Anaesthetics influence leukaemia cell biology and malignancy: Mechanisms and Implications

A thesis submitted to Imperial College London for the degree of Doctor of Philosophy Jiang Cui

November 2019

Anaesthetics, Pain Medicine and Intensive Care section

Department of Surgery and Cancer

Faculty of Medicine

Chelsea & Westminster Hospital Campus

Imperial College London

UK

Declaration

I, Jiang Cui, hereby declare that the work presented in this thesis is my own. Certain experiments were performed with the assistance of Anton Gonzalez, Sara.

Experiments in Figure 5.8a, b, c and Figure 5.9a were performed with the assistance of Anton Gonzalez, Sara, a PhD student under my co-supervisor Professor Cristina Lo Celso.

Copyright Declaration

Abstract

Acute lymphoblastic leukaemia (ALL) is the most common type of cancer in children. During ALL treatments, general anaesthetics are often used on patients undergoing painful procedures. General anaesthetics have been shown to influence cancer cell biology in solid cancer models. However, no study has been published regarding the effects of anaesthetics on leukaemia. To further our understanding, the objective of this thesis is to compare the effects of two commonly used general anaesthetics (intravenous: propofol and inhalational: sevoflurane) on ALL *in vitro* and *in vivo*.

Propofol and sevoflurane reduce proliferation, CXCR4 expression, osteopontin (OPN) secretion and migration of leukaemia cells *in vitro*. In addition, both anaesthetics reduce homing and migration of leukaemia cells *in vivo*. Upon further investigation, hypoxia-inducible factor-1 alpha (HIF-1α) is responsible for induced molecular changes in leukaemia cells. HIF-1α is reduced by propofol in a dose-dependent manner, and its effect is relatively short-term (<24 hours). On the other hand, HIF-1α is inhibited by sevoflurane in a time-dependent manner with more sustainable effects lasting more than 24 hours. The reduction of HIF-1α expression by propofol is likely due to the inhibition of the phosphorylation of ERK and AKT. Sevoflurane only decreases the phosphorylation of ERK. Chemoresistance study reveals both propofol and sevoflurane enhance the cytotoxic effect of the chemotherapeutic agent (Ara-C). Both anaesthetics are shown to potentiate caspase-based apoptotic pathways when given together with Ara-C to leukaemia cells.

In addition to HIF-1α, OPN is shown to regulate anaesthetic induced molecular changes in leukaemia cells *in vitro*. Upon further investigation, OPN forms an auto feedback loop with HIF-1α in leukaemia cells, regulating CXCR4 expression, migration and chemoresistance of leukaemia cells *in vitro.*

In summary, our data demonstrate both propofol and sevoflurane may potentially reduce the malignancy of ALL.

Acknowledgements

I would like to express my sincere gratitude to my supervisor, Professor Daqing Ma, BOC chair professor of Anaesthetics, Section of Anaesthetics, Pain and ICU, Department of Surgery and Cancer in Imperial College London. His guidance has been of great value for me

I would also like to extend my gratitude to my co-supervisor, Professor Cristina Lo Celso, Professor of Stem Cell, Department of Life Sciences, Imperial College London. Her detail and constructive comments really helped me with my project.

I wish to thank Mr Faruq Noormohamed for his kind support.

I wish to thank my wife, Miss Xiaomeng Li, for her support and her patience with me.

I wish to thank everyone who has helped me with my study at Imperial College London.

Table of Contents

List of Figures

List of Tables

Abbreviations

Acute lymphoblastic leukaemia: ALL

Acute promyelocytic leukaemia: APL

Acute myeloid leukaemia: AML

Bone marrow: BM

Central nervous system: CNS

Chronic myeloid leukaemia: CML

Chemokine receptor type: CXCR4

Cytarabine arabinoside: Ara-C

Cytokine receptor-like factor 2: CRLF2

Death inducing signalling complex: DISC

Event-free survival: EFS

Erythropoietin receptor: EPOR

Factor inhibiting HIF: FIH

Foetal bovine serum: FBS

Hypoxia-inducible factor-1 alpha: HIF-1α

Hypoxia-responsive element: HRE

Intravenous: IV

Insulin-like growth factor-1: IGF-1

Ligand stromal-cell-derived factor-1: SDF-1

Minimal residual disease: MRD

Multiplicity of infection: MOI

Naïve control: NC

Natural killer cells: NK cells

Osteopontin: OPN

Overall survival: OS

Phosphatidylinositol 3-kinase: PI3K

Philadelphia chromosome: Ph chromosome

Platelet-derived growth factor receptor beta: PDGFRB

Poly ADP-ribose polymerase: PARP

Prolyl hydroxylase: PHD

Polymerase chain reaction: PCR

Protein kinase C: PKC

Renal cell carcinoma: RCC

Severe combined immunodeficiency: SCID

Total intravenous anaesthesia: TIVA

Vascular endothelial growth factor: VEGF

Vehicle control: VC

Von Hippel-Lindau: VHL

World Health Organisation: WHO

CHAPTER 1

Introduction

Acute lymphoblastic leukaemia (ALL) is a common cause of death before the age of 20 in children with cancer. Although the cure rate for paediatric cases is high (>95%), adult patients still have a poor prognosis. Diagnosis and treatment of ALL consist of multiple stressful and painful procedures (bone marrow (BM) biopsy, BM aspiration and intrathecal chemotherapy). Therefore, the use of anaesthetics is commonly needed for patients. Generally speaking, general anaesthesia is used for most paediatric cases and some adult patients, as general anaesthetics can induce a state of deep sedation and unconsciousness. However, the choice of general anaesthesia technique (inhalational or intravenous (IV)) is entirely down to clinicians without formal guidance indicating which method is beneficial to patient outcomes.

Several reports have been published[1-3] describing how total intravenous general anaesthesia is beneficial to patients with solid cancer, whereas inhalational general anaesthesia worsens patient outcome. The aim of my PhD is to investigate whether two general anaesthesia techniques (IV and inhalational) affect the malignancy of ALL *in vitro* and *in vivo*. In addition, we want to explore the underlying molecular mechanisms.

We propose to treat leukaemia cells with either propofol (an IV general anaesthetic) or sevoflurane (an inhalational anaesthetic) followed by evaluation of 5 aspects of leukaemia malignancy. Well established animal models are used in this study. An overview of the research is illustrated in Figure 1.1. Initially, we studied the effects of general anaesthetics on the proliferation of ALL cells, and we found both general anaesthetics reduced proliferation.

Next, we studied cell viability, migration and homing of ALL cells after general anaesthetic exposure. Migration and homing are vital for cancer cell survival *in vivo*. Migration is responsible for translocating cells to desired locations with optimal growth conditions, whereas homing describes the process of engraftment of ALL cells in the BM. Poor homing leads to early cell death and failure in disease induction. General anaesthetics do not affect cell viability. However, migration and homing of ALL are significantly reduced by general anaesthetics *in vitro* and *in vivo*.

We also focused on the chemoresistance, which is the most substantial challenge for ALL treatment. Our data show that general anaesthetics sensitise ALL cells to chemotherapy.

Finally, our data and existing literature suggest HIF-1α is a primary target of general anaesthetic induced changes in solid and non-solid cancer cells[4]. In addition, we also identified an auto feedback loop between HIF-1α and osteopontin in ALL cells. According to our data, this novel pathway can regulate migration and chemoresistance of ALL cells.

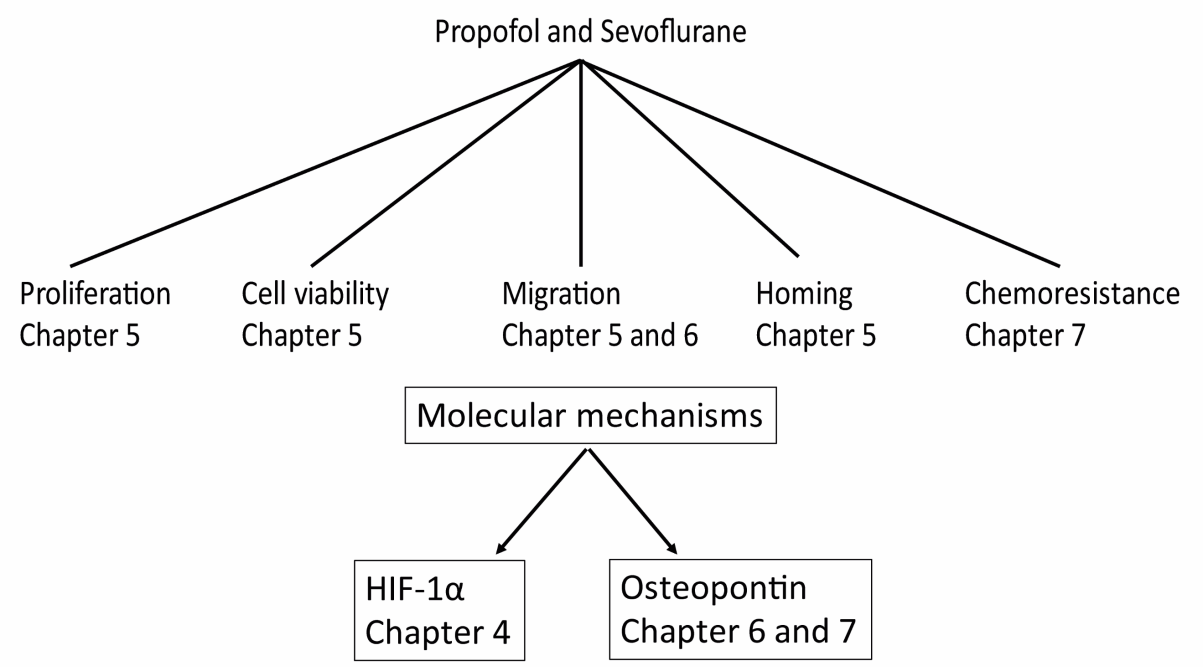

Figure 1.1 Overview of the PhD thesis

In this thesis, the effects of propofol and sevoflurane are evaluated on 5 aspects of leukaemia malignancy. The effects on proliferation, cell viability, migration and homing are included in chapter 5. Migration is discussed in chapter 5 and 6. Chapter 7 illustrates the effect of anaesthetics on the chemoresistance of leukaemia cells. HIF-1α and osteopontin are found to mediate anaesthetic induced effects in leukaemia cells. Chapter 4, 6 and 7 illustrate these mechanisms.

CHAPTER 2

Background

2.1 Acute Lymphoblastic Leukaemia

ALL is most commonly found in children, and it is relatively rare in adults. In children, ALL has an excellent prognosis. However, adults with ALL usually have a 50% chance of survival. Chemotherapy and targeted therapy are the current treatment options. However, chemoresistance is still the major challenge for ALL treatment, so there is a pressing need for innovative ways to reduce chemoresistance and improve the survival rate of ALL.

2.2 ALL epidemiology, aetiology, subtypes and prognostic factors

Leukaemia is the cancer of the blood. More specifically, it is the uncontrolled growth of a particular lineage of blood cells. ALL is a subtype characterised by overgrowth of lymphoblasts, and it manifests in a very rapid manner (6 months from initial symptoms to death).

In this section, I will cover four essential topics for ALL: epidemiology, aetiology, subtypes and prognostic factors.

2.2.1 Epidemiology

ALL is the most common type of cancer in children and a common cause of death before the age of 20 in children with cancer. It has the peak incidence occurring from the age of 2 to 5[(5)]. Every year, around 6000, new cases of ALL are diagnosed in the US, and over 60% of them are younger than 20 years old[(6)]. In the UK, around 400 new cases are diagnosed. Incidence rate of ALL varies significantly according to genders and ethnic groups. For example, Hispanics have higher incidence rate than any other ethnic groups[(5),] and more boys are affected by ALL than girls before the age of 20 (boys: girls = 55%:45%)[(7)].

2.2.2 Aetiology

ALL is a disease with mutations in somatic genes. Usually, ALL is not hereditary but some individuals may inherit genetic abnormalities that increase their risks of developing ALL. Broadly speaking, ALL comprises multiple entities with distinct constellations of somatic genetic alterations including aneuploidy (changes in chromosome number), chromosomal rearrangements, deletions and gains of DNA, and DNA sequence mutations[(5)]. The current proposed sequential acquisition of genetic alterations contributing to the pathogenesis of ALL include three stages: predisposition, initiating translocation and secondary mutations.

Predisposition: Mounting evidence indicates the development of ALL starts from the prenatal period with neonatal and infancy promotion[(6, 8, 9)]. Risks associated with pre-natal period come from inherited gene variants which contribute to the intrinsic vulnerability of precursor blood cells. In addition,

transforming events that occur during the neonatal and infancy period enable the clonal evolution of ALL cells in BM[6]. The common genetic variants at diagnosis including *IKZF1, ETV6-RUNX1* (also known as *TEL-AML1*), *CEBPE* and *ARID5B*. Relatively rare mutations are *pAx5* and *TP53*. However, predisposition of genetic abnormalities alone cannot give rise to ALL later in life. For example, screening of neonatal cord-blood samples reveals the presence of the *TEL-AML1* fusion gene in 1% of all new-borns. However, this frequency is 100 times higher than the prevalence of ALL defined with this fusion[10], suggesting additional disease-related events occur in the neonatal and infancy period.

Initiating translocations: Initiating lesions are acquired in lymphoid progenitors, and they are vital in initiating the disease. Common abnormalities affect self-renewal, developmental arrest, epigenetic reprogramming and proliferation of progenitors.

Secondary mutations: Secondary mutations and structural genetic alterations contribute to an arrest in lymphoid development and perturbation of multiple cellular pathways. Secondary mutations are associated with the progression of the initial disease. These mutations include TP53-retinoblastoma protein tumour-suppressor, Ras, phosphatidylinositol 3-kinase (PI3K), and JAK-STAT signalling and nucleoside metabolism[11, 12]. Some genetic factors are associated with the occurrence of ALL, e.g. Down's syndrome[13], but most cases have no recognised causes.

2.2.3 Subtypes

There are many ways to classify ALL. ALL can be of B-cell or T-cell lineage. However, to aid clinical management and prognosis of the disease, ALL is mainly stratified via chromosomal alterations and genetic mutations.

Hyperdiploidy: The subtype of hyperdiploidy (>50 chromosomes), due to abnormal chromosome gains, comprises around 25-30% of children with B-cell ALL[5]. Patients with this subtype have an excellent response to chemotherapy.

Hypodiploidy: The subtype of hypodiploidy (<44 chromosomes), which only occurs in 2-3 % of patients is a strong negative prognostic factor[14].

Chromosomal translocation: There are two major classes of chromosomal translocations. The first class translocates oncogenes into actively transcribed genes, which in turn cause disruptions in the expression of an existing protein. Examples include rearrangement of cytokine receptor-like factor 2 (CRLF2) and erythropoietin receptor (EPOR) genes in B-cell ALL[15, 16]. The second primary class of translocations combines two genes to encode a chimeric protein which has different functions to previously derived genes. One classic example is the fusion of *ETV6-RUNX1* (also known as *TEL-AML1*) which fuses two hematopoietic transcription factors[5]. Another example is the t(9;22)(q34;q11.2)

translocation that results in the formation of the Philadelphia (Ph) chromosome which encodes *BCR-ABL1* protein. Patients with Ph ALL usually have poor prognoses[17].

Others: Apart from classification, according to lineage and chromosomal alteration, several subtypes of ALL do not have single defining chromosomal alternations. But they are defined by other pathological and genomic features. An example is Ph-like ALL. Patients with this particular subtype have leukaemia cell gene expression similar to patents with Ph-positive ALL, but they lack BCR-ABL1 protein[18].

2.2.4 Prognostic factors

Significant prognostic factors of ALL include followings: clinical feature of patients, biological and genetic feature of leukaemia cells and early response to treatment. Among these factors, early response to treatment is by far the most accurate predictor for outcome.

Clinical feature: the age of patient and initial white blood cell counts are important predictors for outcome. Those patients who have a relatively old age (> or = 10) and a high white blood cell count (> or = 50000/mm^3) at diagnosis are associated with a poor treatment response and a high rate of relapse.

Immunophenotype: The cell-surface and cytoplasmic expression of lineage markers classify ALL into B cell and T cell ALL. In children, B cell ALL is the most common subtype (more than 85%)[5]. Historically, children with T cell ALL had inferior survival rate than those with B cell ALL. However, cell lineages do not provide much prognostic value to disease stratification apart from being reminiscent to lymphoid lineage.

Genetic features: High hyperdiploidy and *ETV6-RUNX1* genetic fusion are associated with favourable outcomes[5]. Hypodiploidy, *MLL* rearrangement, *BCR-ABL1*, Ph-like ALL are associated with poor outcomes[5].

Early response to treatment: This is the most powerful prognostic factor in ALL[19]. The treatment response can be easily measured by polymerase-chain-reaction (PCR) amplification of *IGH* or *TCR* gene rearrangements. Otherwise, the response can also be measured by flow cytometry detection of surface antigens[20]. If a patient has a level of minimal residual disease (MRD) greater than 0.01% at the end of induction therapy, the risk of treatment failure and death increases by 3 to 5 times[21].

2.3 Acute lymphoblastic leukaemia treatments

Treatments of ALL have evolved dramatically over the last few decades. Intensive chemotherapy and disease stratification have turned the ALL from a disease of 100% death rate prior to 1950s to a disease which is treatable in a large proportion of patients today. In this section, a brief history of ALL

treatment is given firstly, followed by a discussion of the contemporary therapy. Then, new strategies in ALL management are illustrated. Finally, I describe the role of anaesthetics in leukaemia treatment.

2.3.1 History of therapy

In the early 19th century, a small number of cases of patients with uncommon alterations in blood cells were reported across Europe. Reported cases had significant age differences and involved both sexes[22]. Of all cases, two of those might suggest symptoms of leukaemia. It was not until March 1845, John Hughes Bennett (an English physician) made the first description of leukaemia as a blood disorder in contrast to the belief of pus and inflammation of blood cells at that time[22]. In 1857, the first acute leukaemia (first time the term was used) case was described by Nikolaus Friedreich, a pathologist in Wurzburg[22]. The short time between the presentation of symptoms and death of the patient granted the name of "acute leukaemia"[22]. Towards the end of the 19th century, clinicians were able to identify the basic cell lineage and subtypes of leukaemia were named[22]. In the late 19th century, leukaemia was generally accepted as a chronic disease, and very limited therapeutic means were available to physicians. Those primitive treatments included quinine used for fever, morphine and opium used for diarrhoea and pain, iron for anaemia, some anti-bacterial and arsenic were also used[22]. However, the efficacies of these remedies were limited, and the deaths of patients were unavoidable. The first treatment that showed some promising results was the use of X-ray[23]. Unfortunately, X-ray treatment was later concluded to be only effective on patients with chronic leukaemia and some lymphomas, but it remained ineffective on all acute leukaemia patients.

The first description of temporary remission of leukaemia induced by folic acid antagonist and 4-aminopropyl-glutamic acid was reported in 1948[24], but acute leukaemia remained invariably fatal until the 1960s. The first milestone in ALL treatment was the introduction of vincristine (an extract from the periwinkle plant) in the 1960s, which showed excellent results when given to children with ALL; 60% of them achieved remission, and the incidence of remission was then further increased to 90% when vincristine was combined with prednisone[25]. In the late 1960s, cranial radiations and intrathecal therapy were used prophylactically to treat potential disease in the central nervous system (CNS). Prophylactic CNS treatment dramatically increased the survivability of ALL patients in 1970s. After 1980s, clinicians and scientists started focusing on stratifying ALL according to the clinical features of patients and biologic characteristics of the leukaemia cells. Thanks to stratification, the survival rate of ALL patients in children has reached 90%[26].

Entering the 21st century, we saw the incorporation of the molecularly targeted tyrosine kinase inhibitor, imatinib mesylate, being used for treatment of patients with Ph ALL. In addition, clofarabine is also being used for patients with recurring ALL[25].

2.3.2 Contemporary therapy

Contemporary therapy of ALL involves several discrete phases. The induction therapy lasts 4 to 6 weeks, and a combination of chemotherapeutic agents are used (prednisone, vincristine and so on). With the development of this chemotherapy protocol over the last 60 years, almost all patients achieve remission, but relapse occurs virtually in all cases if no further therapy is given.

The consolidation phase involves the intensive combination of chemotherapy that is designed to prevent the development of leukaemia cells invading into the CNS. The whole phase lasts 6 to 8 months. Repeated courses of high dose methotrexate are administrated to patients over 24 hours followed by the use of folinic acid, mitigating the side effects of high dose methotrexate.

The maintenance phase consists of low-intensity antimetabolite-based medications for 18 to 30 months. Oral medications include mercaptopurine and methotrexate with some additional regimens of vincristine in some cases. The oral medication brings the problem of adherence. Evidence indicates patients with the adherence rate lower than 90% are 4 times more likely to have relapses[27].

CNS-directed therapy, e.g. cranial irradiation, dramatically improved the survival rates in patients in 1960s. However, cranial irradiations are associated with many complications, e.g. risk of secondary tumours, delayed growth in children, endocrinopathies and neurocognitive deficiencies[28]. In addition, with contemporary chemotherapy, survival rates are similar with or without cranial irradiation[28]. Consequently, the current role of CNS irradiation is controversial.

2.3.3 Challenge and new strategy

Chemoresistance is the major challenge for modern-day treatment. It occurs in 15 to 20% of children with ALL and 50 to 60% in adult patients. Most importantly, the cure rate is much lower after relapses[29]. Factors associated with unfavourable prognosis at relapse include the time to relapse (the shorter i.e. within 2 years, the worse prognosis), certain immunophenotype (e.g. T-ALL) and the site of relapse. Leukaemia cells may reoccur from either the BM or from extramedullary space with the latter being rarer (11%) but achieving a better prognosis[30]. After the first relapse, most patients enter a second remission with the chance for cure around 50%. If relapse occurs again after the second remission, the chance of achieving a third remission is dramatically reduced to 50% to 70%. Those who achieve a third remission have only 20% to 30% chance of survival.

The mechanism by which ALL relapses after remission is still under investigation. The current proposed model is somewhat similar to bacterial resistance to antibiotics. At diagnosis, ALL cells are commonly genetically polyclonal. Initial therapy eliminates clones that are more proliferative predominant, leaving subclones which are insensitive to chemotherapy. Those subclones then harbour or acquire mutations that enable them to be resistance to chemotherapeutic agents. Essentially, chemotherapy

selects drug resistance mutations and promotes resistance. Leukaemia cells obtained from patients with an early relapse show these cells have already developed mutations that decrease sensitivity to chemotherapy[31]. Those common mutations include *CREBBP* (resistance to glucocorticoids)[31], *NT5C2* and *PRPS1* (resistance to thiopurines)[32, 33].

In order to improve the outcome for patients with relapse(s), allogeneic hematopoietic cell transplantation is used. Transplantation is not usually recommended for primary therapy. Only 5% to 10% of patients in the very high-risk group is considered for allogeneic hematopoietic-cell transplantation. Assessment of MRD is required to determine whether patients are suitable for transplantation during therapy for a second remission[34].

Targeted therapy: With the development of targeted therapies in cancer, we are entering a new era of treating ALL. The first successful targeted therapy in leukaemia was using tyrosine kinase inhibitors (imatinib, introduced clinically since 2001) on patients with chronic myeloid leukaemia (CML), a cancer driven by BCR-ABL1 fusion oncoprotein[5]. The effectiveness of imatinib completely changed the treatment landscape of CML. CML treatment used to consist of intensive treatment and stem cell transplantation. However, after the introduction of imatinib, CML became a successfully managed chronic disease with oral medications[5]. Still, 33% of patients do not achieve an optimal response with imatinib[35]. Two major resistance mutations*, E255K* and *T315I*, were identified on BCR-ABL 1 kinase domain[36]. Those two mutations render the shape change of binding domains for imatinib on BCR-ABL 1 kinase[36].

After the successful introduction of imatinib in CML, it is applied to patients with Ph ALL which is also driven by BCR-ABL 1 fusion protein. Before the use of imatinib, the survival rate of Ph ALL was 50% in children and 20 to 30% in adults. With the help of imatinib, the survival rate increased dramatically and potentially minimised the need for hematopoietic-cell transplantation[5].

Ph-like ALL has similar BCR-ABL 1 kinase mutation but has an additional mutation in other kinases including ABL-class and JAK-STAT signalling pathway. Extensive pre-clinical studies have shown activation of abnormal signalling pathways is sensitive to tyrosine kinase inhibitors[5]. Potentially, imatinib may be trialled on patients with Ph-like ALL.

Immunotherapy: Immunotherapy is increasingly becoming a research focus in oncology. In ALL, several groups have developed strategies to transduce T-cell receptors with an anti-CD19 antibody fragment, redirecting cytotoxic T lymphocytes to recognise and kill B-ALL cells[37]. One innovative study showed the effectiveness of T cells transduced with CD19-directed chimeric antigen receptor (CTL019) treatment in patients with multiple relapses[38]. Out of 30 patients (children and adults) treated by transduced T cells, 27 (90%) achieved complete remission. In addition, sustained remission was achieved with a 6-month event-free survival rate of 67% and an overall survival rate of 78%[38].

Remission was durable with 3 years follow-up. One ongoing clinical trial (ClinicalTrial.gov number, NCT0244522) is assessing the role of chimeric antigen receptor T-cell therapy in ALL patients with less advanced disease.

A new strategy in immunotherapy is to use blinatumomab[39]. It is used as a second-line treatment option for ALL patients with relapses. Blinatumomab belongs to a class of constructed monoclonal antibodies and bi-specific T-cell engagers that specifically target CD19 receptor (a B-ALL surface marker) and direct immune system to act against ALL cells. Blinatumomab is constructed as a fusion protein consisting of two single-chain variable fragments to recognise two different antigens. One of the single-chain variable fragments binds to T cells via the CD3 receptor, and the other binds to ALL cells via CD19 receptor[39]. With the help of blinatumomab, T calls can be in direct contact with B-ALL cells and carry out cytotoxic effects.

2.3.4 Use of anaesthetics in ALL treatment

Anaesthetics (both regional anaesthetics and general anaesthetics) are widely used during ALL diagnosis and treatment. Painful and stress-producing procedures, including BM aspiration/biopsy, intrathecal chemotherapy, lumbar puncture, cranial radiation and BM transplantation, all require some forms of analgesia and anaesthesia for both adult and paediatric patients. Currently, there is no guidance on which, if any, anaesthetic or anaesthetic technique is beneficial to patient outcomes. It is largely down to the anaesthetist's belief, training and local hospital policy. The frequency of these painful, anxiety-producing procedures is very high during the diagnosis and treatment of ALL. Patients may receive 2-3 procedures every week for a few weeks during intensification treatment phase to monitor treatment response. Therefore, anaesthetics have good opportunities to have direct effects on cancer cells.

Adult patients: Regional anaesthetics (e.g. lidocaine) are generally used in adults for short painful procedures[40]. One of the most important pain-influencing factors during these procedures is anxiety. In order to improve the quality of the procedure, IV sedatives include lorazepam, midazolam, or diazepam are administered. In addition to their properties of reducing anxiety and decreasing pain perception, IV sedation has been shown to induce a degree of amnesia[41].

Paediatric patients: In 1990, the American Academy of Paediatrics published recommendations on the management of pain and anxiety related to procedures in children with cancer[42]. It recommended the use of general anaesthesia for paediatric patients undergoing short painful procedures in haematological malignancies. Besides pain relief, general anaesthetics may offer potential psychological benefits for patients, improving the overall experience of procedures[43].

Studies examining different methods of sedation for children yielded various results. Some investigators suggested benzodiazepines alone were sufficient[43], while others recommended brief general anaesthesia[44]. There is still some reluctance to offer deep sedation to paediatric patients, a tendency that is more prominent in the US than Europe.

Safety of using general anaesthetics in paediatric patients undergoing short painful procedures has been extensively studied. A recent retrospective review consisting of 137 patients subject to 423 short procedures under general anaesthesia found the majority of procedures had no adverse events during intraoperative and postoperative periods. No procedure was suspended after it had begun and no patient needed cardiopulmonary resuscitation[45].

IV general anaesthetics and inhalational general anaesthetics are both used clinically for short procedures. Both techniques are similar in terms of safety, patient experience and immune response. The notable differences are recovery time and equipment set up. A single-blind study consisted of 21 children undergoing similar procedures (BM biopsy and lumbar puncture) showed IV anaesthesia (propofol and remifentanil) allowed rapid patient recovery time of 13 minutes and patients with inhalational anaesthesia (sevoflurane or nitrous oxide) needed 30 minutes for recovery[44].

They are still some disadvantages of using general anaesthesia in paediatric patients. Firstly, staff with experience in airway management and advanced life support are essential for general anaesthesia. Anaesthetists are usually called upon to administer and monitor patients if general anaesthesia is involved; whereas any trained physicians are competent enough to administer local anaesthesia. In addition, facilities required to carry out general anaesthesia are more complex with additional monitoring, delivery and resuscitation equipment. Usually, short procedures requiring general anaesthesia are carried out in a theatre environment. However, regional anaesthesia requires less equipment.

2.4 Anaesthetics and cancer

Cancer is a major contributor to the global disease burden and the second greatest killer following cardiovascular disease. Surgery is still the first line and the most effective treatment for solid cancer. Anaesthetics (particularly general anaesthetics) are used during surgery to achieve: unconsciousness, amnesia, analgesia, muscle relaxation and diminished motor response to stimuli. Usually, combinations of general anaesthetics are deployed during surgery, as no single general anaesthetic could achieve all 5 properties mentioned above. Not only surgery but also diagnostic procedures e.g. biopsy and palliative intervention all require the use of anaesthetics. Therefore, a high percentage of patients are exposed to a high dose of anaesthetics at least once or multiple times during diagnostic and treatment procedures.

Clinicians and scientists have long been observing the potential effects of anaesthetics on solid cancer. It was thought that the systemic immune modulation of the anaesthetics affects cancer malignancy. Specifically, anaesthetics affect the function of noncancer cells present in tumour microenvironment and cells in the immune system. However, evidence indicates that anaesthetics exert direct biological effects on cancer cells due to cellular signalling changes beyond their primary effect of anaesthesia and analgesia. In this section, I will discuss different mechanisms by which various anaesthetics influence cancer cells directly and indirectly.

2.4.1 Clinical evidence

The hypothesis that anaesthetics and analgesics during cancer surgery affect recurrence or metastasis was initially proposed in 2006[46]. It has become an important research question. The retrospective analysis which proposed this question in the first place suggested paravertebral anaesthesia (regional anaesthesia) plus general anaesthesia reduced the risk of breast cancer recurrence and metastasis during 3 years of follow up when compared to general anaesthesia alone[46]. This raised the first question of which, if any, anaesthetic technique is more favourable for cancer patients: regional anaesthesia vs general anaesthesia. A few years later, the second question surrounding the topic of anaesthetics and cancer was asked: "which general anaesthetic technique is beneficial to cancer patients: inhalational vs IV". I will discuss both questions blow.

Regional anaesthesia vs general anaesthesia: The perioperative period is considered as a time of maximum vulnerability in cancer patients. Perioperative inflammation, immunosuppression and elevated concentrations of catecholamines can facilitate the seeding of circulating cancer cells in distant organs as well as the growth of dormant tumours[47]. Regional anaesthesia is known to prevent or attenuate the above-mentioned surgical stress responses by blocking afferent neural transmissions. A little over a decade ago, research on breast cancer patients concluded regional anaesthesia plus general anaesthesia was more beneficial than general anaesthesia alone[46]. However, in 2015 a consensus statement from the BJA workshop on cancer and anaesthesia stated there was insufficient evidence to support the use of particular regional anaesthesia to improve survival in cancer patients[48]. Since then, over 40 papers have been published (Table 2.1 and 2.2), testing the hypothesis of "the use of regional anaesthetics is associated with better oncological outcomes than the use of general anaesthetics"[46, 49-90].

As we can see from these studies, five of them were conducted as randomised control trials[54, 64-66, 90]. Four of them found regional anaesthesia had no impact on overall survival, recurrence-free survival and recurrence[54, 65, 66, 90]. The one remaining randomised control trial showed benefit of regional anaesthesia only on early overall survival (1.46 years). And beneficial effects were only seen in those

who did not have a metastatic disease. Interestingly, data from a recent randomised control trial indicated that the regional anaesthesia-analgesia may reduce the breast cancer recurrence in Asian patients (Asian vs non-Asian p=0.043) and in those who were treated in Chinese hospitals (Chinese vs non-Chinese; p=0.039)[90].

The rest of the investigations from two tables were retrospective cohort studies. Most of larger sample-sized studies were not able to show any association between regional anaesthesia and improved recurrence-free survival for breast, gastric, colorectal and prostate cancer. After all, several important factors related to retrospective study design e.g. bias, confounding error, random error and sampling error limited the interpretation of these investigations. In addition, most studies have differences and variation in outcome measures and adjuvant therapies. More importantly, tumour-related characteristics (staging, histology and subtypes) were varied from one study to another.

Table 2.1 Summary of studies that show the beneficial effect of regional anaesthesia
EA: epidural anaesthesia; GA: general anaesthesia; IVPCA: Intravenous patient-controlled analgesia; OS: overall survival; PVB: Thoracic paravertebral block; PFS: progression-free survival; RFS: recurrence-free survival; SB: scalp block.

Study (author, year, reference number)	Method	Cancer	Anaesthetics technique	Number of patients received RA	Number of patients received no RA	Outcome
Hiller, 2014, 59	Retrospective	Gastro Esophageal	GA+EA vs GA	97	43	EA showed benefit on recurrence or OS
Wang, 2016, 63	Retrospective	Gastric	GA+EA vs GA	157	116	EA showed benefit on OS
Wang, 2017, 62	Retrospective	Gastric	GA-EA vs GA-IVPCA	1362	2856	EA showed a benefit on OS
Christopherson, 2008, 64	Randomised control trial	Colorectal	GA-EA vs GA	85	92	EA showed a benefit on early OS
Gupta, 2011, 75	Retrospective	Colorectal	GA-EA vs Spinal vs GA	562	93	EA showed a marginal benefit on OS in colon cancer but not on rectal cancer
Holler, 2013, 68	Retrospective	Colorectal	GA-EA vs GA	442	307	EA showed a benefit on OS
Cummings, 2012, 56	Retrospective	Colorectal	GA-EA vs GA	9278	4037	EA showed a benefit on RFS but not on OS
Lai, 2012, 50	Retrospective	Hepatocellular	EA vs GA	62	117	GA showed a benefit in RFS
Biki, 2008, 70	Retrospective	Prostate	GA-EA vs GA	103	102	EA showed a marginal benefit on BRFS
Wuethrich, 2010, 72	Retrospective	Prostate	GA-EA vs GA	103	158	EA showed a benefit on PFS but not on OS
Scavonetto, 2014, 82	Retrospective progression-free survival	Prostate	GA-EA vs GA	1642	1642	EA showed a marginal benefit on OS

DE Oliveira, 2011, 74	Retrospective	Ovarian	Intraop EA vs Postop EA vs GA	55	127	Introp EA showed marginal benefit on PFS
Lin, 2011, 77	Retrospective	Ovarian	GA-EA vs GA	106	37	EA showed benefit on OS
Merquiol, 2013, 84	Retrospective	Head and neck	GA-EA vs GA	111	160	EA showed marginal benefit on OS
Zimmitti, 2016, 49	Retrospective	Metastatic liver resections	GA-EA vs GA	390	120	EA is associated with longer PFS
Zheng, 2017, 88	Retrospective	Glioblastoma	GA-SB vs GA	67	52	SB associated with longer PFS
Cata, 2018, 87	Retrospective	Mix of gliomas	GA-SB vs GA	120	56	SB associated with longer PFS

Table 2.2 Summary of studies that do not show the beneficial effect of regional anaesthesia
EA: epidural anaesthesia; GA: general anaesthesia; IVPCA: Intravenous patient-controlled analgesia; OS: overall survival; PVB: Thoracic paravertebral block; PFS: progression-free survival; RFS: recurrence-free survival; SB: scalp block.

Study (author, year, reference number)	Method	Cancer	Anaesthetic technique	Number of patients received RA	Number of patients received no RA	Outcome
Cummings, 2014, 55	Retrospective	Gastric	GA-EA vs GA	766	1979	GA did not show benefit on OS
Shin, 2017, 61	Retrospective	Gastric	GA_EA vs GA	3425	374	EA did now show benefit on RFS
Heinrich, 2015, 60	Retrospective	Esophageal	GA-EA vs GA	118	35	GA did not show benefit on OS
Gottschalk, 2010, 80	Retrospective	Colorectal	GA-EA vs GA	256	253	EA did not show benefit on RFS
Myles, 2011, 66	Randomised controlled trial sub-analysis	Colorectal	GA-EA vs GA	230	216	EA did not show benefit on OS
Day, 2012, 79	Retrospective	Colorectal	GA-EA vs Spinal vs GA	251	173	EA did not show benefit on OS
Binczak, 2013, 67	Retrospective	Colorectal	GA-EA vs GA	69	63	EA did not show benefit on RFS
Exadaktylos, 2006, 46	Retrospective	Breast	PVB vs GA	50	79	PVB did not show a benefit on recurrence
Starnes-Ott, 2015, 53	Retrospective	Breast	PVB-GA vs GA	193	165	PVB did not show benefit on recurrence
Kairaluoma, 2016, 51	Retrospective	Breast	PVB-GA vs GA	45	41	PVB did not show on recurrence but longer OS
Tsigonsis, 2016, 58	Retrospective	Breast	RA vs GA	646	461	No benefit
Cata, 2016, 52	Retrospective	Breast	PVB vs GA	197	197	PVB did not show benefit on RFS or OS
Finn, 2017, 54	Randomised control trial	Breast	PVB-GA vs Placebo-GA	26	28	PVB did not show benefit on RFS
Tsui, 2010, 65	Randomised control trial	Prostate	GA-EA vs GA	49	50	EA did not show benefit on RFS

Forget, 2011, 76	Retrospective	Prostate	GA-EA vs GA	578	533	EA did not show benefit on RFS
Wuethrich, 2013, 73	Retrospective	Prostate	GA-EA vs GA	67	81	No benefit on RFS or OS
Roiss, 2014, 81	Retrospective	Prostate	GA-spinal vs GA	3047	1725	No benefit on RFS or OS
Sprung, 2014, 83	Retrospective	Prostate	GA-EA vs GA	486	483	No benefit on cancer recurrence
Tseng, 2014, 85	Retrospective	Prostate	GA-EA vs GA	1166	798	No benefit on RFS
Lee, 2015, 57	Meta-analysis	Prostate	GA-EA vs GA	7504	6261	No benefit on RFS
Capmas, 2012, 78	Retrospective	Ovarian	GA-EA vs GA	47	47	No benefit on OS or RFS
Lacassie, 2013, 69	Retrospective	Ovarian	GA-EA vs GA	37	43	No benefit on OS
Ismail, 2010, 71	Retrospective	Cervical	GA-EV vs GA	63	69	No benefit on RFS
Cata, 2013, 86	Retrospective	Non-small cell lung	IVPCA vs EA-IVPCA vs EA alone	343	102	EA showed no benefit on RFS or OS
Gottschalk, 2012, 89	Retrospective	Melanoma	GA vs spinal	52	221	Spinal showed no benefit in survival
Sessler, 2019, 90	Randomised control trial	Breast	GA-EA vs GA	1043	1065	RA showed no benefit in cancer recurrence and OS

Inhalational general anaesthetics vs IV general anaesthetics: The use of general anaesthesia is considered as an unreplaceable part in modern-day surgery. They are used in induction and maintenance of anaesthesia during procedures.

The second question regarding anaesthetics and cancer is which, if any, general anaesthetic technique (inhalational or IV) is beneficial to cancer patients. Not many clinical publications with cancer outcome are available for considerations. However, two recent[3, 91] retrospective investigations with large patient size both suggested total intravenous anaesthesia (TIVA) is associated with better overall survival and recurrence-free survival in many types of cancer patients. In 7030 patients undergoing cancer surgeries regardless of cancer types, those who received inhalational general anaesthetics (isoflurane and sevoflurane) had around 50% higher mortality rate than those who received TIVA with an adjusted hazard ratio of 1.46[3]. Jun et al reported similar findings. Inhalational anaesthetics were associated with worse overall survival with a hazard ratio of 1.45 and worse recurrence-free survival with a hazard ratio of 1.44 in patients who had oesophageal cancer surgeries[91]. However, a recent randomised control trial suggested that propofol did not reduce cancer recurrence compared with sevoflurane in breast cancer patients[90]. Overall, there is insufficient evidence to potentially change clinical practice.

2.4.2 Pre-clinical evidence

Regional anaesthesia vs general anaesthesia:

Tumour growth, metastasis, immune surveillance and angiogenesis are hallmarks of cancer. There is both *in vivo* and *in vitro* evidence showing regional anaesthetics might have some "anti-cancer" effects.

Lidocaine and ropivacaine triggered apoptosis in lung and breast cancer cells *in vitro* by inhibiting Src kinase phosphorylation and blocking voltage-gated sodium channels[92, 93]. In addition, both bupivacaine and levobupivacaine inhibited colon cancer growth and invasion *in vitro* (a publication from our group)[94]. The mechanism of inhibition was currently not known. However, it is reasonable to assume that voltage-gated sodium channels may be involved as a voltage-gated sodium channel SCN5A is shown to be a key regulator of the gene transcriptional network that controls colon cancer invasion[95]. Furthermore, both ester and amide local anaesthetics activated the tumour suppressor genes following inhibition of DNA methylation in human hepatoma cells and breast cancer cells[96, 97].

The excitability of cancer cells is linked to their ability of metastasis. Amide local anaesthetics reduced the excitability of cancer cells (lung, breast and transient receptor potential cation vanilloid subfamily member 6 (TRPV6) expressing cancer cells) by blockage of voltage-gated sodium channels (Nav 1.5

and 1.7), modulation of voltage-gated potassium channel, decreasing calcium availability and reducing the expression of TRPV6[98-101].

The immune system acts against the development and growth of cancer cells through elimination, equilibrium and escape. Many immune cells including neutrophils, macrophages, dendritic cells, natural killer (NK) cells, B cells, and T cells participate in the maintenance of immune system balance and they constantly surveil any cancer growth. Several human studies demonstrated that regional anaesthesia preserved the cell count and function of circulating NK cells and increased the presence of T helper cells near tumour sights[102-104]. Associated with these findings, they also showed increased concentrations of antitumoral cytokines such as interleukin-2 and interferon-γ[105].

The goal of angiogenesis is to adequately supply cancer cells with blood and nutrients to facilitate their survival, proliferation and metastasis. This process is regulated by proangiogenic and antiangiogenic factors. Regional anaesthesia is shown to reduce proangiogenic factors systemically[106]. Circulating concentrations of vascular endothelial growth factor (VEGF) were reduced in colorectal patients who received epidural anaesthesia[106]. In addition, local anaesthetics were shown to modulate the function of the endothelium and systemic vasculature[107].

Inhalational general anaesthetics vs propofol: Evidence from *in vitro* and *in vivo* studies demonstrated inhalational general anaesthetics potentially increased cancer malignancy and metastasis. On the contrary, IV general anaesthetics (i.e. propofol) are generally considered harmful to cancer cells under experimental settings. However, responses to anaesthetics are entirely cancer-specific and largely down to cancer cell biology. My colleagues, Benzonana et al, demonstrated that isoflurane enhanced renal cell (RCC) carcinoma growth and malignant potential through hypoxia-inducible factor (HIF) signalling pathway[108]. Shortly after, Huang et al (from our group) demonstrated isoflurane increased characteristics associated with malignancy in prostate cancer. However, propofol attenuated those effects of isoflurane through HIF mediated mechanisms[4]. In addition, Luo et al also showed isoflurane potentiated malignancy of ovarian cancer cells including increased insulin-like growth factor-1 (IGF-1) expression, increased cell cycle progression, enhanced cell proliferation, increased VEGF expression and increased migration[109]. Propofol, on the other hand, was shown to reduce factors associated with the malignancy of cancer cells which include inhibition of invasion, induction of apoptosis and disruption of aerobic glycolysis in ovarian cancer cells and colorectal cancer cells [110] [111].

2.4.3 Opioids

Opioids (e.g. morphine, fentanyl and remifentanil) are essential for pain management during surgical procedures. They are given together with general anaesthetics to achieve three main

clinical outcomes: unconsciousness, immobility and the control of autonomic nervous system responses to surgical stimulation. Over the past decade, the hypothesis that the use of opioids preoperatively may influence cancer recurrence and metastasis has received increasing attention[112]. *In vitro* and *in vivo* studies have evaluated the effects of opioids on host immune system, cancer angiogenesis, apoptosis, and invasion, showing discrepant results[113-118]. A limited number of retrospective clinical studies in this area could not draw a clear conclusion[119]. Most retrospective studies have focused on the hypothesis that using reginal anaesthesia/analgesia in cancer patients may reduce the rate of recurrence and improve overall survival. Studies suggesting benefits with regional anaesthesia/analgesia techniques (opioids sparing) in cancer surgery patients cannot clearly show if this benefit arises directly from the avoidance of opioids or an added benefit afforded by regional anaesthesia/analgesia[64, 65, 89]. Nevertheless, data from a recent randomised control trial with a large sample size indicated opioids and volatile anaesthesia (sevoflurane) did not increase breast cancer recurrence compared with regional anaesthesia-analgesia (paravertebral block and propofol)[90]. Overall, there is insufficient evidence to indicate whether or not opioids may affect metastasis and recurrence after cancer surgery.

2.5 Proposed mechanisms by which general anaesthetics affect ALL cell biology

For many years, it has been the belief that general anaesthetics exert a reversible effect on the CNS which is returned to its original state once the agent is eliminated from the body. However, there is increasing evidence to suggest general anaesthetics exert long-term biological effects due to strongly induced cellular signalling changes beyond their primary effect of anaesthesia and analgesia. Indeed, our group has been investigating such 'long term' effects of general anaesthetics. In particular, we found that an inhalational anaesthetic, xenon, potently protected against kidney ischaemia refusion injury via HIF activation[120]. This encouraged us to explore the role of general anaesthetics on cancer cell biology, as hypoxia is intrinsic to the tumour. Since then, we have interrogated the effect of both inhalational and propofol on prostate, ovarian, lung and renal cancer models[4, 108, 109, 121, 122]. According to our data, inhalational general anaesthetics potentially exhibit 'pro-cancer' effects and IV general anaesthetics potentially have 'anti-cancer' effects. The mechanism by which general anaesthetics affect cancer biology still largely remains elusive. And it is extremely difficult to predict the precise effects of general anaesthetics on each cancer type as those effects are largely cancer type specific.

A very important issue in leukaemia research has been neglected. That is to investigate whether general anaesthetics may play any role in cancer biology of leukaemia.

Currently, there is no literature published describing the effects of general anaesthetics on human acute lymphoblastic leukaemia *in vitro*, *in vivo* or in a clinical setting. I attempt to fill this knowledge gap with this study. In this section, I will discuss potential mechanisms by which general anaesthetics may affect leukaemia biology and I will summarise the hypotheses for my PhD.

2.5.1 Hypoxia Inducible Factor (HIF)

Hypoxia-inducible factors (HIF) are a family of oxygen-sensitive basic helix-loop-helix transcription factors that direct the transcriptional response to hypoxia. They were initially identified in the 1990s by Semenza et al[123]. HIF-1α and HIF-1β were initially identified, followed by the discovery of HIF-2s and HIF-3s. HIF-1s are ubiquitously expressed in human cells, whereas HIF-2s and-3s are only expressed in specific tissues and cell types[124].

The role of HIF-1s is well defined in cancer but the parts played by HIF-2s and HIF-3s in cancer are still under investigation. Therefore, I have focused on investigating the role of HIF-1s in my study and the roles of HIF-2s and HIF-3s are beyond the scope of my research.

Under normoxia, α-ketoglutarate-dependent prolyl hydroxylases (PHDs) catalyse the hydroxylation of proline residues within oxygen-dependent degradation domains of HIF-1α[124]. The hydroxylation reaction catalysed by PHDs requires oxygen and α-ketoglutarate as co-substrates. The hydroxylated proline residues are then recognised by the Von Hippel-Lindau (VHL) E3 ubiquitin ligase complex (consisting of pVHL, Cul-2 and TCEB), leading to HIF-1α ubiquitination and degradation[124] (Figure 2.1). An additional asparagine residue in the C-terminal activation domain is hydroxylated by the Factor inhibiting HIF (FIH)[124]. The hydroxylated asparagine prevents the binding of p300 to HIF, inhibiting HIF transcriptional potential[124]. When under hypoxia (oxygen concentration <5%), HIF-1 α is stabilised and translocated into the nucleus. Then, it combines with HIF-1β, ARNT and p300 to form a heterodimer complex. The complex binds to the hypoxia-responsive element (HRE) and activates the transcription of the target gene[124]. The oxygen-dependent hydroxylase stabilisation of HIF-1α is one of the two ways of HIF-1α stabilisation and activation.

In addition to hypoxic activation of HIF-1α, growth factor-dependent non-hypoxic pathways also regulate HIF-1α signalling. Three intracellular pathways (PI3K-AKT-mTOR, MAPK-ERK and JAK-STAT3) associated with growth factors increase cap-dependent translation of HIF-1α mRNA, resulting in increased expression of HIF-1α[124-126].

In cancer cells, frequent activation of the PI3K-AKT-mTOR axis due to mutation stimulates HIF-1α activity and promotes tumour angiogenesis[126]. In the PI3K-AKT-mTOR axis, PTEN acts as an inhibitor of AKT phosphorylation. Mutation of PTEN enhances activation of HIF-1α in many cancer cell types. HIF-1α modulation by the JAK-STAT3 pathway is initially identified in lymphocytes[127]. Pro-

inflammatory cytokines such as interleukin-6 have been found to activate transcription of HIF-1α through JAK-STAT3 pathway[127]. In cancer cells with Ras-Raf mutation, the MAPK-ERK pathway is activated, leading to an increase in transcriptional activity of HIF-1α. Activation of HIF-1α elevates the expression of downstream target genes include: angiogenesis, migration and cell survival[124].

In leukaemia, the role of HIF-1α is not sufficiently studied. In solid tumours, the primitive and chaotic tumour neovasculature is unable to meet all requirements of oxygen and nutrients. The poor and hostile location drives cancer cell survival, maintenance, metabolic reprogramming, angiogenesis and modulation of the immune response[128]. As leukaemia does not have a primary tumour, the role of hypoxia in leukaemia was initially presumed to be inconsequential. However, the BM environment is hypoxic when compared to normal tissue. Spencer et al measured the absolute PO_2 of BM in live mice by using two-photon phosphorescence lifetime microscopy[129]. They found the average absolute PO_2 of BM was quite low (<32 mm Hg, <5%) despite very high vascular density[129]. In addition, the lowest PO_2 (9.9 mm Hg, 1.3%) was found in deeper per-sinusoidal regions[129]. Therefore, hypoxia is indeed a hallmark of the BM.

An elevated expression of HIF-1α is considered to be a marker of poor prognosis in solid cancer[130]. In theory, HIF-1α should drive the transcription of genes involved in many pathways promoting angiogenesis, proliferation, survival and invasion in leukaemia cells. An elevated level of HIF-1α is reported in almost all subtypes of leukaemia including acute myeloid leukaemia (AML)[130-132], acute promyelocytic leukaemia (APL)[133], ALL[130], and CML[134]. However, the subject is somewhat complex and controversial in leukaemia. It appears the elevated level of HIF-1α expression can either be beneficial or harmful to leukaemia cells and its role is subtype dependent. Several studies showed that inhibition of HIF-1α resulted in a failure of primary leukaemia cells forming *in vitro* colonies. At the same time, tumour growth and leukemic progression were observed to be impaired by inhibition of HIF-1α in ALL and CML *in vivo*[132, 135]. In addition, a dramatic decrease and potential eradication of leukaemia cell xenografts were demonstrated with HIF-1α inhibited ALL cells *in vivo*[132]. On the contrary, Talia et al found a faster development of the disease and an enhanced leukaemia phenotype were observed in murine AML models lacking *hif-1α*[136]. And they also observed that *hif-1α* deficiency in mice accelerated leukaemogenesis. Therefore, they proposed *hif-1α* might act as a tumour suppressor gene in AML[136]. Although the increased expression of HIF-1α was reported in many leukaemia subtypes, the outcome of its elevated expression has not been correlated with its expression pattern[131, 132]. Further studies are still needed to understand and stratify the role of HIF-1α in leukaemia.

HIF-1α becomes a central pathway in the recent research topic of “effects of general anaesthetics on cancer”. Our group, for the first time, showed that short exposure of isoflurane, a commonly used

inhalational general anaesthetics, enhanced the expression of HIF-1α through increased phosphorylation of AKT in renal cell carcinoma cells (RCC4). Increased HIF-1α then potentiated the cancer cell malignancy[108]. Others have found similar phenomena in non-small cell lung cancer and glioma cancer cells *in vitro*[137, 138], where inhalational general anaesthetics was associated with the increased expression of HIF-1α. Inhalational general anaesthesia was shown to activate downstream target genes include VEGF, CD133 (a stem cell marker), MMP2 and MMP9[138]. Whereas, propofol (a general anaesthetic) was found to reduce HIF-1α expression and decrease the expression of HIF-1α target genes[138].

2.5.2 CXCR4/SDF-1 axis

Homing and subsequent adhesion of leukaemia cells to a specific niche in BM are vital in leukaemogenesis, migration and propagation of the disease and chemoresistance. The chemokine receptor, C-X-C chemokine receptor type 4 (CXCR4), and its ligand stromal-cell-derived factor (SDF-1 or CXCL12) mediates the homing process in ALL[139]. Sipkins et al. demonstrated B-ALL (NALM-6) cells selectively homed to the adhesion molecule E-selectin and SDF-1 expressing vessels via a CXCR4 dependent process. Disruption of the interaction between SDF-1 and CXCR4 inhibited the homing process[139]. Further study revealed circulating leukaemia cells engrafted around these vessels, suggesting a potential microenvironment for early metastasis[139]. The role of the SDF-1/CXCR4 axis in chemoresistance of leukaemia was also profoundly studied. A recent study showed that stromal cells conferred a remarkable chemoprotective effect on T-ALL cells which was specifically blocked by a CXCR4 blocker (AMD3100). This phenomenon suggests that stromal cell-mediated chemoresistance is SDF-1/CXCR4 dependent in T-ALL[140].

In the context of anaesthetics and cancer, one publication reported that lidocaine inhibited the migration of human breast cancer cells through inhibition of CXCR4[141]. It is reasonable to assume that general anaesthetics like propofol and sevoflurane may affect the SDF-1/CXCR4 axis as both SDF-1 and CXCR4 are well-known downstream targets of HIF-1α [142, 143].

2.5.3 Osteopontin

Osteopontin (OPN) is an acidic arginine-glycine-aspartate containing adhesive glycoprotein with a molecular mass of approximately 44 kDa[144], interacting with several integrins ($\alpha_V\beta_3$, (α_4, α_9, α_5)β_1, and $\alpha_4\beta_2$) and CD44[144, 145].

It serves many functions in both physiological and pathophysiological conditions. In BM, the function of OPN is very complex, and it can be cleaved by thrombin, forming different fragments with various

functions[146]. Generally speaking, OPN has been found to carry out functions like being an adhesion molecule, regulator of hematopoietic stem cell pool and regulator of cell trafficking[147] in BM.

In BM, OPN is primarily secreted by osteoblasts and hematopoietic stem cells[145, 148]. Recently, OPN was also shown to be secreted by ALL cells. It adhered ALL cells to anatomic locations supporting leukaemia cell dormancy and avoiding chemotherapeutic agents[148].

OPN interacts with HIF-1α in solid cancer models. OPN was shown to increase HIF-1α via the PI3K/AKT pathway in ovarian cancer and breast cancer model[149] [150].

Importantly, results from our group demonstrated sevoflurane increased expression of OPN and migration in RCC4 cells[121]. It can be speculated that general anaesthetics may affect expression of OPN secreted by ALL cells through HIF-1α mediated process.

2.5.4 Chemoresistance

There are currently two proposed means that leukaemia cells protect themselves from chemotherapy. Firstly, anatomic locations inside bone marrow with poor vasculature may provide a physical barrier for leukaemia cells[140, 148]. These locations include the endosteal niche, which is hypoxic and rich in quiescent hematopoietic stem cells. It is thought that leukaemia cells hijack normal hematopoietic stem cell niches, taking advantage of a physical barrier and staying quiescence while chemotherapy eradicates actively proliferating cells. It was shown during T-ALL progression, leukaemia cells selectively remodelled the endosteal space, resulting in a complete loss of mature osteoblastic cells[151]. This process is thought to be important in T-ALL chemoresistance. In B-ALL, instead of remodelling niches, leukaemia cells are anchored to stromal locations rich in OPN expressions via integrin[148]. The anchorage of leukaemia cells in discreet locations protects ALL cells from chemotherapy. Similarly, SDF-1/CXC4 axis regulates interactions between ALL cells and stroma which provide physical locations for ALL cells to 'hide' from chemotherapy[128]. It is relatively unrealistic for general anaesthetics affecting above-mentioned mechanisms as they are carried around via the bloodstream with chemotherapeutic agents. General anaesthetics are less efficient in accessing poorly perfused areas.

The second proposed mechanism of chemoresistance in leukaemia cells is through activating molecular signalling pathways: resistance to apoptosis, mutation in receptors, rapid self-renew and autophagy. It is hard to predict whether general anaesthetics may have any effects on the above-mentioned pathways due to insufficient evidence. However, the effect of general anaesthetics on autophagy has been extensively studied in the field of neurodegeneration and cognitive dysfunction[152-154]. In particular, inhalational general anaesthetics, e.g. sevoflurane and isoflurane, are potent activators of autophagy. Wang et al found that sevoflurane exposure significantly increased

the level of LC3-II and the ratio of LC3-II/LC3-1 was also increased. In addition, sevoflurane treatment decreased the level of p62 in the hippocampus of the young mice at P8, indicating the induction of autophagy[152]. Given the fact, general anaesthetics could modulate autophagy; we proposed to study whether general anaesthetics might affect chemosensitivity of ALL cells through modulation of autophagy.

2.5.5 Summary of hypothesises

Currently, there is insufficient guidance for clinicians to choose from a wide range of anaesthetics for pain management during ALL treatment. It is imperative to establish and stratify the optimal anaesthesia technique for leukaemia patients and, if possible, give them the edge over cancer. Accumulative advantage at each stage of diagnosis and treatment will eventually turn into improvement in survival and maybe one day curing the disease. Unfortunately, stratifying optimal anaesthetics for better outcomes in leukaemia patients has been long neglected.

Therefore, we conducted this study with the aim to answer two broad questions: 1) can general anaesthetics affect ALL cell biology 2) if they can, which technique (inhalational or IV) reduces malignancy of the disease.

Given the fact that HIF-1α plays a vital role in leukaemia, and general anaesthetics modulates it in other cancer models, we hypothesised that general anaesthetics may alter the expression of HIF-1 α in ALL cells. We studied cell survival and proliferation as they are classic target genes of HIF-1α in other cancer models. We were also very interested in defining whether general anaesthetics might disrupt the CXCR-4/SDF-1 axis, affecting migration of leukaemia cells. Study of chemo-sensitivity is crucial, as most relapse is primarily due to chemoresistance. We hypothesised general anaesthetics might induce autophagy in leukaemia cells, as they strongly induced autophagy in cognitive dysfunctions models[152]. Then, we explored whether the elevated level of autophagy protected leukaemia cells from chemotherapy or enhancing the cytotoxic effect of chemotherapy.

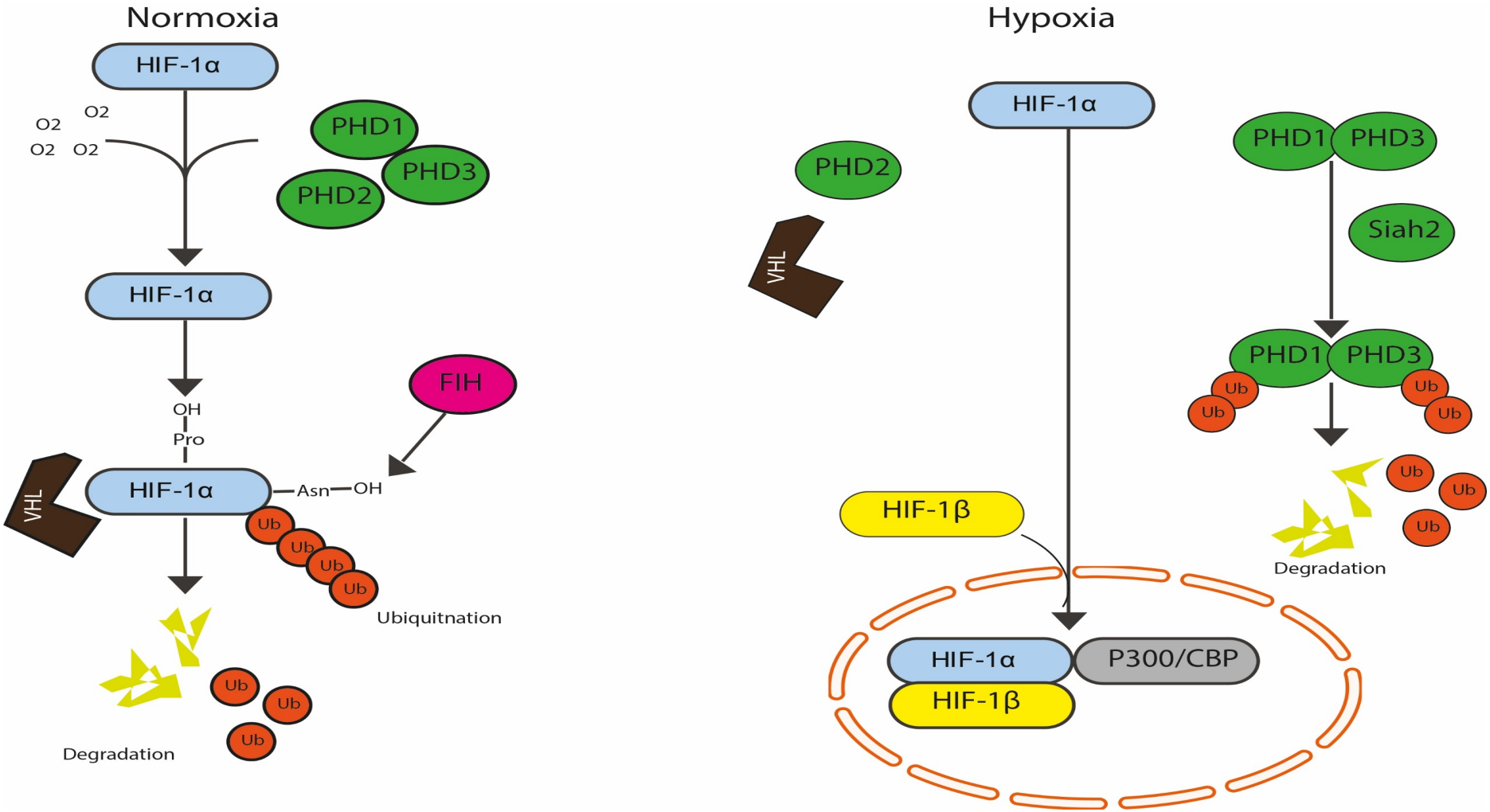

Figure 2.1 Oxygen dependent regulation of HIF-1α

Under normoxia, the HIF-1α protein is recognised by prolyl hydroxylase proteins (PHD), which hydroxylate prolines in the oxygen-dependent degradation domain. Von Hippel-Lindau (VHL) recognises the hydroxylated prolines and whole complex is degraded by proteasome. Under hypoxic conditions, PHD activity is inhibited. HIF-1α is stabilised and translocated into nucleus before forming the heterodimer with HIF-1β. Then, the heterodimer binds to the hypoxia-responsive element (HRE) and actives target genes.

CHAPTER 3

Materials and methods

This chapter introduces the experimental models and methods applied in this PhD study, including specific laboratory skills and techniques.

3.1 *In vitro* model

3.1.1 Cell culture

The following cell lines are used for this PhD study (Table 3.1)

NALM-6: NAML-6 cell line (DSMZ, Germany) is an immortalised cell line established from peripheral blood of a 19-year-old man with ALL in relapse. NALM-6 is classified as B-ALL by phenotype, and it is commonly used to study ALL *in vitro* and *in vivo*.

GFP-NALM-6: NALM-6 cells are transduced with GFP lentivirus (System Biosciences, USA) to produce GFP-NALM-6 cells. They are particularly useful in *in vivo* tracking of leukaemia cells.

Reh: Reh cell line (DSMZ, Germany) is another classical ALL cell line. It was initially established from the peripheral blood of a 15-year-old North African girl with ALL in 1973. It has been used in many publications to study ALL.

All cell lines were maintained in T175 tissue culture flasks at 37 °C in RPMI 1640 medium (Invitrogen) supplemented with 10% foetal bovine serum (FBS) (Invitrogen), 2 mM L-glutamine (Invitrogen), and 100 U/mL penicillin-streptomycin (Invitrogen) in a humidified air with 5% CO_2 atmosphere. The media was changed every two days. After reaching more than a cell density of $2.0X10^7$, cells were centrifuged and passed to the next generation.

Table 3.1 Cell lines and cell culture medium

Cell Lines	Species	Culture medium	Supplement
NALM-6	Human immortalised cell line	RPMI 1640	10 % foetal bovine serum (FBS), 2 mM L-glutamine, and 100 U/mL penicillin-streptomycin
GFP-NALM-6	Human immortalised cell line transduced with GFP lentivirus	RPMI 1640	10 % foetal bovine serum (FBS), 2 mM L-glutamine, and 100 U/mL penicillin-streptomycin
Reh	Human immortalised cell line	RPMI 1640	10 % foetal bovine serum (FBS), 2 mM L-glutamine, and 100 U/mL penicillin-streptomycin

3.1.2 Sevoflurane exposure

Before gas exposure, NALM-6 and Reh cells were cultured at 1 X 10^6 per ml density on 30-mm^2 Petri dishes (VWR, Leicestershire, UK), or on 24 well plates with a seeding density of 5 X 10^4 per ml. Cells were used 12 hours later after seeding. Cells were placed in 1.5 L purpose-built airtight, temperature-controlled chambers equipped with inlet and outlet valves and an internal electric fan was used to provide continuous delivery and mixture of gases. The chamber was connected to calibrated flow meters and an in-line vaporiser was used to deliver the desired composition (Datex gas monitor, Helsinki, Finland) of sevoflurane (3.6%, MAC 2.0) (Abbott Laboratories, Maidenhead, UK) in 21% oxygen and 5% CO_2 balanced with nitrogen (BOC, Guildford, UK). The chamber was pre-flushed with the aforementioned gas mixture to ensure that a stable gas composition was achieved, and a closed system was established to prevent leakage. Gas treatment was given at the desired sevoflurane concentration for 2, 4 and 6 hours at 37°C. At the end of treatment, cells were harvested for further analysis. Cells used as the naïve control group were placed in an identical gas chamber containing 21% oxygen and 5% CO_2 balanced with nitrogen at 37°C. For recovery experiment, cells were supplied with fresh media and they were returned to a standard incubator containing humidified air and 5% CO_2 at 37°C for further analysis analysed at different time points ranging from 0–24 h post gas exposure.

3.1.3 Propofol treatment

A clinical formulation of propofol (Diprivan, Astra-Zeneca, London, UK) was used. It was dissolved in 10% intralipid (Astra-Zeneca, London, UK). Before treatment, NALM-6 and Reh cells were cultured as described above.

On the day of the experiment, the stock solution of propofol was diluted with medium to the final concentrations of 1–10μg/ml (5.6–56μM). For the intralipid control, 10% intralipid was added to the cell medium to recreate the amount of intralipid in the highest 10μg/ml dose of propofol being used. Propofol-supplemented medium was then added to the cell cultures for 6 hours. For recovery experiments, the propofol medium was replaced with fresh medium and cells were returned to a standard incubator containing humidified air and 5% CO_2 at 37°C for further analysis at 24 hours post propofol treatment.

3.1.4 Hypoxia induction

Cells were placed in a gas chamber as described earlier and exposed to a mixture of low concentration oxygen (<1%) balanced in nitrogen and 5% CO_2 for 6 h at 37°C. For some experiments, propofol (1–10μg/ml) and sevoflurane (3.6%) were added to the cell culture medium. For hypoxia experiments, cells were subject to an extreme level of hypoxia (<1%).

3.1.5 *In vitro* siRNA administration

Human HIF-1 α and human OPN siRNA were predesigned with the following sequences

Table 3.2 Sequences of human HIF-1 α and human OPN siRNA

HIF-1α	
Target sequences	5'-AGGAAGAACTATGAACATAAA-3'
Sense sequence	5'-GAAGAACUAUGAACAUAAATT-3'
Antisense sequence	5'-UUUAUGUUCAUAGUUCUUCCT-3'
OPN	
Target sequence	5'-TGCGGCAAGCATTCTGAGGATG-3'
Sense Sequence	5'-GGUUGUCCAGCAAUUAAUATT-3'
Antisense sequence	5'-UAUUAAUUGCUGGACAACCGT-3'

Leukaemia cells were transfected with high-quality human-specific siRNA (Qiagen, Sussex, UK). A scrambled non-sense siRNA (Qiagen) without specific gene-silencing activity was used as a negative control. Transfection was achieved using lipofectamine RNAi MAX (Invitrogen). Cells were cultured at the density of 0.4 X 10^6 per ml and treated with siRNA. Human Specific targeted or scrambled siRNA was dissolved in siRNA suspension buffer supplement with lipofectamine which was administered to cells in a dose of 20nM. Cells were incubated with siRNA for 6 hours at 37°C in humidified air containing 5% CO_2, after which the cells were washed with medium then serum-free medium was added. For OPN experiments, 200ng/ml of human OPN was given to culture after OPN knockdown. For chemotherapy experiment, 0.5-200μM of Ara-C was given to cells after OPN knockdown.

3.1.6 OPN treatment

NALM-6 cells were treated with rising concentration of human recombinant OPN (R&D system, catalogue number: 1433-OP-050, Host: Goat, Target: Human, Concentration: 50 to 200ng/ml) or cells were treated with polyclonal goat IgG (Abcam, catalogue number: ab37373, Host: Goat concentration: 200ng/ml). Then, treated cells were incubated for 6 hours at 37°C in humidified air containing 5% CO_2. After incubation, cells were harvested for western blot and flow cytometry analysis.

In some experiments, human anti-OPN neutralising antibody was used (155) (R&D system, Catalogue number: AF1433, Host: Goat, Target: Human, concentration: 2μg/ml) to treat NALM-6 cells. Then, treated cells were incubated for 6 hours at 37°C in humidified air containing 5% CO_2. After incubation, cells were harvested for western blot and flow cytometry analysis.

3.1.7 Generation of GFP expressing NALM-6 cells

Initially, 5 X 10^4 of NALM-6 cells were seeded in a 24 well plate. After 12 hours, TransDux and TransDUX MAX enhancer (System Biosciences, Palo Alto, USA) were mixed and added to culture with a concentration of 1X. Then, pre-packed GFP lentivirus (System Biosciences, Palo Alto, USA) were given

to NALM-6 cells at a multiplicity of infection (MOI) of 20. Cells were incubated at 5% CO_2 at 37°C for 72 hours. Finally, GFP-expressing NALM-6 cells were sorted using FACS Aria-II cell sorter (BD, USA), before seeding in T175 flask with fresh medium.

3.1.8 Chemotherapy treatment

A typical anti-mitotic chemotherapeutic agent for leukaemia, cytosine arabinoside (Ara-C), was used. For general anaesthetics treatment, 0.5-50μM of Ara-C (Sigma-Aldrich, UK) and general anaesthetics (sevoflurane 3.6% and propofol 10μg/ml or 56μM) were given to cells for 6 hours. After treatment, cells were processed for western blot and flow cytometry analysis. For the OPN experiment, 0.5-100μM of Ara-C was given to cells in conjunction with 200ng/ml of OPN (R&D system, UK) or OPN siRNA (Qiagen, UK).

3.2 *In vivo* model

3.2.1 Animals

C57/BL6 mice (20-22g) and SCID mice (20-22g) were purchased from Charles River, UK and breed in temperature and humidity-controlled cages in a specific pathogen-free facility at the Chelsea and Westminster Campus, Imperial College London. This study was approved by the Home Office, United Kingdom, and all procedures were carried out in accordance with the United Kingdom Animals (Scientific Procedures) Act of 1986. C57/BL6 mouse was used for the homing and migration study. Severe combined immunodeficiency (SCID) mouse was used for the disease induction study.

3.2.2 ALL induction and tracking of disease progression in SCID mice

ALL was induced in SCID mice and progression of the disease was tracked. 1 X 10^6 of NALM-6 cells were injected into SCID mice IV at day 0. 10 days later, mice were sacrificed using terminal anaesthesia (sodium pentobarbital, intraperitoneal injection). Blood samples were taken via cardiac puncture, then samples were processed for enzyme-linked immunosorbent assay (ELISA) and flow cytometry. Bone marrow flush samples were also taken for flow cytometry analysis. Same procedures were carried out on mice after 20, 30 and 40 days post leukaemia cell injections respectively. The use of terminal anaesthesia may affect the cell biology of injected ALL cells *in vivo*, which may affect ELISA and flow cytometry results. However, those effects are applied to all samples across different treatment groups. Therefore, statistical differences we observed among different treatment groups should be caused by the treatment not the terminal anaesthesia.

3.2.3 Intravital microscopy (equipment)

We used intravital microscopy to monitor ALL homing and migration *in vivo*. This procedure was only carried out on C57/BL6 mice. Intravital microscopy was performed using a Leica SP5 and a Zeiss LSM 780 upright confocal microscope with a motorized stage. The SP5 was fitted with the following lasers: Argon, 546, 633 and a tunable infrared multiphoton laser (Spectraphysics Mai Tai 690-1020). The Zeiss LSM 780 was fitted with the following lasers: Argon, 561, 633 and a tunable infrared multiphoton laser (Spectraphysics Mai Tai DeepSee 690-1040). The signal was visualized with a Leica HCX IRAPO L ×25 water immersion lens (0.95 N.A) and a W Plan-Apochromat ×20 DIC water immersion lens (1.0 N.A). GFP signals were generated through excitation at 840 and 870 nm and detected with external detectors. Internal detectors were used to collect GFP and Cy5 signals. Prior to surgery, mice were administered isoflurane (Mac 4.0 isoflurane in 4L/min O_2 for induction and Mac 1.0–2.0 isoflurane in 1L/min O_2 for maintenance). This was gradually reduced to approximately Mac 1.0 as anaesthesia stabilized. We have considered the fact that isoflurane (an inhalational anaesthetic) may affect factors associated with leukaemia malignancy, as isoflurane has been shown to increase migration and proliferation of prostate cancer cells *in vitro*[4]. Prior to isoflurane, we tried to use the combination of ketamine and xylazine during procedures in pilot studies. However, we found that ketamine-xylazine was associated with issues like inadequate depth of anaesthesia and the death of animals. In fact, we had 2 mice died prior to the end of procedures. These issues were not seen with isoflurane. In addition, isoflurane was used to induce anaesthesia in all animals. The effects of isoflurane, if any, are applied to all animals across different treatment groups. Therefore, statistical differences we observed among different treatment groups should be caused by the treatment not isoflurane.

A headpiece was placed onto the calvarium by following ways:

1) Using sterile forceps and scissors, carefully remove the central portion of the scalp to expose the calvarium area to be imaged: make a small incision at the back of the head between the ears by lifting the skin up with the forceps. While holding the skin up, slide the scissors under the skin and gently cut along the outside of the desired imaging area.

2) Mix an adequate amount of dental cement in a weigh boat until it becomes a paste and quickly apply to the bottom surface of the headpiece that will attach to the skull.

3) Before the cement sets, place the headpiece onto the skull of the mouse, making sure not to get any dental cement on the imaging area, then wait for it to set.

4) Attach the headpiece to the holder and secure in place using the screw, ensuring that the grooves fit within the holder notches.

IVM equipment and methodology is summarised in Figure 3.1.

3.2.4 Intravital microscopy (Tile scan and time-lapse)

Large three-dimensional 'tile scans' of the entire BM cavity space were acquired by stitching adjacent, high-resolution *z*-stack images using a surgically implanted imaging window that ensures steady positioning of mice on the microscope. Time-lapse was taken by focusing on one area of BM. One image was taken every 3 minutes for the entire 22 images. Then, all 22 images were combined together to produce a movie (time-lapse). The calvarium has been demonstrated to be equivalent to the long bones such as the femur with regards to haematopoietic stem cell frequency, function and localization[156], and is the only BM compartment that allows longitudinal imaging through minimally invasive surgery. Blood vessels were highlighted by i.v. injection of 50µl of 8mg/ml 500kDa Cy5-Dextran (Nanocs, MA). Injection of Cy5-Dextran was done 5 to 10 minutes before each imaging session. All mice were terminally anaesthetised at the end of imaging procedures.

3.2.5 Intravital microscopy (Data processing)

Microscopy data was processed using multiple platforms. Tile scans were stitched using Leica Application Systems (LAS; Leica Microsystems, Germany) and ZEN black (Zeiss, Germany) software. Raw data were visualised and processed using Fiji/Image J (National Institutes of Health, Maryland, USA). Cell tracking was performed using FIJI plugin MTrackJ. For accuracy in cell tracking data, videos were registered when required before using four-dimensional data protocols implemented in Fiji. Three-dimensional data rendering and measurement of cell distances were performed in Volocity (Perkin Elmer, MA, USA).

3.3 Immuno-histochemistry

Immunostaining is a laboratory technique, which uses antibodies to detect the target proteins.

3.3.1 Immunofluorescence

NALM-6 cells are suspension cells that do not adhere to the bottom of Petri dishes. 10µg/ml of poly-L-Lysine was used to adhere to NALM-6 cells to petri dishes 24 hours prior to the experiment. After treatment, cells were fixed in paraformaldehyde and incubated in 10% normal donkey serum in 0.1M PBS-T prior to overnight incubation with primary antibody (Table 3.3), followed by secondary antibody (Table 3.4) for 1 hour. Slides were counterstained with DAPI nuclear dye and mounted with VECTASHIELD Mounting Medium (Vector lab, USA). 10 high-power fields at x20 and x40 magnification were photographed using an AxioCam digital camera (Zeiss, Germany) mounted on an Olympus BX60 microscope (Olympus, Middlesex, UK) with Zeiss KS-300 software. Ten representative regions per field *in vitro* were randomly selected by an assessor blinded to the treatment groups. Immunofluorescence

was visualised using Fiji/Image J. For Ki-67 experiments, the number of Ki-67 positive cells were counted, and this number was used to against the number of all cells in the field of the view. Ki-67 index= the number of Ki67 positive cells/ the total number of cells.

Table 3.3 Primary antibodies for immunochemistry

Primary antibodies	Host Species	Target Species	Source	Product Code	Dilution
Ki-67	Mouse	Human	Santa Cruz	Sc-23900	1 in 200
HIF-1 α	Rabbit	Human	Novus	NB100-479	1 in 100

Table 3.4 Secondary antibodies for immunochemistry

Secondary antibodies	Host Species	Target Species	Conjugate	Source	Product Code	Dilution
Donkey anti Rabbit Ig	Donkey	Rabbit	FITC	Millipore	AP182F	1 in 200
Donkey anti Mouse Ig	Donkey	Mouse	FITC	Millipore	AP192F	1 in 200

3.4 Western Blot

Cultured cells were homogenised in lysis buffer and centrifuged at 3,000g for 30 minutes at 4°C and the supernatant was then collected. Total protein concentration in the supernatant was quantified by the Bradford protein assay (BioRad, Hemel Hempstead, UK). The protein extracts (40 to 60µg/sample) were heated for 10 min in 95°C and denatured in sodium dodecyl sulphate (SDS) sample buffer (Invitrogen). The samples were then loaded on a NuPAGE 4 to 12% Bis-Tris gel (Invitrogen) for electrophoresis and then transferred to a PVDF membrane. The membrane was treated with blocking solution (5% non-fat dry milk in TBS with 0.1% Tween-20) for 2 hours and was probed with the following primary antibodies (Table 3.5) in TBS-T overnight at 4°C, followed by HRP-conjugated secondary antibody for 1 hour (Table 3.6). The loading control was the constitutively expressed protein GAPDH (1:20000, Sigma-Aldrich). The membrane was washed with TBST for 5 minutes three times and visualised with enhanced chemiluminescence (ECL) system (Santa Cruz, USA). The protein bands were captured with the image processor, GeneSnap (Syngene, Cambridge, UK), and the intensity of the bands corresponding to the protein expression level was measured with software Image J (National Institutes of Health, Maryland, USA) and normalised to GAPDH and expressed as ratio of control for data analysis.

Table 3.5 Primary antibodies for western blot

Primary antibodies	Host species	Target species	Source	Product code	Dilution
HIF-1α	Rabbit	Human	Novus	NB100-479	1 in 100

Osteopontin (OPN)	Mouse	Human	Abcam	Ab166709	1 in 500
Phospho-p44/42 MAPK (Erk1/2)	Rabbit	Human	Cell signalling	9101S	1 in 500
P44/42 MAPK (Erl1/2)	Rabbit	Human	Cell signalling	9102S	1 in 500
Phospho-Akt (Ser473)	Rabbit	Human	Cell signalling	9271S	1 in 500
Akt	Rabbit	Human	Cell signalling	9272S	1 in 500
Phospho-Stat3	Rabbit	Human	Cell signalling	9131S	1 in 500
Stat3	Rabbit	Human	Cell signalling	4904T	1 in 500
PARP	Rabbit	Human	Cell signalling	9542S	1 in 500
Caspase-8	Mouse	Human	Cell signalling	9746S	1 in 500
Pro Caspase-3	Rabbit	Human	Abcam	Ab32150	1 in 1000
LC3B	Rabbit	Human	Cell signalling	2775S	1 in 1000
ATG5	Rabbit	Human	Cell signalling	12994S	1 in 1000
GAPDH	Rabbit	Human	Millipore	ABS16	1 in 20000

Table 3.6 Secondary antibodies for western blot

Secondary antibodies	Species	Target species	Conjugate	Source	Product Code	Dilution
Donkey anti-Rabbit Ig	Donkey	Rabbit	HRP	Cell signalling	7074	1 in 1000
Donkey anti Mouse Ig	Donkey	Mouse	HRP	Cell signalling	7076	1 in 1000

Table 3.7 Buffer solutions for western blot

Tris-HCl solution	12.1 g Trizma base 0.5 L dH_2O Titrate to pH 8.0 with HCL
Tris-buffered saline (TBS)	8.8 g NaCl 50 ml Tris-HCL Top up to 1L with dH_2O
Tris-buffered saline with 0.05% Tween-20 (TBST)	8.8 g NaCl 50 ml Tris-HCL Top up to 1 L with dH_2O 0.5 ml Tween-20

3.5 Enzyme-linked immunosorbent assay (ELISA)

Human OPN concentration in serum and cell supernatant were measured by ELISA (R&D Systems, UK). *In vivo* serum samples from mouse blood and *in vitro* cell samples were diluted in standard diluents

buffer. And standards (100µl/well) were added, and the plate was incubated at room temperature as per manufacture instructions. All samples were developed by reacting with 100µl stabilised chromogen. Absorbance was read by the photometric reader at 450nm.

Table 3.8 Primary antibodies for ELISA

Primary antibodies	Target Species	Source	Product Code
Human osteopontin (OPN)	Human	R&D system	DOST00

3.6 Flow cytometry (FACS)

Flow cytometry is a laser-based technology for cell counting and biomarker detection.

3.6.1 Determination of cell death *in vitro*

Leukaemia cells were centrifuged and washed with PBS (Sigma, UK). Those cells were then stained with propidium iodide (e-Bioscience, Cambridge, UK) and incubated in the dark at room temperature for 5 minutes before flow cytometry analysis. 50000 cells per sample were analysed with a flow cytometer (CyAn ADP; Beckman Coulter, US). Propidium iodide is a fluorescent dye that binds to DNA. In addition, it cannot pass cell membranes. When excited by 488nm laser light, it can be detected within the PE-Texas Red channel. The scatter plot of forward scatter versus the PE-Texas red was initially analysed in naïve control samples to determine the population of healthy cells. We found that healthy cells had an intensity smaller than 10^2 in the PE-Texas Red channel. Any cells with an intensity larger than 10^2 in PE-Texas Red channel were considered as dead cells. Then, the scatter plot of cells with various treatments was analysed to determine the population of dead cells.

3.6.2 Determination of cell cycle *in vitro*

Cells were centrifuged and washed with PBS. Then, cells were stained with Vybrant DyeCycle green stain (Thermo Fisher, UK) at the concentration of 10µM. Cells were incubated at 37°C for 30 minutes. After staining, cells were run on BD FACS Aria-III (Becton Dickinson, US). A count of 50000 cells per sample was acquired.

3.6.3 Migration assay *in vitro*

In vitro migration assay was performed by loading 20000 cells to the upper chamber of migration chamber. Cells were allowed to mitigate for 6 hours before being collected in the lower chamber. Then, cells were centrifuged and washed with PBS. Finally, samples were run on a flow cytometer

(CyAn ADP; Beckman Coulter, US) with Accu check counting beads (Thermo Fisher, UK) to determine absolute cell counts in each sample.

3.6.4 Determination of protein expression *in vitro*

Leukaemia cells were washed with PBS and centrifuged. NALM-6 and Reh cells were then incubated with antibodies (Table 3.9) and respective isotypes for 30 minutes at 37°C. After incubation, cells were washed with PBS and samples were run on a flow cytometer (CyAn ADP; Beckman Coulter, US). Each assay included 50000 gated events.

Table 3.9 *In vitro* primary antibodies and isotypes used in flow cytometry analysis

Primary antibodies	Host species	Target species	Source	Product code	Conjugation	Dilution
CXCR4	Mouse	Human	eBioscience	17-9999-42	APC	1 in 400
CXCR4	Mouse	Human	eBioscience	12-9991-82	PE	1 in 400
CD49d	Mouse	Human	eBioscience	12-0499-42	PE	1 in 400
IgG2b kappa Isotype	Mouse	Human	eBioscience	17-04031-82	APC	1 in 400
IgG2b kappa Isotype	Mouse	Human	eBioscience	12-4031-82	PE	1 in 400
IgG1 kappa Isotype	Mouse	Human	eBioscience	12-4714-82	PE	1 in 400

3.6.5 Determination of protein expression *in vivo*

Blood samples and bone marrow samples were collected via terminal cardiac puncture and bone marrow flushing, respectively. Then, blood and flushed bone marrow samples were centrifuged at 350g for 5 minutes in the presence of red blood cell lysis buffer (Biolegend, UK). Then, primary antibodies (Table 3.10) were given to cells, and these cells were incubated for 40 minutes at 37 °C. Finally, samples were acquired on a flow cytometer (CyAn ADP; Beckman Coulter, US). Each assay included 100000 gated events.

Table 3.10 *In vivo* primary antibodies and isotypes used in flow cytometry analysis

Primary antibodies	Host species	Target species	Source	Product code	Conjugation	Dilution
CD10	Mouse	Human	Thermo Fisher	MA1-19627	PE	1 in 200
CD19	Rat	Human	ebioscience	17-0193-82	APC	1 in 400
IgG2b kappa Isotype	Mouse	Human	eBioscience	12-4031-82	PE	1 in 400

Rat IgG2a kappa Isotype	Rat	Human	eBioscience	17-4321-81	APC	1 in 400

3.7 Animal survival

For the disease induction study, animals were monitored on a daily basis with a scoring system based on body weight, activity, general appearance and behaviour (Table 3.11). Any animal that scored over 7 was terminated. All animals were terminated humanly 40 days post initial leukaemia cell injection.

Table 3.11 Post-injection scoring system

Criteria	**Score**
Weight (g)	
> or = pre-injection weight	0
90-100% pre-injection weight	1
80-90% pre-injection weight	3
< 80% pre-injection weight	8
Activity	
Normal	0
Moves around cage spontaneously, but reduced	1
Moves to stimulus, but not spontaneously	2
Huddled, not moving to stimulation	4
General Appearance	
Normal	0
Evidence of poor grooming	1
Harsh Starring coat	3
Flabby appearance due to rapid accumulation of fluid under the skin and abdominal areas	6
Behaviour	
Traumatisation of wound	1
Muscle twitching	3
Back arching	5
Judgment: 0: No evidence of symptoms 1-4: Continue to monitor closely, at least on a daily basis 5-7: Consider humane endpoint > Or = 8: Institute humane endpoint	

3.8 Statistical analysis

All numerical data were expressed as mean ± standard error (SE). Data were initially tested for normality by Prism 6.0 (GraphPad, US). Having established data were normally distributed, one-way ANOVA followed by Bonferroni's post-hoc test was used for experiments with more than two variables. Unpaired T-test was used for experiments with two variables. If data were not normally distributed,

one-way non-parametric ANOVA test (Kruskal-Wallis test) was used. A p-value < 0.05 was considered statistically significant.

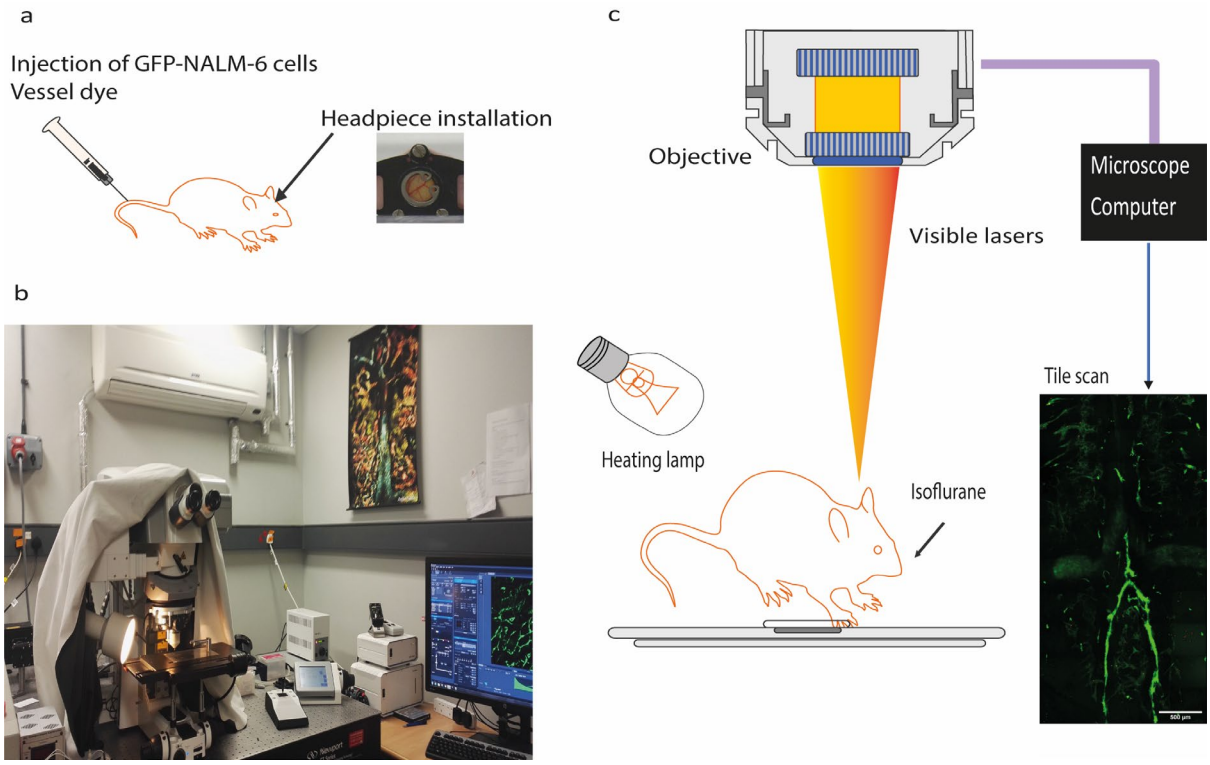

Figure 3.1 Intravital microscopy set up

a) Before each imaging session, $1X10^6$ of GFP-NALM-6 cells and vessel dye were injected IV. Then a headpiece was installed on the calvarium of the mouse. **b)** A picture of procedure room **c)** A schematic representation of the microscope. Heating lamp is provided to maintain the optimal body temperature of the mouse. Deep anaesthesia is maintained by continuous flow of isoflurane. Inverted objectives are set to focus on the mouse calvarium. Imaging processing computer produces a tile scan.

CHAPTER 4

General anaesthetics reduce HIF-1α expression and they reduce the phosphorylation of ERK and AKT

4.1 Introduction

Our initial hypothesis was that propofol and sevoflurane might affect HIF-1α expression in NALM-6 and Reh cells. Both of cell lines are classic examples of B cell ALL, and each represents distinctive genetic alterations. Reh cells feature chromosome rearrangement of *TEL-AML* fusion genes and NALM-6 cells have the near diploid karyotype[157]. The aim of this chapter is to explore the effect of propofol and sevoflurane on HIF-1α expression and identify underlying mechanisms.

4.2 Experiment Design

NALM-6 cells were treated with a rising concentration of propofol from 1 to 10μg/ml (5.6–56μM). After treatment with propofol, western blot and immunostaining were carried out to probe with specific antibodies. In recovery time studies, fresh medium was given to cells after 6 hours of propofol treatment, and 24 hours of additional recovery time was given. After treatment, western blot and immunostaining analyse were carried out.

The chosen concentrations of propofol were derived from previous studies[4, 110, 111, 138]. When injected into the bloodstream, propofol quickly binds to erythrocytes and serum proteins (almost exclusively to albumin). One study demonstrated 40% of propofol molecules bund to erythrocytes and serum proteins[158] at clinically relevant concentrations of propofol (0.5 to 16μg/ml). The clinical formulation of propofol was used (Diprivan). So, intralipid control was included in our experiments. 10% intralipid was added to the cell medium to recreate the amount of intralipid in the highest 10μg/ml (56μM) dose of propofol being used.

NALM-6 cells were also treated by 3.6% (MAC 2.0) of sevoflurane for 2, 4 and 6 hours followed by western blot and immunostaining analysis. 2, 4 and 24 hours recovery time were given in recovery time experiments.

Hypoxia treatment (<1% of oxygen) was also given to cell culture in conjunction with propofol and sevoflurane for 6 hours. At the end of exposure, cells were subjected to western blot and immunostaining analysis. Some experiments were replicated by using Reh cells.

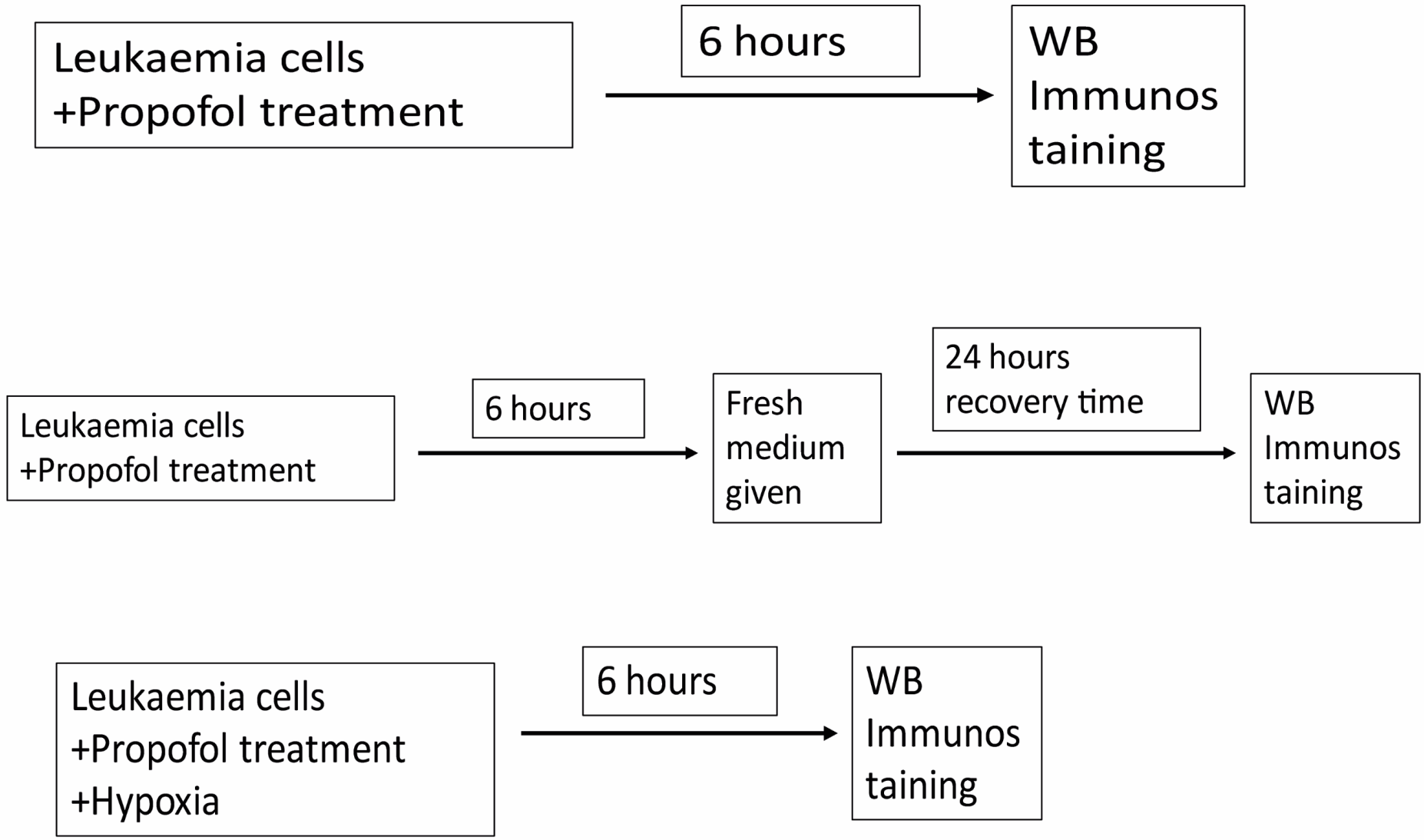

Figure 4.1 Experiment Design for propofol experiment
WB: western blot

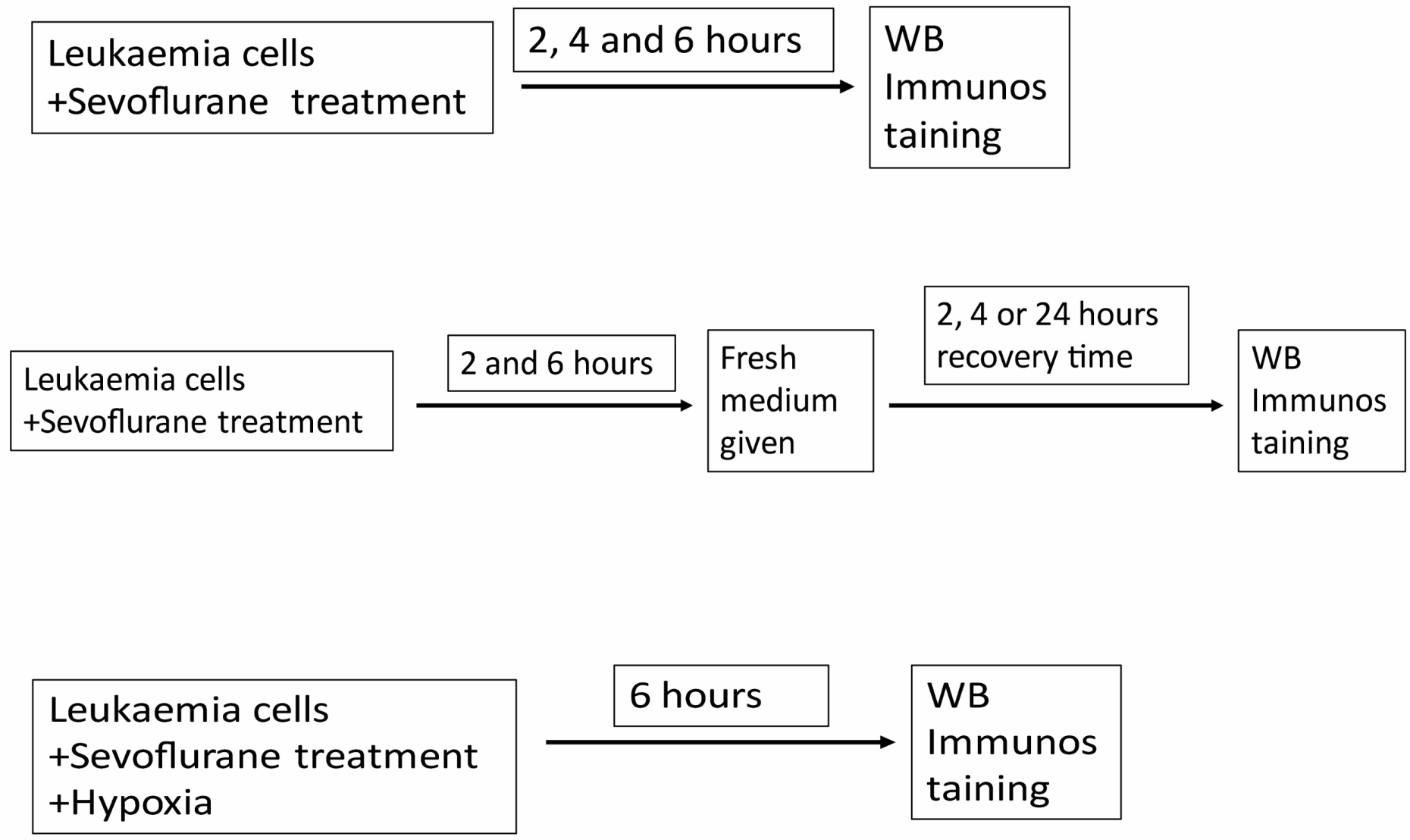

Figure 4.2 Experiment Design for sevoflurane experiment
WB: western blot

4.3 Results

4.3.1 Propofol reduces HIF-1α expression in a concentration-dependent manner, and its effect is relatively short-lived

As we can see from Figure 4.3, NALM-6 cells express high level of HIF-1α even under normoxia. This is possibly due to the mutations in tyrosine receptors or mutations in upstream pathways leading to enhanced transcription of HIF-1α[159]. Our data showed 6 hours of clinically relevant concentrations of propofol (1 to 10μg/ml) reduced the expression of HIF-1α in a concentration-dependent manner (Figure 4.3a). 10% intralipid (VC: vehicle control) did not affect the expression of HIF-1α (Figure 4.3a). To further demonstrate the inhibitory effect of propofol on HIF-1α expression, we treated cells with 6 hours of hypoxia (O_2 < 1%) and 10μg/ml of propofol. After hypoxia treatment, the HIF-1α level was elevated (Figure 4.3b) which was abolished by propofol (Figure 4.3b). Intralipid did not affect the expression of HIF-1α.

Then, we studied the longevity of propofol's effect on HIF-1α expression. NALM-6 cells were initially treated with 10μg/ml of propofol for 6 hours followed by 24 hours recovery time of incubation with fresh culture medium. Clearly, after 24 hours of recovery time, the reduction effect of propofol pre-treatment was diminished (Figure 4.3c).

Interestingly, HIF-1ß expression was not changed after propofol treatment (Figure 4.3e)(n=4). The inhibitory effect of HIF-1α by propofol was validated by using Reh cells (Figure 4.3d)(n=4). The image shown here in Figure 4.3 is a representative image selected from 4 images.

In order to confirm results obtained from Western blot, confocal microscopy images were taken on NLAM-6 cells treated with 6 hours hypoxia (O_2 < 1%) or hypoxia + 10μg/ml propofol for 6 hours (Figure 4.4)(n=3). The image shown here in Figure 4.4 is a representative image selected from 3 images. We observed some translocations of HIF-1α from cytoplasm to nucleus (indicated by white arrows), which was then successfully reversed by propofol treatment. Given the fact we only gave 6 hours of hypoxia, only a small amount of cells with HIF-1α translocation was expected[127].

4.3.2 HIF-1α is reduced by sevoflurane in a time-dependent manner and its effect is long-term

NALM-6 cells were treated with 3.6% of sevoflurane for 2, 4 and 6 hours. After treatment, cells were harvested for western blot and immunostaining analysis. Our data demonstrated HIF-1α was only reduced significantly after 6 hours of exposure (Figure 4.5a). 6 hours of hypoxia (O_2 < 1%) increased the expression of HIF-1α which was then reduced by 3.6% of sevoflurane (Figure 4.5b). In addition, the increased translocation of HIF-1α into the nucleus after 6 hours of hypoxia was abolished by sevoflurane (Figure 4.4)(n=3). The image shown here in Figure 4.4 is a representative image selected from 3 images. We also studied the longevity of sevoflurane's effect on HIF-1α expression (Figure 4.5c and d). NALM6 cells were initially treated by 2 hours of sevoflurane followed by 4 and 24 hours of recovery time (Figure 4.5c). HIF-1α expression was continuously reduced after 24 hours of recovery time. Then, we extended the initial exposure of sevoflurane to 6 hours followed by 24 hours of recovery time (Figure 4.5d). HIF-1α was significantly reduced after 6 hours of exposure and its expression was reduced further after 24 hours of recovery time. We confirmed the inhibitory effect of sevoflurane on HIF-1α by using Reh cells (Figure 4.5e) (n=4). Similar to propofol, HIF-1ß expression was not altered by exposure of sevoflurane (Figure 4.5f) (n=4). The image shown here in Figure 4.5 is a representative image selected from 4 images

4.3.3 Propofol reduced the phosphorylation of AKT and ERK

As we discussed earlier, cellular elevation of HIF-1α protein is achieved through hypoxic and non-hypoxic means. Previous literature suggested that general anaesthetics affected upstream pathways associated with transcription of *hif-1α* gene rather than affecting degradation pathways of HIF-1α[4, 120]. Therefore, we studied three upstream pathways of HIF-1α: PI3K-AKT, MAPK-ERK, and JAK-STAT3 pathways.

NALM-6 cells were treated with 1 to 10µg/ml of propofol for 6 hours then cells were harvested for western blot. Propofol reduced the phosphorylation of AKT $^{ser\ 473}$ and ERK 1/2 in a concentration-dependent manner (Figure 4.6a). However, STAT3 phosphorylation was not affected, suggesting STAT3 was not involved in the action of propofol. Then, we gave 24 hours of recovery time to NALM-6 cells which were initially treated by 10 µg/ml of propofol. The inhibitory effect of propofol on the phosphorylation of ERK and AKT was not observed after 24 hours of recovery time (Figure 4.6b). This phenomenon corresponded with the reduction of HIF-1α expression after propofol treatment. Finally, we showed 6 hours of hypoxia did not increase the phosphorylation of ERK and AKT, but propofol reduced their phosphorylation (Figure 4.7a).

4.3.4 Sevoflurane reduced the phosphorylation of ERK

NALM-6 cells were treated with 3.6% of sevoflurane for 2, 4 and 6 hours followed by western blot analysis. We found neither JAK-STAT3 nor PI3K-AKT pathways were affected by sevoflurane. However, 3.6% of sevoflurane greatly reduced phosphorylation of ERK (Figure 4.8a). Reduction in the phosphorylation of ERK was not seen after 2 hours of sevoflurane exposure. However, after 4 hours of exposure, a dramatic decrease in ERK phosphorylation was observed. Surprisingly, after 6 hours of exposure, nearly all phosphorylation of ERK was inhibited (Figure 4.8a).

We were encouraged by these results. Then, we studied phosphorylation of ERK after sevoflurane treatment with recovery time. Expectedly, after a short exposure of sevoflurane (2 hours), a strong inhibition of ERK phosphorylation was neither seen straight after exposure nor after 4 hours of recovery time, rather it was observed after 24 hours of recovery time (Figure 4.8b). When a longer exposure of sevoflurane was given initially (6 hours), a strong inhibition of ERK phosphorylation was recorded both at the end of exposure (6 hours) and after 24 hours of recovery time (Figure 4.8c).

6 hours of hypoxia did not significantly increase the phosphorylation of ERK, and sevoflurane reduced its phosphorylation under hypoxia (Figure 4.8d).

4.4 Discussion

Currently, there is no literature describing the effects of general anaesthetics on human leukaemia. We attempted to fill this knowledge gap with our study. In contrast to some of the current literature on other cancer cell types, we found inhalational general anaesthetic sevoflurane reduced HIF-1α instead of increasing it[4, 160, 161]. Our propofol data is in line with most current literature[4, 138]. The discrepancy between our data and data reported elsewhere may lie in the difference of cancer types. According to our data, leukaemia cells have a high expression of HIF-1α, even under normoxia. We suggest two reasons are associated with this phenomenon. Firstly, the elevated level of HIF-1α is intrinsic to leukaemia cells as hypoxia is an integral component of BM[129]. Secondly, HIF-1α protein synthesis is thought to be enhanced in ALL. Mutations of tyrosine kinase leading to HIF activation and mutations in HIF upstream pathways are identified in ALL. These mutations include enhanced activation of PI3K and JAK pathway and mutation of platelet-derived growth factor receptor beta (PDGFRB)[162] [163].

Apart from HIF-1α, we demonstrated HIF-1ß expression was not affected by general anaesthetics. This confirmed the work of others[4]. In future experiments, we propose to study whether general anaesthetics affect expression of HIF-2α. Two reports demonstrated the general anaesthetics affected the expression of HIF-2α in a solid cancer model[108] [128].

A few studies investigated the underlying mechanism by which HIF-1α was affected by general anaesthetics[4, 120, 161]. They confirmed general anaesthetics did not affect the degradation of HIF-1α but modulated HIF in a translational dependent pathway[4, 120, 161]. In our study, the level of *hif-1α* gene expression after general anaesthetics was not investigated. It will be explored in future experiments. In our study, propofol reduced the phosphorylation of ERK and AKT and sevoflurane only affected the ERK pathway. It could be speculated that the inhibitory effect of propofol and sevoflurane on the expression of HIF-1α is possibly mediated by ERK and AKT pathways, as they are both upstream pathways of HIF-1α[159]. Inhibitory studies with ERK and AKT inhibitors are needed to confirm those two pathways are, indeed, responsible for the inhibitory effect of general anaesthetics on HIF-1α expression[4].

We propose to validate our *in vitro* results under *in vivo* and clinical settings. The ALL leukaemia model is established via injection of NALM-6 cells to mouse IV and cells are allowed to multiply and propagate *in vivo*[164]. A few weeks after disease induction, general anaesthetic treatment protocol is given to the disease-bearing mouse. When the disease-bearing mouse is sacrificed, NALM-6 cells are sorted via flow sorter. HIF-1α expression of sorted NALM-6 cells is detected via western blot. This will confirm whether general anaesthetics reduce HIF-1α *in vivo*.

For the human study, we propose to treat clinical human B-ALL cells with general anaesthetics *in vitro*. Clinical human cancer cells have few advantages over immortalised cancer cell lines[165, 166]. Cancer cell lines are known to evolve in culture. The extent of the resultant genetic and transcriptional heterogeneity has been proved to be dramatically different from original cells. Ben-David et al demonstrated cells within the same cell line with different passage numbers are highly heterogeneous in terms of their genetics, transcriptomics and responses to therapeutics[166]. Thus, cell culture conditions and passage number of cell lines influence experimental outcomes. Experiments on clinical human B-ALL cells will provide excellent validation to our existing data.

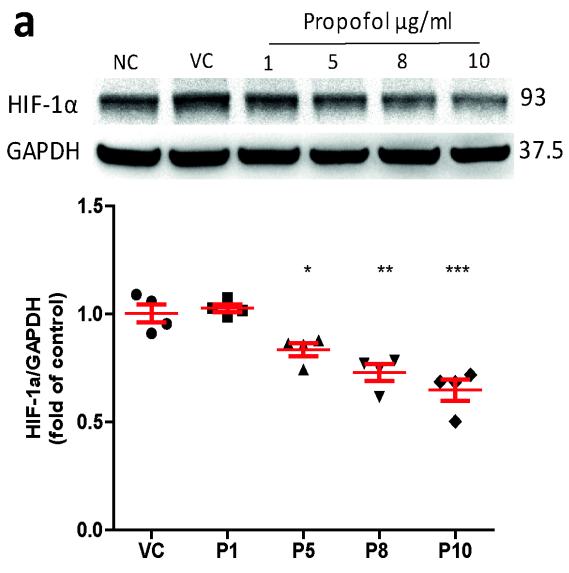
a
Propofol μg/ml
NC VC 1 5 8 10
HIF-1α
GAPDH
93
37.5
HIF-1a/GAPDH (fold of control)
1.5
1.0
0.5
0.0
*
**
***
VC P1 P5 P8 P10

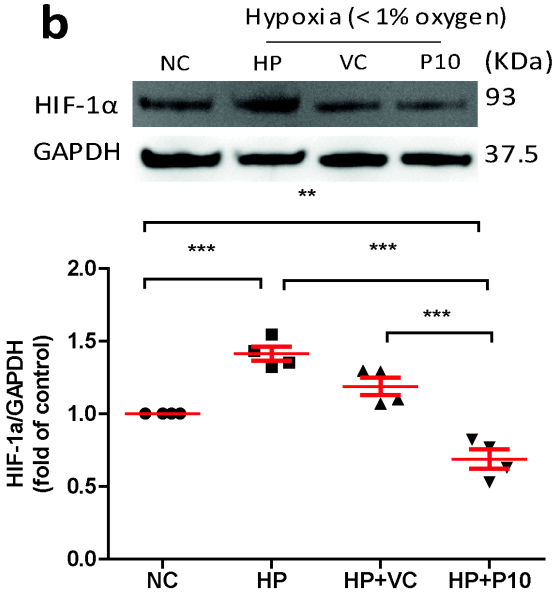
b
Hypoxia (< 1% oxygen)
NC HP VC P10 (KDa)
HIF-1α
GAPDH
93
37.5
**
***
***
***
HIF-1a/GAPDH (fold of control)
2.0
1.5
1.0
0.5
0.0
NC HP HP+VC HP+P10

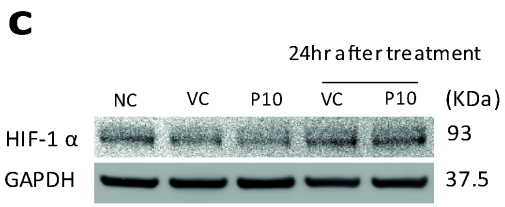
c
24hr after treatment
NC VC P10 VC P10 (KDa)
HIF-1 α
GAPDH
93
37.5

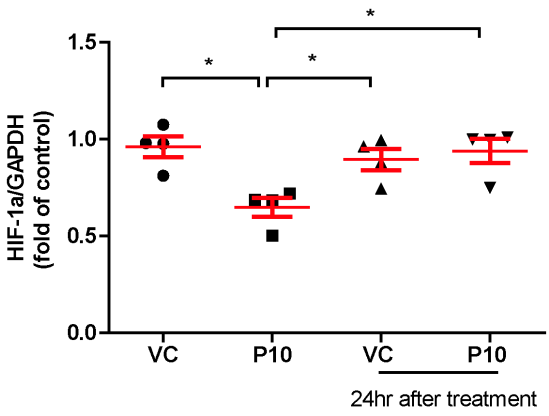
*
*
*
HIF-1a/GAPDH (fold of control)
1.5
1.0
0.5
0.0
VC P10 VC P10
24hr after treatment

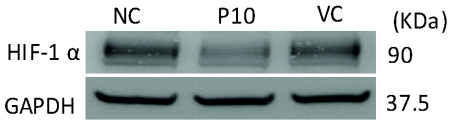
d
NC P10 VC (KDa)
HIF-1 α
GAPDH
90
37.5

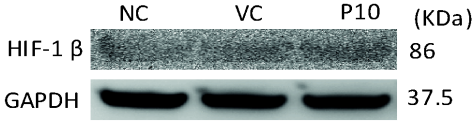
e
NC VC P10 (KDa)
HIF-1 β
GAPDH
86
37.5

Figure 4.3 Propofol reduces HIF-1α expression in NALM-6 cells
a) Western blot and densitometry of HIF-1α expression in NALM-6 cells following 6 hours treatment of intralipid (vehicle control) and propofol (1-10μg/ml). Data are illustrated as mean±s.e.m (n=4) *P<0.05, **P<0.01, ***P<0.001 vs vehicle control (VC). Data are analysed by one-way ANOVA followed by Bonferroni's post-hoc test. NC: Naïve control, VC: Vehicle control, P1-P10: 1-10μg/ml of propofol. **b)** 6 hours of 10μg/ml of propofol treatment clearly reduce the hypoxia-induced expression of HIF-1α in NALM-6 cells. Data are illustrated as mean±s.e.m (n=4). **P<0.01, ***P<0.001. Data are analysed by one-way ANOVA followed by Bonferroni's post-hoc test. NC: Naïve control, P10: 10μg/ml of propofol, HP: hypoxia, VC: vehicle control. **c)** The effect of propofol on HIF-1α expression is relatively short-lived. 10μg/ml of propofol was used to treat NALM-6 cells, then 24 hours recovery time was given. Data are illustrated as mean±s.e.m (n=4). *P<0.05. Data are analysed by one-way ANOVA followed by Bonferroni's post-hoc test. NC: naïve control, P10: 10μg/ml of propofol, VC: vehicle control. **d)** Reh cells were treated with propofol (1-10μg/ml) and intralipid (vehicle control) for 6 hours followed by western blot analysis. NC: naïve control, VC: vehicle control and P10: 10μg/ml. The image shown here is a representative image selected from 4 images (N=4). **e)** HIF-1ß expression is not affected by 6 hours treatment of propofol (10μg/ml) and intralipid (VC) in NALM-6 cells. NC: naïve control, VC: vehicle control and P10: 10μg/ml. The image shown here is a representative image selected from 4 images (N=4).

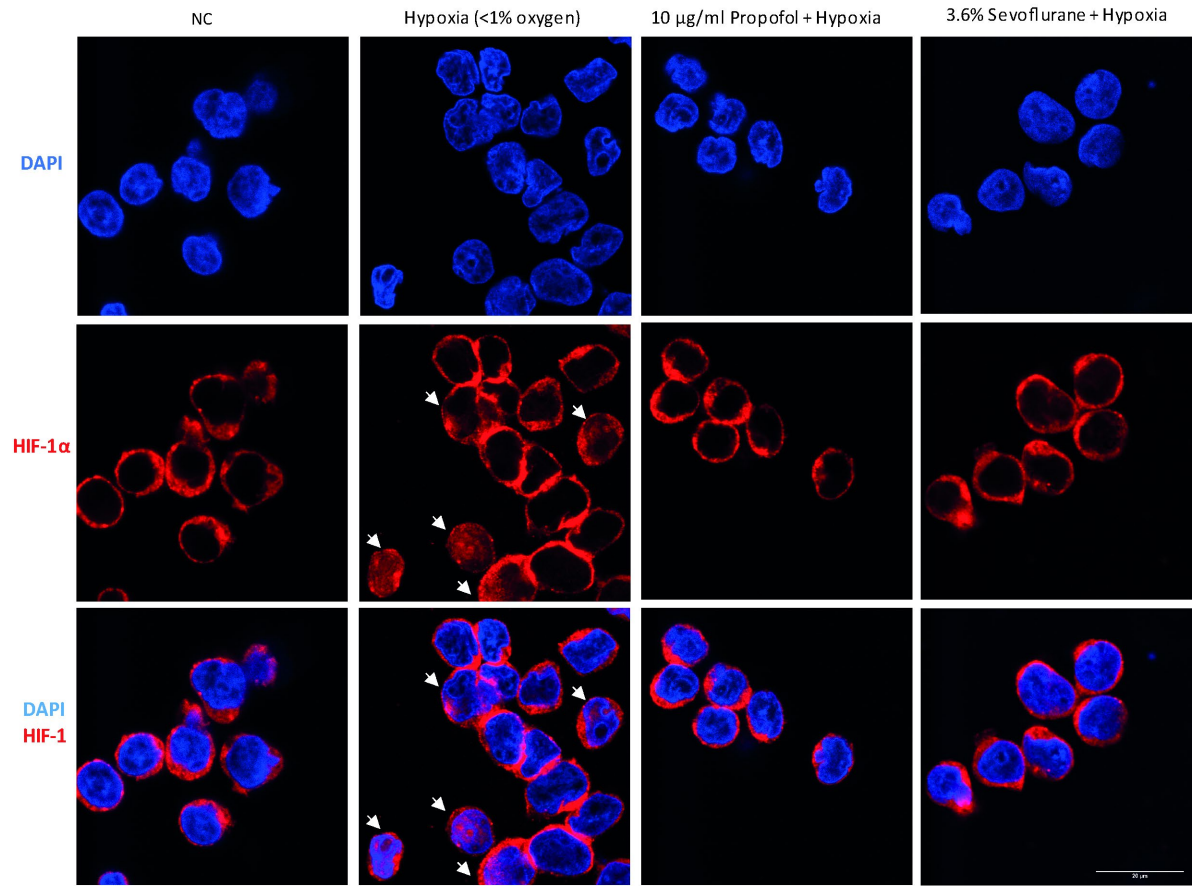

Figure 4.4 General anaesthetics reduce the translocation of HIF-1α into the nucleus
Confocal microscopy images show the translocation of HIF-1α after different treatments. After 6 hours of hypoxia, not all cells exhibit a significant translocation of HIF-1α. 5 cells are indicated with white arrows. Those cells show a significant translocation of HIF-1α (red) from the cytoplasm to the nucleus (blue). However, when propofol or sevoflurane is given to cells under hypoxia, the translocation of HIF-1α (red) from the cytoplasm to the nucleus (blue) could no longer be observed in any cells. Scale bar: 20 µm

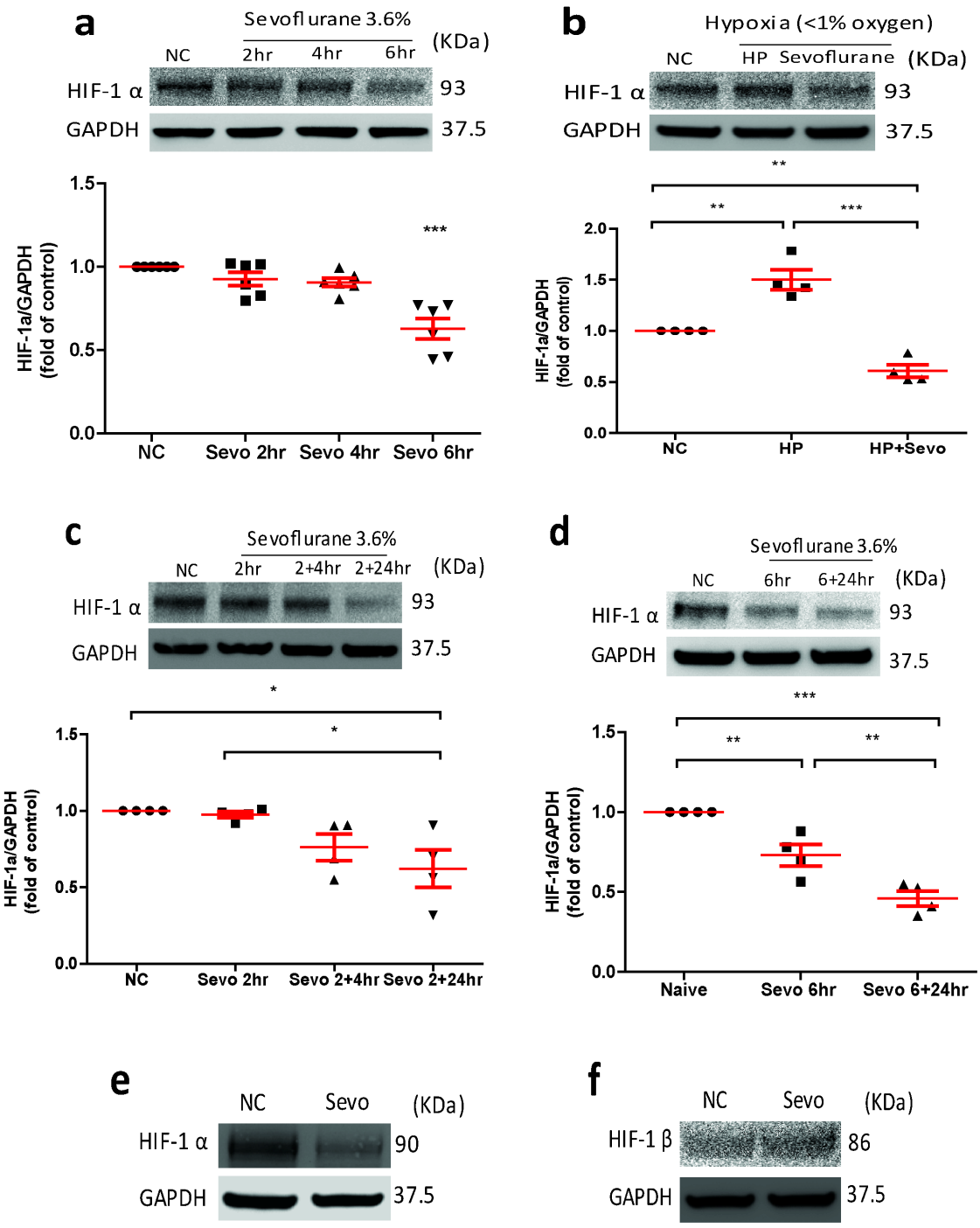
a
Sevoflurane 3.6%
NC
2hr
4hr
6hr
(KDa)
HIF-1 α
93
GAPDH
37.5
HIF-1a/GAPDH (fold of control)
1.5
1.0
0.5
0.0
***
NC
Sevo 2hr
Sevo 4hr
Sevo 6hr
b
Hypoxia (<1% oxygen)
NC
HP
Sevoflurane
(KDa)
HIF-1 α
93
GAPDH
37.5
**
**
***
HIF-1a/GAPDH (fold of control)
2.0
1.5
1.0
0.5
0.0
NC
HP
HP+Sevo
c
Sevoflurane 3.6%
NC
2hr
2+4hr
2+24hr
(KDa)
HIF-1 α
93
GAPDH
37.5
*
*
HIF-1a/GAPDH (fold of control)
1.5
1.0
0.5
0.0
NC
Sevo 2hr
Sevo 2+4hr
Sevo 2+24hr
d
Sevoflurane 3.6%
NC
6hr
6+24hr
(KDa)
HIF-1 α
93
GAPDH
37.5
***
**
**
HIF-1a/GAPDH (fold of control)
1.5
1.0
0.5
0.0
Naive
Sevo 6hr
Sevo 6+24hr
e
NC
Sevo
(KDa)
HIF-1 α
90
GAPDH
37.5
f
NC
Sevo
(KDa)
HIF-1 β
86
GAPDH
37.5

Figure 4.5 Sevoflurane reduces HIF-1α expression in NALM-6 cells

a) Sevoflurane reduces HIF-1α expression in a time dependent manner. NALM-6 cells were treated with 3.6 % of sevoflurane (MAC 2.0) for 2, 4 and 6 hours respectively. Data are illustrated as mean±s.e.m (n=6) ***P<0.001 vs Naïve control (NC). Data are analysed by one-way ANOVA followed by Bonferroni's post-hoc test. NC: Naïve control, Sevo 2hr: Sevoflurane 2 hours, Sevo 4hr: Sevoflurane 4 hours, Sevo 6hr: Sevoflurane 6 hours. **b)** 6 hours of sevoflurane significantly reduced HIF-1α expression induced by hypoxia (6 hours) in NALM-6 cells. Data are illustrated as mean±s.e.m (n=4). **P<0.01, ***P<0.001. Data are analysed by one-way ANOVA followed by Bonferroni's post-hoc test. NC: Naïve control, HP: Hypoxia, HP+Sevo: Hypoxia+sevoflurane (6 hours). **c)** NALM-6 cells were treated with 3.6% of sevoflurane for 2 hours followed by 4 and 24 hours recovery. Data are illustrated as mean±s.e.m (n=4). *P<0.05. Data are analysed by one-way ANOVA followed by Bonferroni's post-hoc test. NC: Naïve control, Sevo 2hr: Sevoflurane 2 hours, Sevo 2+4hr: Treatment of sevoflurane for 2 hours followed by 4 hours of recovery time, Sevo 2+24hr: Treatment of sevoflurane for 2 hours followed by 24 hours of recovery time. **d)** the effect of sevoflurane on HIF-1α in NALM-6 cells were relatively long term. Cells were initially treated with 3.6% of sevoflurane for 6 hours followed by 24 hours recovery. Data are illustrated as mean±s.e.m (n=4). **P<0.01, ***P<0.001. Data are analysed by one-way ANOVA followed by Bonferroni's post-hoc test. NC: Naïve control, Sevo 6hr: Sevoflurane 6 hours, Sevo 6+24hr: Treatment of sevoflurane for 6 hours followed by 24 hours of recovery time. **e)** Reh cells were treated with 3.6% of sevoflurane for 6 hours followed by western blot analysis. NC: Naïve control, Sevo: Sevoflurane treatment for 6 hours. The image shown here is a representative image selected from 4 images (N=4). **f)** HIF-1ß expression was not affected by 6 hours treatment of sevoflurane (3.6%) in NALM-6 cells. Naïve control (NC), Sevo: Sevoflurane treatment for 6 hours. The image shown here is a representative image selected from 4 images (N=4).

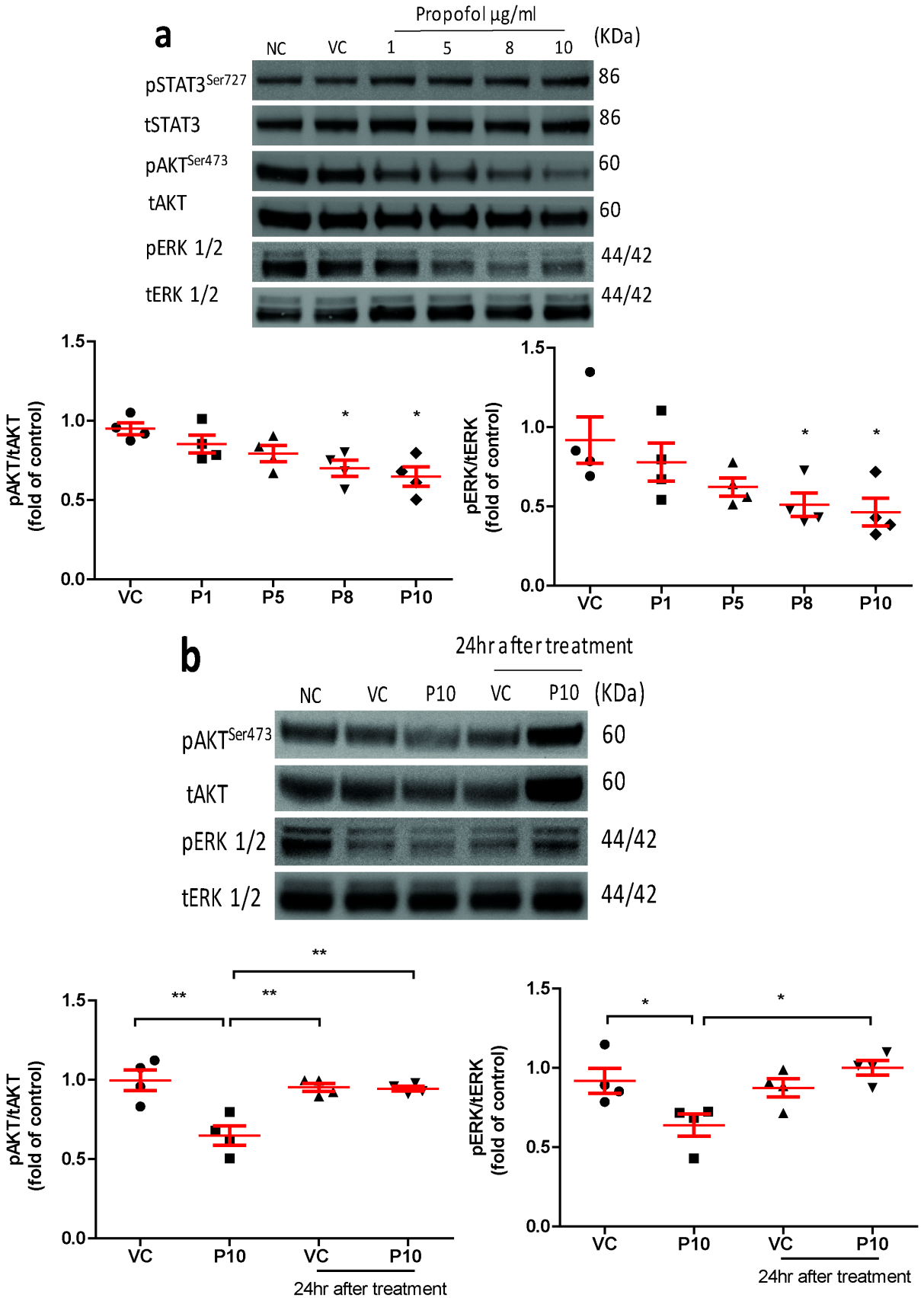
a
Propofol μg/ml
NC
VC
1
5
8
10
(KDa)
pSTAT3Ser727
tSTAT3
pAKTSer473
tAKT
pERK 1/2
tERK 1/2
86
86
60
60
44/42
44/42
pAKT/tAKT (fold of control)
pERK/tERK (fold of control)
1.5
1.0
0.5
0.0
VC
P1
P5
P8
P10
b
24hr after treatment
NC
VC
P10
VC
P10
(KDa)
pAKTSer473
tAKT
pERK 1/2
tERK 1/2
60
60
44/42
44/42
**
*
24hr after treatment

Figure 4.6 Propofol reduces the phosphorylation of AKT and ERK
a) Western blot analysis and densitometry of pSTATA, pAKT, pERK in NALM-6 cells. Cells were treated with 6 hours treatment of intralipid and propofol (1-10μg/ml). Then, cells were harvested for western blot analysis. Data are illustrated as mean±s.e.m (n=4). *P<0.05 vs Vehicle control (VC). Data are analysed by one-way ANOVA followed by Bonferroni's post-hoc test. NC: Naïve control, VC: Vehicle control, P1-P10: 1-10μg/ml of propofol. **b)** NALM-6 cells were treated with 10μg/ml of propofol followed by 24 hours of recovery time. Then, cells were harvested for western blot analysis. Data are shown as mean±s.e.m (n=4). *P<0.05, **P<0.01. Data are analysed by one-way ANOVA followed by Bonferroni's post-hoc test. NC: Naïve control, VC: Vehicle control, P1-P10: 1-10μg/ml of propofol.

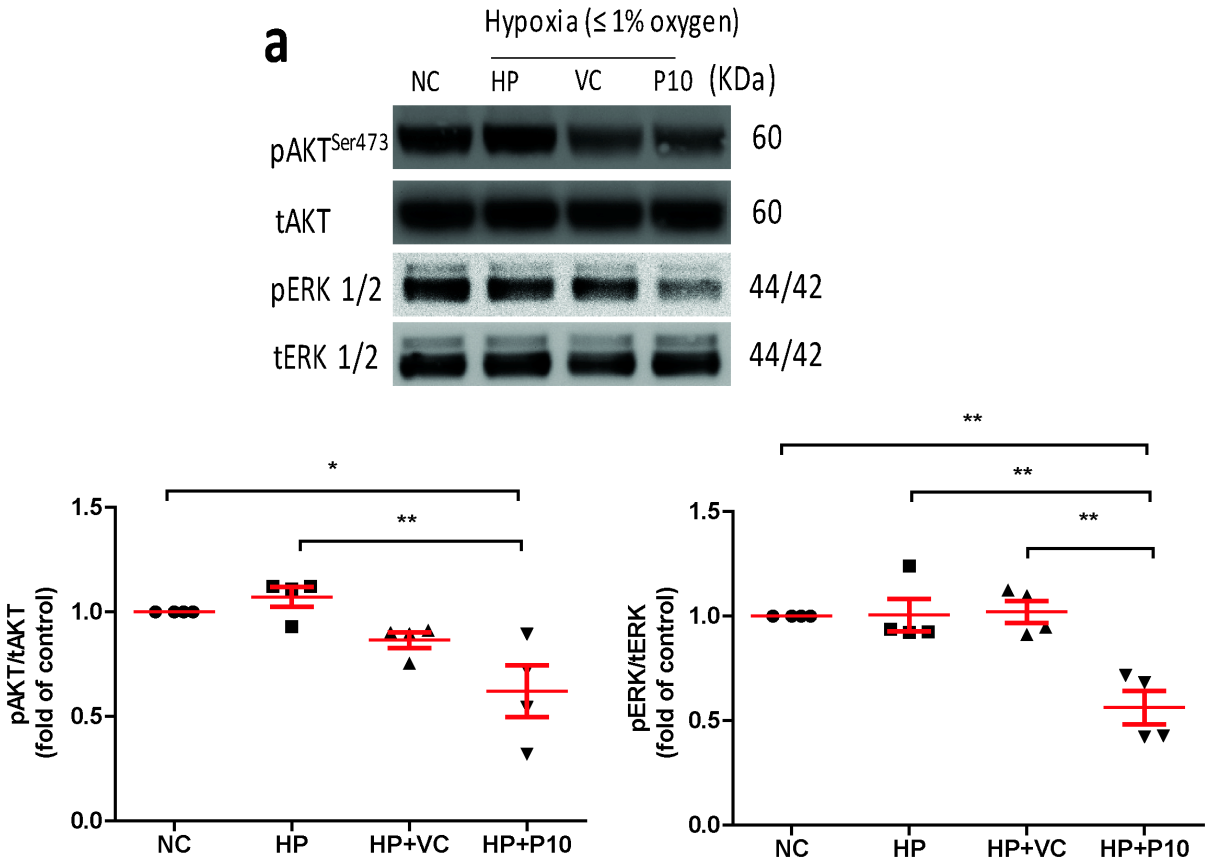

Figure 4.7 Propofol reduces the phosphorylation of AKT and ERK under hypoxia
a) NALM-6 cells were treated with 10μg/ml of propofol and hypoxia (<1% of oxygen) for 6 hours. Data are shown as mean±s.e.m (n=4). *P<0.05, **P<0.01. Data are analysed by one-way ANOVA followed by Bonferroni's post-hoc test. NC: Naïve control, VC: Vehicle control, HP: Hypoxia, HP+VC: Hypoxia+vehicle control(intralipid), HP+P10: Hypoxia+10μg/ml of propofol.

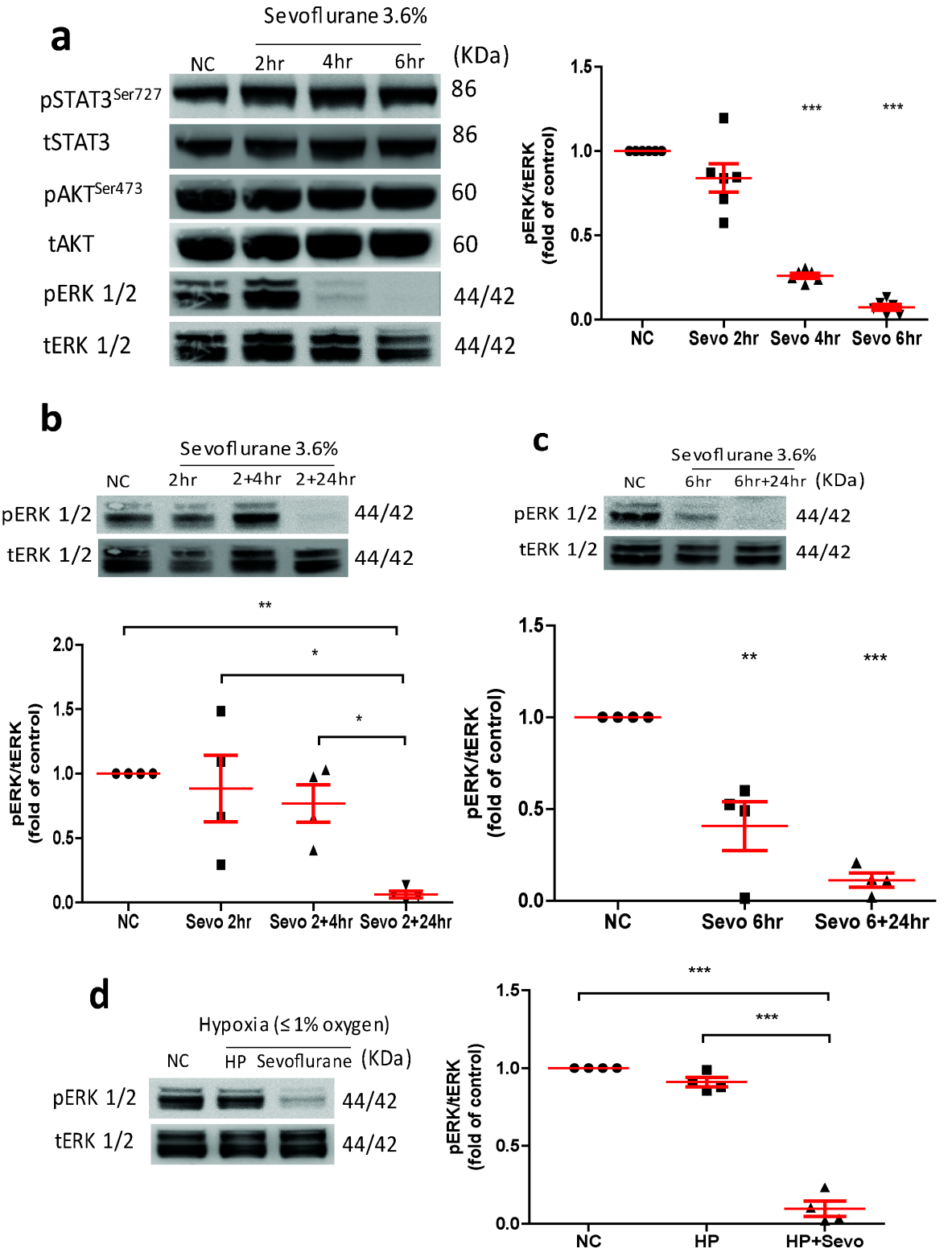
a
Sevoflurane 3.6%
NC
2hr
4hr
6hr
(KDa)
pSTAT3Ser727
86
tSTAT3
86
pAKTSer473
60
tAKT
60
pERK 1/2
44/42
tERK 1/2
44/42
pERK/tERK (fold of control)
1.5
1.0
0.5
0.0
***
***
NC
Sevo 2hr
Sevo 4hr
Sevo 6hr
b
Sevoflurane 3.6%
NC
2hr
2+4hr
2+24hr
pERK 1/2
44/42
tERK 1/2
44/42
**
*
*
2.0
1.5
1.0
0.5
0.0
pERK/tERK (fold of control)
NC
Sevo 2hr
Sevo 2+4hr
Sevo 2+24hr
c
Sevoflurane 3.6%
NC
6hr
6hr+24hr
(KDa)
pERK 1/2
44/42
tERK 1/2
44/42
1.5
1.0
0.5
0.0
**
***
pERK/tERK (fold of control)
NC
Sevo 6hr
Sevo 6+24hr
d
Hypoxia (≤1% oxygen)
NC
HP
Sevoflurane
(KDa)
pERK 1/2
44/42
tERK 1/2
44/42
***
***
1.5
1.0
0.5
0.0
pERK/tERK (fold of control)
NC
HP
HP+Sevo

Figure 4.8 Sevoflurane reduces the phosphorylation of ERK
a) Western blot analysis and densitometry of pAKT and pERK in NALM-6 cells. Cells were treated with 2, 4 and 6 hours of sevoflurane (3.6%). Data are shown as mean±s.e.m (n=4). ***P<0.001 vs Naïve control (NC). Data are analysed by one-way ANOVA followed by Bonferroni's post-hoc test. NC: Naïve control, Sevo 2hr: Sevoflurane 2 hours, Sevo 4hr: Sevoflurane 4 hours, Sevo 6hr: Sevoflurane 6 hours. **b)** NAML-6 ells were treated with 3.6% of sevoflurane for 2 hours, then 4 and 24 hours of recovery time were given. Data are shown as mean±s.e.m (n=4) *P<0.05, **P<0.01. Data are analysed by one-way ANOVA followed by Bonferroni's post-hoc test. NC: Naïve control, Sevo 2hr: Sevoflurane 2 hours, Sevo 2+4hr: Treatment of sevoflurane for 2 hours followed by 4 hours of recovery time, Sevo 2+24hr: Treatment of sevoflurane for 2 hours followed by 24 hours of recovery time. **c)** Cells were treated with 3.6% of sevoflurane for 6 hours, then 24 hours of recovery time was given. After treatment, cells were harvested for western blot analysis. Data are illustrated as mean±s.e.m (n=4). **P<0.01, ***P<0.001 vs Naïve control (NC). Data are analysed by one-way ANOVA followed by Bonferroni's post-hoc test. NC: Naïve control, Sevo 6hr: Sevoflurane 6 hours, Sevo 6+24hr: Treatment of sevoflurane for 6 hours followed by 24 hours of recovery time. **d)** NALM-6 cells treated with 3.6% of propofol and hypoxia (<1% of oxygen) for 6 hours. Data are illustrated as mean±s.e.m (n=4). ***P<0.001. Data are analysed by one-way ANOVA followed by Bonferroni's post-hoc test. NC: Naïve control, HP: Hypoxia, HP+Sevo: Hypoxia+sevoflurane (6 hours).

CHAPTER 5

General anaesthetics reduce leukaemia malignancy

5.1 Introduction

In the last chapter, we identified that HIF-1α protein synthesis was reduced by sevoflurane and propofol. It is important to understand whether any potential downstream effectors of HIF-1α are modulated by general anaesthetics.

5.2 Experiment Design

5.2.1 In vitro

HIF-1α is implicated in many physiological and pathological processes. In this study, we studied the viability, proliferation, CXCR4 expression and migration of NALM-6 cells after treatment of sevoflurane and propofol *in vitro.* In addition, HIF-1α siRNA and nonsense siRNA were also used to confirm the above-mentioned parameters were, indeed, downstream to HIF-1α. Migration data was replicated by using Reh cell lines *in vitro*. Figure 5.1 and Figure 5.2 illustrate the *in vitro* experiment design.

In our study, we used the ki-67 protein to study the proliferation of leukaemia cells. The ki-67 protein (or ki-67) is a cellular marker for proliferation, and it can be used in both western blot and immunohistochemistry. It is strictly associated with cell proliferation, and it is present during all active phases of the cell cycle (G_1, S, G_2 and mitosis). However, ki-67 is absent in resting cells (G_0)[167]. We stained ALL cells with the ki-67 antibody and it can be visualised under the microscope.

5.2.2 In vivo

After observing the potential effects of general anaesthetics on leukaemia cells *in vitro*, we developed a mouse model to validate *in vitro* data. We developed *in vivo* homing and migration assay with two photon intravital confocal microscopy.

NALM-6 cells were pre-treated with 10μg/ml of propofol and 3.6 % of sevoflurane for 12 hours (overnight). Then, cell number and viability were recorded using flow cytometry. We found after 12 hours of treatment, no cell death was seen by flow cytometry or by trypan blue exclusion assay. $1X10^6$ NALM-6 cells were injected into C57BL/6J mice IV followed by a small incision to expose mouse calvarium. Then, a calvarium window was fixed before injection of vessel dye IV. Finally, the imaging session was carried out to capture tile scans and time-lapse scans. They are two main reasons that calvarium was the chosen site for imaging. Firstly, mouse calvarium is the very thing which allows easy penetration of the laser beam. In addition, calvarium is superficial and could be easily exposed with small incisions. Long bones like femur and tibia are deep and surrounded by muscle and tissue. From the animal warfare point of view, small incisions on calvarium are less invasive with fewer complications. Figure 5.3 shows the sequential events before each imaging session.

Before we were able to establish GFP-NALM-6 cells, we used pre-stained cells for mice injections. NALM-6 cells were pre-stained with CD19-PE, CD-10-APC and/or Vybrant DiD cell labelling solution for 45 minutes. We found stained cells were inferior to GFP tagged cells in terms of resolution and signal to noise ratio. Therefore, experiments with stained cells were only used for counting the number of cells in the BM.

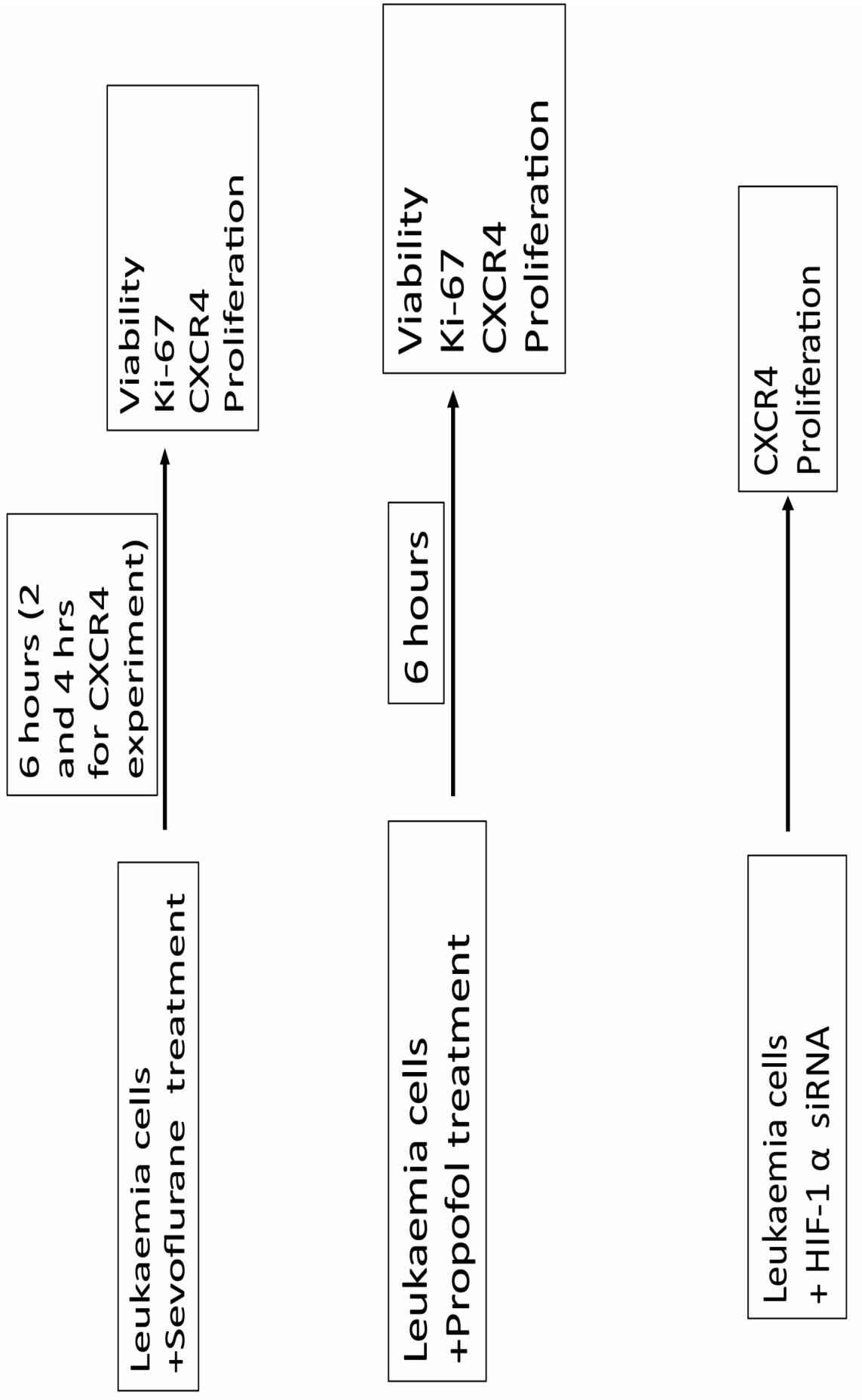

Figure 5.1 ***In vitro*** **experiment design**

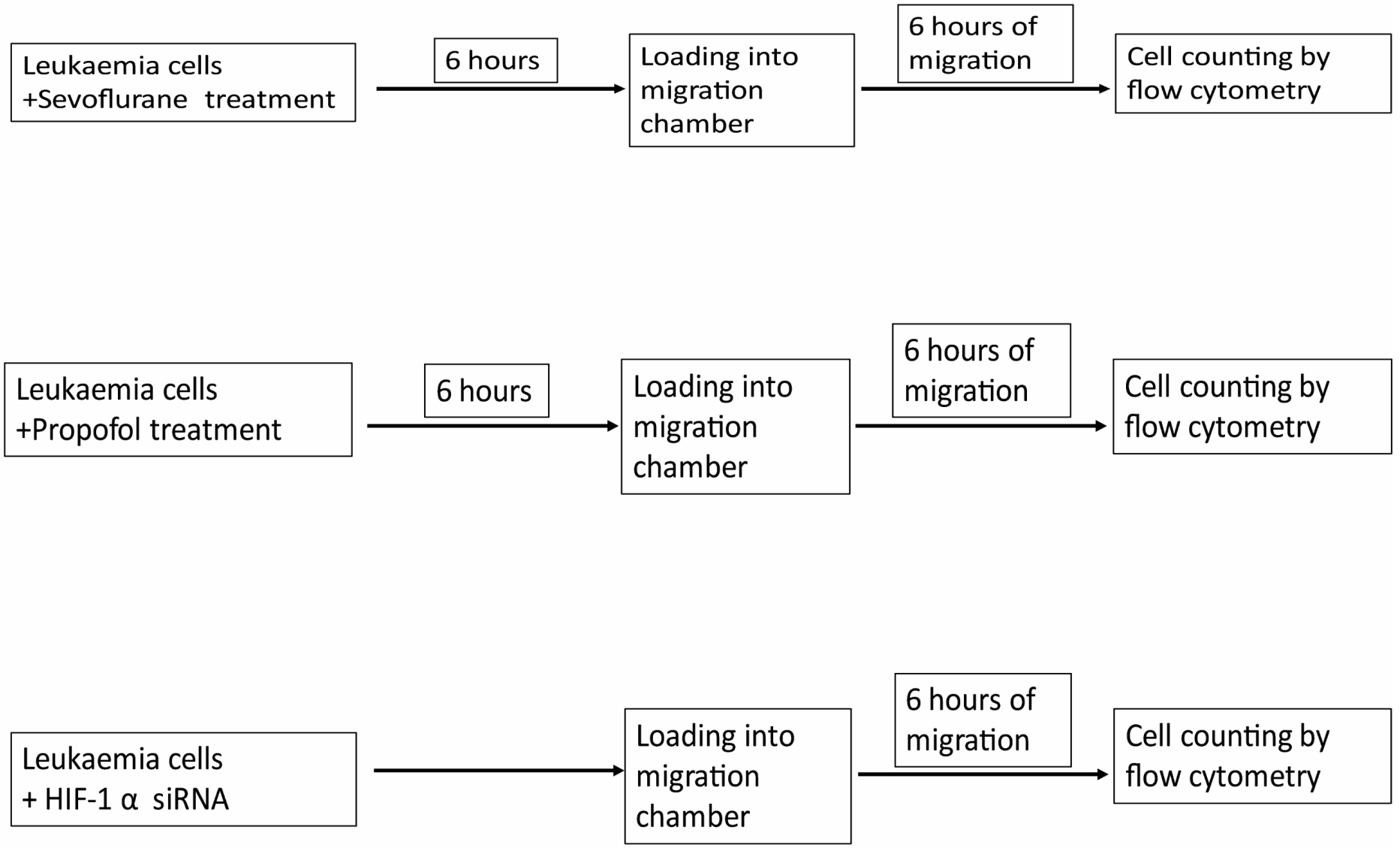

Figure 5.2 *In vitro* migration assay

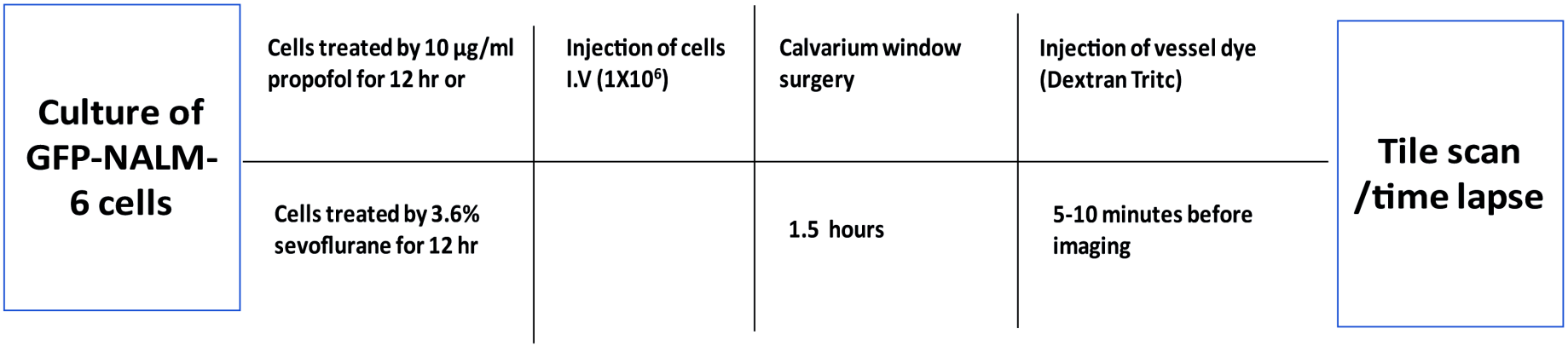

Figure 5.3 Sequential events before imaging session

5.3 Results

5.3.1 Propofol reduces the proliferation and the CXCR4 expression of NALM-6 cells

NALM-6 cells were treated with clinically relevant concentrations of propofol (5 and 10μg/ml) for 6 hours followed by cell viability, ki-67, cell cycle and CXCR4 expression analysis (Figure 5.4a, b and c).

Initially, we used the haemocytometer to study the viability of leukaemia cells after the treatment of propofol *in vitro*. NALM-6 cells were treated with 10μg/ml (56μM) for 6 hours. After propofol treatment, cells were stained with trypan blue. Then, a haemocytometer was filled with stained cells, and cells were counted under a microscope. Live cells have intact cell membranes that exclude trypan blue, whereas dead cells do not. Blue cells were considered as dead cells. Results showed that 6 hours of propofol treatment did not significantly affect the viability of NALM-6 cells *in vitro* (data not shown, n=6). Ki-67 analysis showed a reduction of Ki-67 positive cells after the treatment of 10μg/ml propofol for 6 hours (Figure 5.4a). In order to confirm this data, we used flow cytometry-based Vybrant DyeCycle stain to study cell proliferation in NALM-6 cells after propofol treatment. Our data confirmed 10μg/ml of propofol increased G0/G1 phases, introducing the cell cycle arrest in NALM-6 cells (Figure 5.4b).

In terms of surface CXCR4, its expression was significantly reduced by 5 and 10μg/ml propofol (Figure 5.4c). 6 hours of hypoxia treatment increased surface CXCR4 expression roughly by 20%. Propofol significantly reversed the elevated expression of CXCR4 induced by hypoxia (Figure 5.4d).

5.3.2 Sevoflurane reduces the proliferation and the CXCR4 expression of NALM-6 cells

Similar to propofol, results from the haematocytometer study showed that sevoflurane (3.6%, MAC 2.0) did not significantly affected the viability of NALM-6 cells *in vitro* (data not shown, n=6). 3.6 % of sevoflurane reduced the proliferation of NALM-6 cells after 6 hours of exposure. Treated NALM-6 cells had a smaller proportion of Ki-67 positive cells when compared to naïve control cells (Figure 5.5a). We confirmed the results by using flow cytometry-based Vybrant DyeCycle stain to study cell proliferation (Figure 5.5b). 6 hours of sevoflurane clearly increased the proportions of G1/G0 phase in NALM-6 cells, inducing the cell cycle arrest (Figure 5.5b). Then, NALM-6 cells were exposed to 2, 4 and 6 hours of sevoflurane. Sevoflurane treatment reduced the CXCR4 expression in a time-dependent manner (Figure 5.5c). Finally, sevoflurane remarkably reduced the elevated CXCR4 expressions induced by 6 hours hypoxia (Figure 5.5d).

5.3.3 General anaesthetics may reduce the migration and the proliferation of NALM-6 cells through HIF-1α mediated mechanisms

CXCR4 is responsible for migration of haematological cells include leukaemia cells.

After observing the inhibitory effect of propofol and sevoflurane on CXCR4 expression in NLAM-6 cells, we hypothesised that the general anaesthetics might reduce the migration of leukaemia cells. An *in vitro* migration chamber was set up consisting of treated NALM-6 cells on the upper chamber and stromal cell-derived factor 1 (SDF-1 also known as CXCL12) in the lower chamber. SDF-1 is the ligand for CXCR4, acting as a chemoattractant. NALM-6 cells were allowed to migrate for 6 hours. Our data demonstrated the significant difference in the number of cells that migrated from the upper to lower chamber. Both 5 and 10μg/ml of propofol and 3.6 % of sevoflurane significantly reduced migration of NALM-6 cells *in vitro*. The number of cells that migrated in 10μg/ml propofol treated group was reduced to 1/3 of cells when compared to control group (Figure 5.6a). Sevoflurane roughly reduced the cell migration by 50% when compared to control (Figure 5.6b).

As shown previously (Figure 4.3 and Figure 4.5), propofol and sevoflurane reduced the HIF-1α expression in ALL cells and they both reduced the proliferation of ALL cells. It was reasonable to hypothesise that proliferation was a downstream effector of HIF-1α. HIF-1α was temporarily knocked down with HIF-1α siRNA (the knock down was validated via western blot. data not shown, n=4), followed by cell cycle analysis using flow cytometry. A reduction in HIF-1α expression was positively associated with an increase of G1/G0 phase in NAML-6 cells (cell cycle arrest) and a subsequent decrease of cell proliferation was seen (Figure 5.6c).

We confirmed CXCR4 was a downstream effector of HIF-1α by using siRNA. After HIF knockdown, CXCR4 expression was reduced by 50% (Figure 5.6d). Migration of NALM-6 cells was reduced from around 4000 cells in control to 2000 cells after HIF-1α siRNA treatment (Figure 5.6e). It was surprising to find that propofol reduced the migration the most among (control: 6000 cells vs treated: 2000) all treatments including HIF knockdown, suggesting propofol may have additional mechanisms to influence migration.

We replicated the *in vitro* migration data by using Reh cell line. As expected, general anaesthetics greatly reduced migration of Reh cells (Figure 5.7a). Both general anaesthetics reduced the number of migrated cells by around 50% (around 3000 in control and 1500 in treated) (Figure 5.7a).

5.3.4 General anaesthetics reduce the migration of NALM-6 cells *in vivo*

We validated the *in vitro* migration data by an *in vivo* migration assay. A *in vivo* model of migration assay was set up by using multi-photon intravital microscopy. GFP- expressing NALM-6 cells were engineered by transducing NALM-6 cells with GFP packed lentivirus. 1 X 10^6 of pre-treated (sevoflurane or propofol) GFP-NALM-6 cells were injected into C57/BL6 mice IV followed by calvarium window placement and injection of vessel dye IV. Then, a time-lapse was taken by a specially made microscope. Each time-lapse lasted 66 minutes with one image taken every 3 minutes for a total of 22 images (Figure 5.8a, b and c). 22 images were, then, combined together to produce a time-lapse. Image J was used to analyse the track length and speed of each cell. After analysis, we found propofol and sevoflurane profoundly reduced the displacement of NLAM-6 cells *in vivo*. With anaesthetic treatment, all displacements of GFP-NALM-6 cells were below 50 µm (Figure 5.8d). Displacement here means the linear distance between the initial position of the cell and the last position of the cell. We believe this measurement can, to a large extent, represent the migratory ability of cells *in vivo*. The mean speed of GFP-cells was also calculated. We only measured the mean speed of cells in BM not the speed of cells in blood vessels. Propofol and sevoflurane significantly mitigated the migration speed of cells *in vivo* (Figure 5.8e). The speed of most cells was below 0.05µm/s after anaesthetic treatment (Figure 5.8e). In addition to the two measurements we used above, we found total track length to be important. It represents all distances a cell has travelled in the entire movie. For example, a cell might have travelled a great distance in the first 30 minutes but then returned to the original spot at the end of the movie. The displacement (a vector quantity) of the cell would be 0 µm but the total track (a scalar quantity) would be considerably larger. Displacement / total track (Figure 5.6f) gives a figure between 0 and 1. The figure close to 0 means the cell is travelling in a relatively round track and the number close to 1 means the cell is travelling in a more linear fashion. We observed propofol and sevoflurane did not affect how straight the cells travel *in vivo* (Figure 5.8f).

Examples of time-lapse movies are submitted (Appendix) to examiners in memory sticks.

5.3.5 General anaesthetics reduce the number of NALM-6 cells entering BM *in vivo* and increase the distance between leukaemia cells and endosteal surface *in vivo*

It is known that B-ALL cells migrate to unique anatomic regions in BM defined by specialised endothelium that expresses SDF-1 and adhesion molecule E-selectin[139]. This process is called homing and it is critical in leukaemia development and maintenance. It was shown that disruption of the CXCR4/SDF-1 axis severely inhibited the homing process[139] and resulted in poor engraftment of leukaemia cells in BM. We showed general anaesthetics modulated CXCR4 expression through HIF-1α (Figure 5.6). Therefore, we hypothesised general anaesthetics may disrupt the homing process of B-ALL cells *in vivo*. A mouse model similar to that of migration study was set up for imaging. 1X10^6 of GFP-NALM-6 cells (or NALM-6 cells stained with PE-CD19 and/or DiD dye) were injected IV. A calvarium window was fixed followed by injection of vessel dye. Figure 5.9 illustrates the location of the imaging window on calvarium and strategy of imaging (tile scan) (Figure 5.9a). Then, tile scan was used to count the number of cells entered BM space and calculate the distance between each cell and bone surface.

After careful analysis, we found there were fewer cells entered the BM space after general anaesthetic treatment, possibly due to the disruption of CXCR4/SDF-1 axis by general anaesthetics (Figure 5.9b). Experiments conducted with NALM-6 cells stained with PE-CD19 and/or DiD dye were included in the analysis. It is clear that after treatment of propofol and sevoflurane, fewer than 100 cells entered BM compared to 100-300 cells in BM space in naïve control group (Figure 5.9b).

We took the endosteal surface of the bone as a reference point for homing location rather than distance to nearby blood vessels. As the bone surface signal was acquired by a separate laser (Main Tai), it provided better structural integrity for images, and the captured images were less likely to be distorted. Our results showed that propofol and sevoflurane altered the distance between the endosteal surface of the bone and NALM-6 cells, hence changing the homing location of NALM-6 cells (Figure 5.9c). This potentially could result in poor engraftment and homing failure.

Examples of tile scan are submitted (Appendix) to examiners in memory sticks.

In addition, we analysed the data collected from tile scans and time lapses with a threshold approach. For displacement data, we set the median of naïve control cells as the threshold (Median=10.937μm) (Figure 5.10 a). Then, we counted the number of cells with a displacement larger than the median in all treatment groups. We found that general anaesthetics reduced the number of cells with a displacement larger than 10.937μm. We performed the same data analysis on migration data. The median of naïve control cells was determined initially (Median=0.013μm/s). We found that general anaesthetics reduced the number of cells with a mean speed larger than 0.013μm/s (Figure 5.10 b). Finally, the median distance of naïve control cells to the nearest endosteal surface was calculated

(Median=7.79µm). Expectedly, general anaesthetics increased the number of cells with a distance to the nearest endosteal surface larger than 7.79µm (Figure 5.10 c).

5.4 Discussion

In our *in vitro* data, we determined CXCR4 expression, proliferation and migration were reduced by propofol and sevoflurane via HIF-1α mediated mechanisms. And we also found cell viability was not affected by treatment with the general anaesthetics.

Our data on propofol reducing proliferation is consistent with many current literature[4, 168-170]. Propofol was shown to reduce proliferation and migration in breast cancer cells, prostate cancer cells, hepatocarcinoma cells and choriocarcinoma cells. An increase of HIF-1α was associated with both reduction and an increase in cell proliferation[171], and it seems that the cell type ultimately determines the role of HIF-1α in proliferation. In prostate cancer cells and neuroblastoma cells, HIF-1α was positively associated with cell proliferation[4, 172]. In both of those two cell lines, proliferation was reduced by propofol in HIF-1α mediated pathways. On the other hand, B lymphocytes demonstrated reduced proliferation under hypoxic conditions, but not when the same cell type from *hif-1α* deficient mice were exposed to hypoxia[173], suggesting HIF-1α was negatively correlated with proliferation in B lymphocytes.

Currently, the effects of sevoflurane on cell proliferation are not well understood, and it is highly dependent on the cell type. Sevoflurane was shown to promote proliferation in glioma stem cells[137] and canine mammary tumour cells[174]. However, sevoflurane was associated with suppression of proliferation in breast cancer cells[175]. Finally, sevoflurane did not show any effects on proliferation in human embryonic stem cells[176]. Our data demonstrated that clinically relevant concentrations of sevoflurane decreased proliferation of leukaemia cells in HIF-1α mediated pathways.

Although we did not study the intracellular mechanism by which HIF-1α regulated proliferation, we speculated it could be one of 3 mechanisms.

1): interaction between HIF-1α and Myc (a family of proto-oncogenes). HIF-1α overexpression leads to displacement of Myc from its DNA binding site, causing the depression of genes encoding p21 and p27. Both of them are important cell proliferation regulators[177].

2): The HIF-mediated transcriptional activation is linked to the Jumonji C domain-containing family of histone demethylases. They induce cellular senescence and can be influenced by HIF-1α activation[178, 179]. In particular, JMJD1A and JMJD2B are downstream targets of HIF-1α[178].

3): HIF-1α has a direct effect on the DNA replication machinery, as it has been shown that HIF-1α binds directly to multiple components of the MCM DNA helicase and the helicase loading factor Cdc6[180, 181]. This is associated with an increase in Cdc6 and MCM chromatin interaction and decreased recruitment of the activating kinase Cdc 7, leading to a decreased replication and a reduction in cell proliferation[181]. Additional studies should be granted to interpret which downstream pathways are associated with the inhibitory effect of propofol on proliferation.

The NALM-6 cell line is a suspension cell line. Immunostaining of ki-67 on the suspension cell is rather difficult. Unlike adherent cells, suspension cells require an additional biological agent (poly-L lysine) to anchor them to the petri dish. The strength of anchoring is relatively weak which makes cells vulnerable to washing steps. In addition, primary and secondary antibodies are likely be adhere to peri dishes, making artefacts far more frequent. This explains the inconstancy of image quality captured from ki-67 experiments.

CXCR4 is a well-known downstream target for HIF-1α in many cells include hematopoietic stem cells[182], osteosarcoma cells[183], and RCC cells[184]. In particular, a feed-forward loop between nuclear translocation of CXCR4 and HIF-1α was identified where CXCR4 was translocated into the nucleus and interacted with HIF-1α. Increased HIF-1α expression, in turn, promoted CXCR4 expressions in RCC cells *in vitro*[184]. Our data illustrated both propofol and sevoflurane dramatically reduced CXCR4 expression and mitigated migration of B-ALL cells presumably via HIF-1α pathway. Propofol was associated with the reduction of migration in human leukocytes[185], osteoblastoma cells[186], hepatocellular carcinoma cells[169], gastric cancer cells[187], pancreatic cancer cells[188] and endometrial cancer cells[189]. However, none of the above studies investigated the role of CXCR4 in migration.

Vast majority of studies reported sevoflurane increased migration. Sevoflurane was shown to promote migrations in glioblastoma cells[190], breast cancer cells[191], and ovarian cancer cells[122]. In particular, the ovarian cancer model demonstrated CXCR2 gene expression was enhanced by sevoflurane exposure[122]. The contrast between our data and current literature might lie in the difference of cell type. Migration of cancer cells are complex. Locally, they may rely on the morphology changes and acquire the migratory force by the fibronectin/integrin[192]. Migration of B-ALL cells almost solely relies on CXCR4[139]. The absence or low abundance of CXCR receptors on solid tumour cancer surface may grant them different responses to sevoflurane treatment.

It would be interesting to study the profile of proliferation and CXCR4 expression of the cells that migrated to the lower chamber after propofol and sevoflurane exposure. According to our data, it is entirely possible that the treatment of general anaesthetics only affects a proportion of leukaemia cells, leaving a small proportion of unaffected cells. These proliferative leukaemia cells may still process a high level of CXCR4 and migrate to the lower chamber. The non-proliferative or slowly proliferative cells with reduced expression of CXCR4 do not migrate to the lower chamber. In future experiments, we will collect migrated cells in the lower chamber after general anaesthetic treatment and co-stain them with CXCR4 and Ki-67 antibodies to study proliferation and CXCR4 expression.

Currently, there is no literature describing the effect of general anaesthetics on the migration of cancer cells *in vivo*. Part of the reason is due to the complexity and difficulty of tracking live cells *in vivo*. We deployed a novel imaging technique (intravital microscopy) to achieve our aims here.

Conventional *in vivo* migration assay usually require many complex steps including the sacrifice of animals, additional processing of samples, flow cytometry and immunohistochemistry analysis[193]. However, with intravital microscopy, animals are still alive during the imaging session, and no additional processing of the sample is needed. Therefore, the 'freshness' of the sample is preserved and we, as viewers, can directly observe the movement of cells in real-time.

Our study showed propofol and sevoflurane treated cells had a significant reduction in displacement and mean speed. As cells were pre-treated with propofol and sevoflurane, potentially, the reduction in both CXCR4 and HIF-1α expression were responsible for the decrease of displacement and mean speed. Cells treated with HIF-1α siRNA should be used in the future to confirm these results. It would be interesting to sort GFP-cells after calvarium experiments and pass them through the *in vitro* migration assay again for confirmation. In addition, we would like to determine whether relatively fast migrating cells in the treatment group might have higher proliferation than slow-moving cells in the treatment group *in vivo*.

In 2005, Sipkins et al. demonstrated NALM-6 cells home to unique anatomic regions in BM[139]. These locations are close to blood vessels, and they express a high level of SDF-1 and adhesion molecule E-selectin[139]. The homing process is exclusively mediated by the CXCR4/SDF-1 axis[139]. However, they did not define the location with statistical methods to show the distance between cells and close by reference points (i.e. blood vessel or endosteal surface of the bone). Our data indicated that those cells homed to a location reasonably close to the endosteal surface of the bone (below 100 μm). After treatment with propofol and sevoflurane, the distance was dramatically increased, suggesting the disruption of homing. We speculate that the interruption of the CXCR4/SDF-1 axis was the main reason for the phenomena. HIF-1α might have played a role, but additional confirmation is needed by using HIF-1α siRNA treated cells. Finally, we showed general anaesthetic pre-treatment reduced the number of cells entering BM space. Entering BM space from the bloodstream is the first stage of homing, circulating cells need to attach to structures in BM before engraftment[139]. However, the exact mechanism for attaching is still not known but likely candidates including CXCR4/SDF-1 and E-selectin. Here, we hypothesise that the reduction of CXCR4 from general anaesthetic treatment causes reduced attachment of leukaemia to BM structures and ultimately leads to a smaller number of cells entering the BM space.

There are some limitations to our study. Firstly, we used immune-competent C57BL/6 mice instead of SCID mice for our experiment due to animal license issue. The total length of each imaging session was below 2 hours. So, a strong immune rejection response was not expected. We are still interested in studying whether SCID mice could replicate our existing results, especially our homing assay results. Secondly, the current experiment protocol used cells pre-treated by propofol and sevoflurane *in situ*

prior to animal injections. This eliminates the complexity of bioavailability of medications if general anaesthetics were injected into mice directly. However, pre-treating cells makes the experimental protocol less clinically applicable. A more realistic approach should involve the use of SCID mice and treat them with general anaesthetics for some time after the injection of GFP-NALM-6 cells before imaging session. This approach is closer to the clinical application of general anaesthetics. Finally, we have only investigated the homing of leukaemia cells *in vivo* in a short time frame (a few hours). Although homing is a relatively quick process which takes place only minutes after injection, it is still necessary to understand locations of injected cells in a longer time frame (weeks). It is in those locations where leukaemia cells multiply, propagate and acquire secondary mutations for chemoresistance[194].

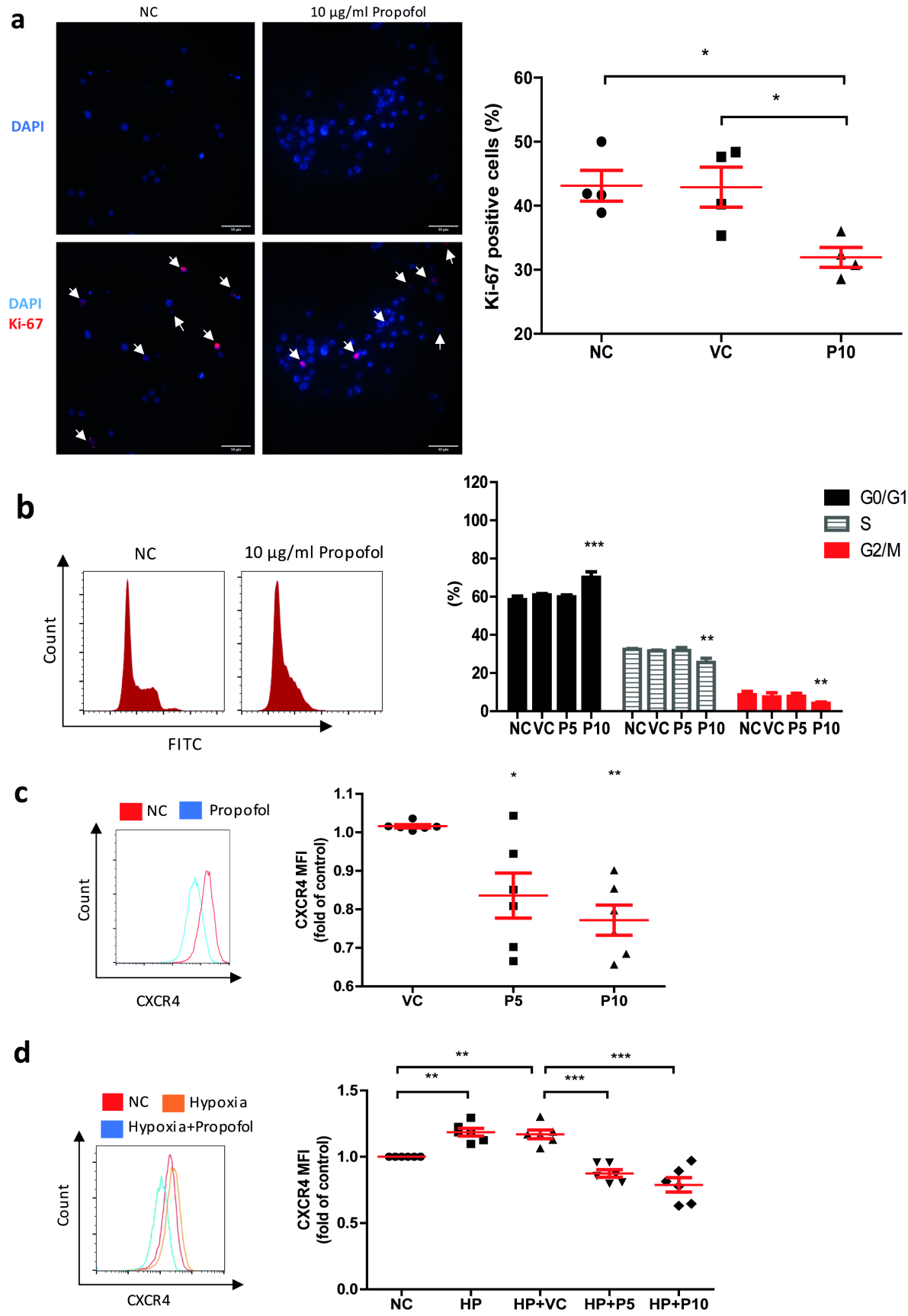
a
NC
10 μg/ml Propofol
DAPI
DAPI
Ki-67
Ki-67 positive cells (%)
NC
VC
P10
b
NC
10 μg/ml Propofol
Count
FITC
G0/G1
S
G2/M
(%)
NC VC P5 P10
NC VC P5 P10
NC VC P5 P10
c
NC
Propofol
Count
CXCR4
CXCR4 MFI (fold of control)
VC
P5
P10
d
NC
Hypoxia
Hypoxia+Propofol
Count
CXCR4
CXCR4 MFI (fold of control)
NC
HP
HP+VC
HP+P5
HP+P10

Figure 5.4 Propofol reduces the proliferation and the CXCR4 expression in NALM-6 cells
a) NALM-6 cells were treated with 10μg/ml of propofol for 6 hours. Then, treated cells were stained with ki-67 antibody. The number of Ki-67 positive cells (red) was divided by the number of all cells in the field of view. Blue: DAPI, red: Ki-67. Propofol reduced the number of ki-67 positive cells. scale bar: 20 μm. Data are shown as mean±s.e.m (n=4). *P<0.05. Data are analysed by one-way ANOVA followed by Bonferroni's post-hoc test. NC: Naïve control, VC: Vehicle control (intralipid), P10: 10μg/ml Propofol. **b)** NALM-6 cells were treated by 5 and 10 μg/ml of propofol and 10% intralipid (vehicle). Then, cells were stained with Vybrant DyeCycle green dye followed by acquiring data on a flow cytometer. FlowJo (a flow cytometry software) determines the percentage of cells in G1, S and G2/M phase. Data are illustrated as mean±s.e.m. (n=4). **P<0.01, ***P<0.001 vs Naïve control (NC). Data are analysed by two-way ANOVA followed by Bonferroni's post-hoc test. NC: Naïve control, VC: Vehicle control (intralipid), P5: 5μg/ml of Propofol, P10: 10μg/ml of Propofol. **c)** After studying the proliferation, we evaluated the effect of propofol on the CXCR4 expression. NALM-6 cells were treated with 5-10μg/ml of propofol and 10% intralipid (VC) for 6 hours. Then, treated cells were stained with the CXCR4 antibody followed by acquiring data on a flow cytometer. The mean fluorescent intensity (MFI) was calculated by FLowjo, and the MIF was compared between groups. After propofol treatment, the curve of propofol treated cells on the histogram shifted to the left-hand side (blue) when compared to the curve of naïve control cells (red). This means the MFI and the CXCR4 expression are reduced in propofol treated cells. Data are illustrated as mean±s.e.m (n=6). *P<0.05, **P<0.01, vs Vehicle control (VC). Data are analysed by one-way ANOVA followed by Bonferroni's post-hoc test. VC: Vehicle control, P5: 5μg/ml propofol, P10: 10μg/ml of propofol. **d)** NLALM-6 cells were treated by hypoxia, propofol (10μg/ml) and intralipid (VC) for 6 hours. Then, the CXCR4 expression was compared between groups by using the above-mentioned method. Data are illustrated as mean±s.e.m (n=6). **P<0.01, ***P<0.001. Data are analysed by one-way ANOVA followed by Bonferroni's post-hoc test. NC: Naïve control, HP: Hypoxia, HP+VC: Hypoxia+vehicle control, HP+P5: Hypoxia+5μg/ml of propofol, HP+P10: Hypoxia+10μg/ml of propofol.

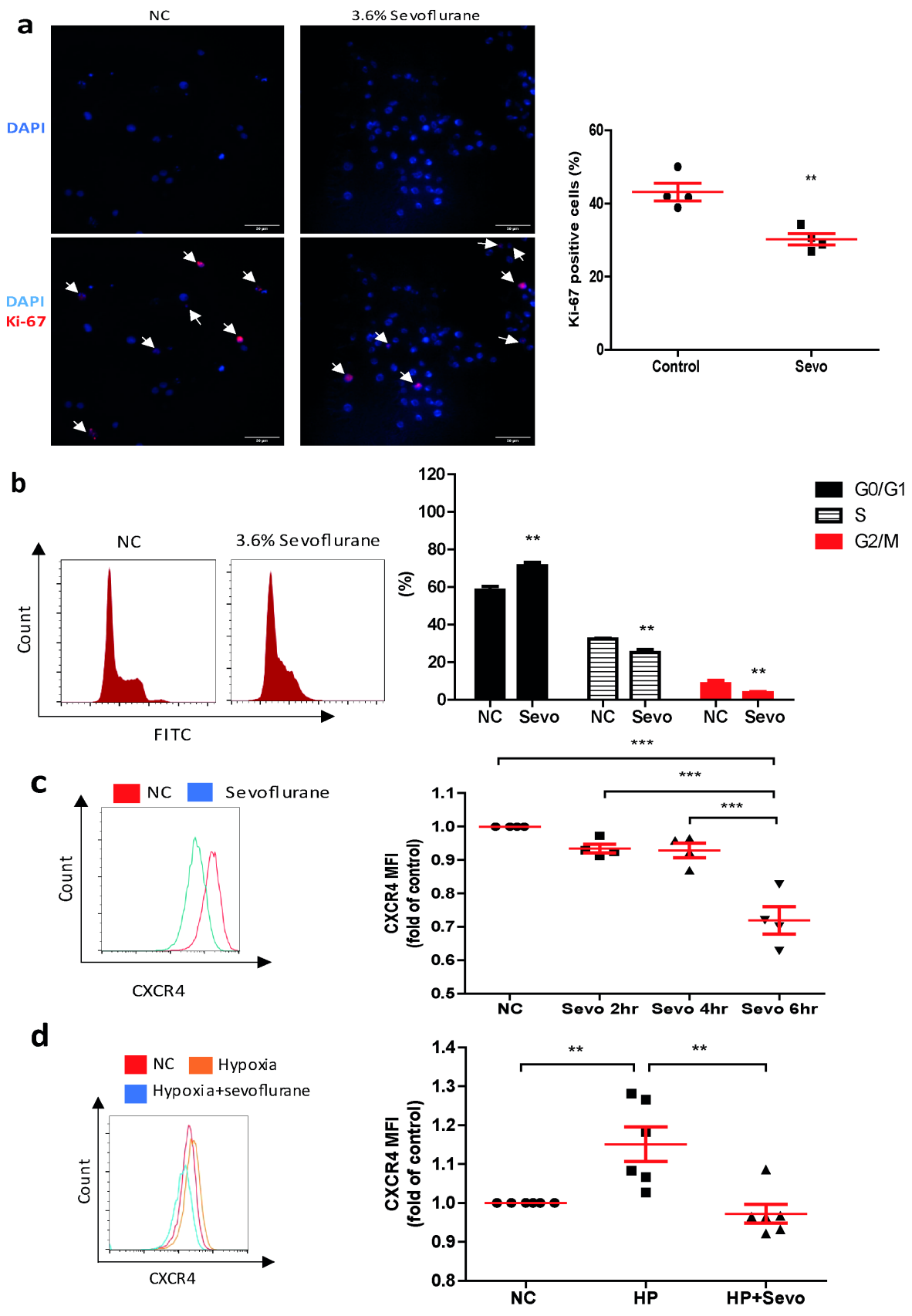
a
NC
3.6% Sevoflurane
DAPI
DAPI
Ki-67
Ki-67 positive cells (%)
60
40
20
0
**
Control
Sevo
b
NC
3.6% Sevoflurane
Count
FITC
120
100
80
60
40
20
0
(%)
**
**
**
NC
Sevo
NC
Sevo
NC
Sevo
G0/G1
S
G2/M
c
NC
Sevoflurane
Count
CXCR4
***
***
***
CXCR4 MFI (fold of control)
1.1
1.0
0.9
0.8
0.7
0.6
0.5
NC
Sevo 2hr
Sevo 4hr
Sevo 6hr
d
NC
Hypoxia
Hypoxia+sevoflurane
Count
CXCR4
**
**
CXCR4 MFI (fold of control)
1.4
1.3
1.2
1.1
1.0
0.9
0.8
NC
HP
HP+Sevo

Figure 5.5 Sevoflurane reduces the proliferation and the CXCR4 expression in NALM-6 cells
a) NALM-6 cells were treated with 3.6% of sevoflurane for 6 hours. Then, treated cells were stained with ki-67 antibody. The number of Ki-67 positive cells (red) was divided by the number of all cells in the field of view. Blue: DAPI, red: Ki-67. Sevoflurane reduced the number of ki-67 positive cells. scale bar: 20 μm. Data are illustrated as mean±s.e.m (n=4). **P<0.01, vs control. Data are analysed by unpaired T-test. Sevo: Sevoflurane 6 hours. **b)** NALM-6 cells were treated by 3.6% sevoflurane for 6hours. Then, cells were stained with Vybrant DyeCycle green dye followed by acquiring data on a flow cytometer. FlowJo (a flow cytometry software) determines the percentage of cells in G1, S and G2/M phase. Data are illustrated as mean±s.e.m. (n=4). **P<0.01 vs Naïve control (NC). Data are analysed by two-way ANOVA followed by Bonferroni's post-hoc test. NC: Naïve control, Sevo: Sevoflurane 6hours. **c)** After studying the proliferation, we evaluated the effect of sevoflurane on the CXCR4 expression of NALM-6 cells. NALM-6 cells were treated with 3.6% of sevoflurane for 2, 4 and 6 hours. Then, treated cells were stained with the CXCR4 antibody followed by acquiring data on a flow cytometer. The mean fluorescent intensity (MFI) was calculated, and the MIF was compared between groups. After sevoflurane treatment, the curve of sevoflurane treated cells on the histogram shifted to the left-hand side (blue) when compared to the curve of naïve control cells (red). This means the MFI and the CXCR4 expression are reduced in sevoflurane treated cells. Data are illustrated as mean±s.e.m (n=4). ***P<0.001. Data are analysed by one-way ANOVA followed by Bonferroni's post-hoc test. NC: Naïve control, Sevo 2hr: Sevoflurane 2 hours, Sevo 4hr: Sevoflurane 4 hours, Sevo 6hr: Sevoflurane 6hours. **d)** NLALM-6 cells were treated by hypoxia and sevoflurane for 6 hours. Then, the CXCR4 expression was compared between groups by the above-mentioned method. Data are shown as mean±s.e.m (n=6) **P<0.01. Data are analysed by one-way ANOVA followed by Bonferroni's post-hoc test. NC: Naïve control, HP: Hypoxia, HP+Sevo: Hypoxia+Sevoflurane.

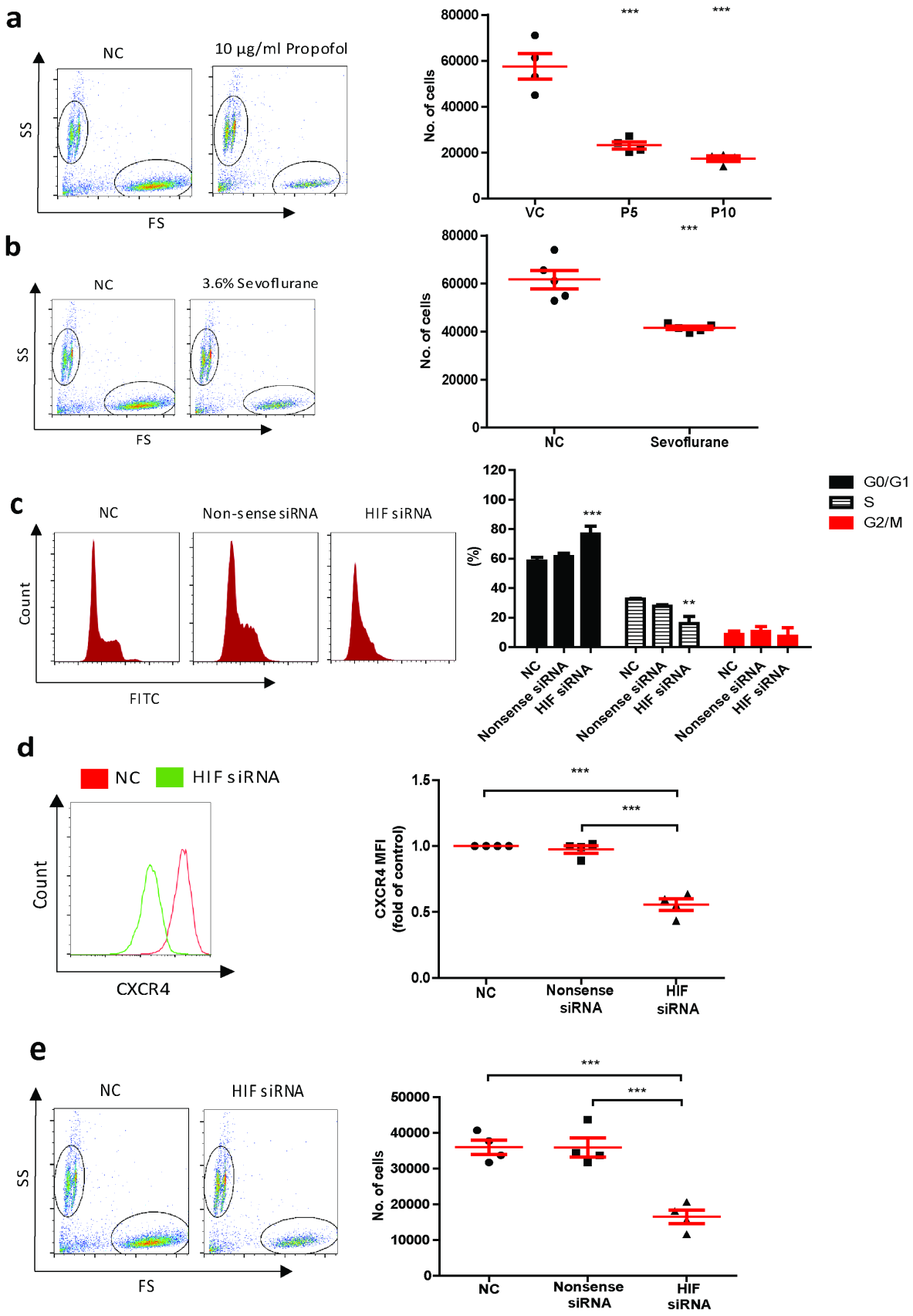
a
NC
10 μg/ml Propofol
SS
FS
No. of cells
VC
P5
P10
b
NC
3.6% Sevoflurane
SS
FS
No. of cells
NC
Sevoflurane
c
NC
Non-sense siRNA
HIF siRNA
Count
FITC
(%)
G0/G1
S
G2/M
NC
Nonsense siRNA
HIF siRNA
d
NC
HIF siRNA
Count
CXCR4
CXCR4 MFI (fold of control)
e
NC
HIF siRNA
SS
FS
No. of cells

Figure 5.6 Migration and proliferation are downstream targets of HIF-1α
a) NALM-6 cells were initially treated with intralipid and 10μg/ml propofol for 6 hours. Then, NALM-6 cells were allowed to pass through chambers for 6 hours. Cells in lower chamber were collected and counted by a flow cytometer. Data are shown as mean±s.e.m (n=4). ***P<0.01 vs Vehicle control (VC). Data are analysed by one-way ANOVA followed by Bonferroni's post-hoc test. VC: Vehicle control, P5: 5μg/ml propofol and P10: 10μg/ml propofol. **b)** NALM-6 cells were treated with sevoflurane for 6 hours. Then, NALM-6 cells were allowed to pass through chambers for 6 hours. Cells in lower chamber were collected and counted in a flow cytometer. Data are illustrated as mean±s.e.m (n=6). ***P<0.01 vs Naïve control (NC). Data are analysed by unpaired T-test. NC: Naïve control, Sevo: Sevoflurane 6 hours. **c)** NALM-6 cells were treated with HIF-1α siRNA or nonsense siRNA. Then, cells were stained with Vybrant DyeCycle green dye followed by acquiring data on a flow cytometer. FlowJo (a flow cytometry software) determines the percentage of cells in G1, S and G2/M phase. Data are illustrated as mean±s.e.m. (n=4). **P<0.01, ***P<0.001 vs Naïve control (NC). Data are analysed by two-way ANOVA followed by Bonferroni's post-hoc test. NC: Naïve control. **d)** NALM-6 cells were treated with HIF-1 α siRNA or nonsense siRNA. Then, treated cells were stained with the CXCR4 antibody followed by acquiring data on a flow cytometer. The mean fluorescent intensity (MFI) was calculated, and the MIF was compared between groups. After HIF siRNA treatment, the curve of HIF siRNA treated cells on the histogram shifted to the left-hand side (green) when compared to the curve of naïve control cells (red). This means the MFI and the CXCR4 expression are reduced in HIF siRNA treated cells. Data are illustrated as mean±s.e.m (n=4). ***P<0.001. Data are analysed by one-way ANOVA followed by Bonferroni's post-hoc test. NC: Naïve control. **e)** NALM-6 cells were treated with HIF-1α siRNA or nonsense siRNA, after which cells were allowed to pass through chamber for 6 hours. Cells in lower chamber were collected and counted by a flow cytometer. Data are shown as mean±s.e.m (n=4) ***P<0.01 vs Naïve control. Data are analysed by one-way ANOVA followed by Bonferroni's post-hoc test. NC: Naïve control.

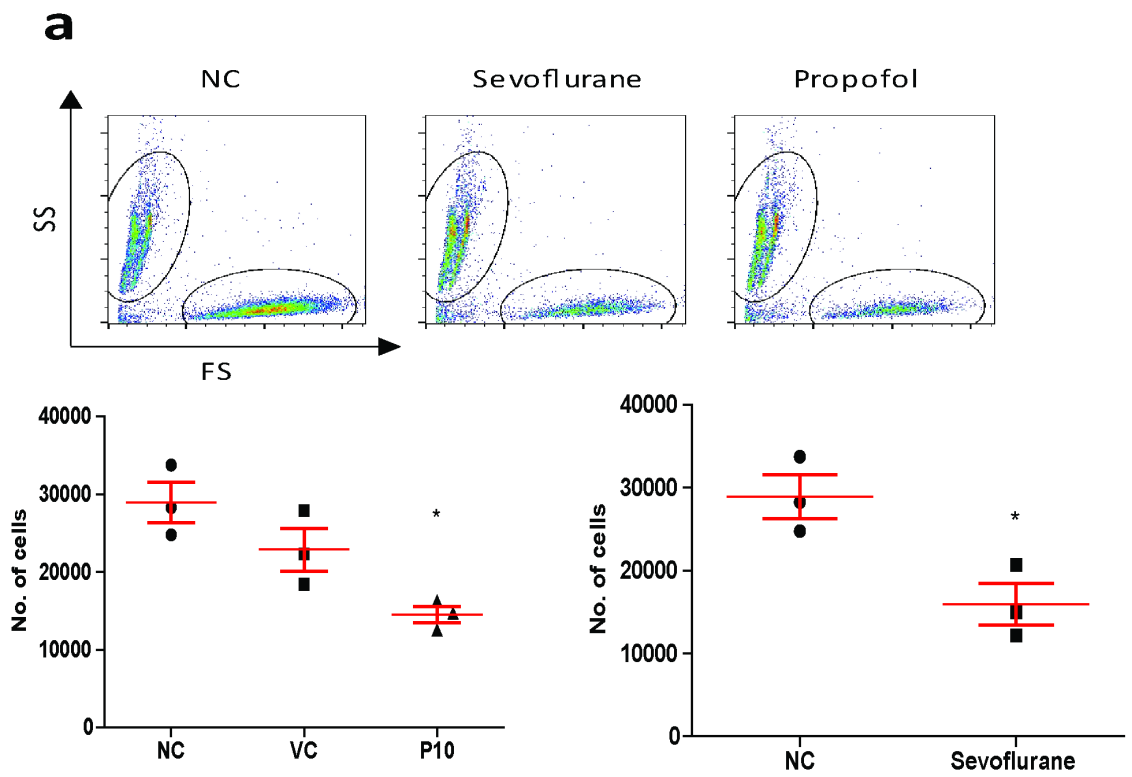

Figure 5.7 General anaesthetics reduce migration of Reh cells

a) Reh cells were initially treated with intralipid and 10µg/ml propofol for 6 hours. In addition, Reh cells were treated with 3.6% of sevoflurane for 6 hours. Then, Reh cells were allowed to pass through chambers for 6 hours. Cells in the lower chamber were collected and counted by a flow cytometer. Data are illustrated as mean±s.e.m (n=3). *P<0.05 vs Naïve control (NC). For propofol experiment, data are analysed by one-way ANOVA followed by Bonferroni's post-hoc test. For sevoflurane experiment, data are analysed by unpaired T-test. NC: Naïve control, VC: Vehicle control, P10: 10µg/ml propofol.

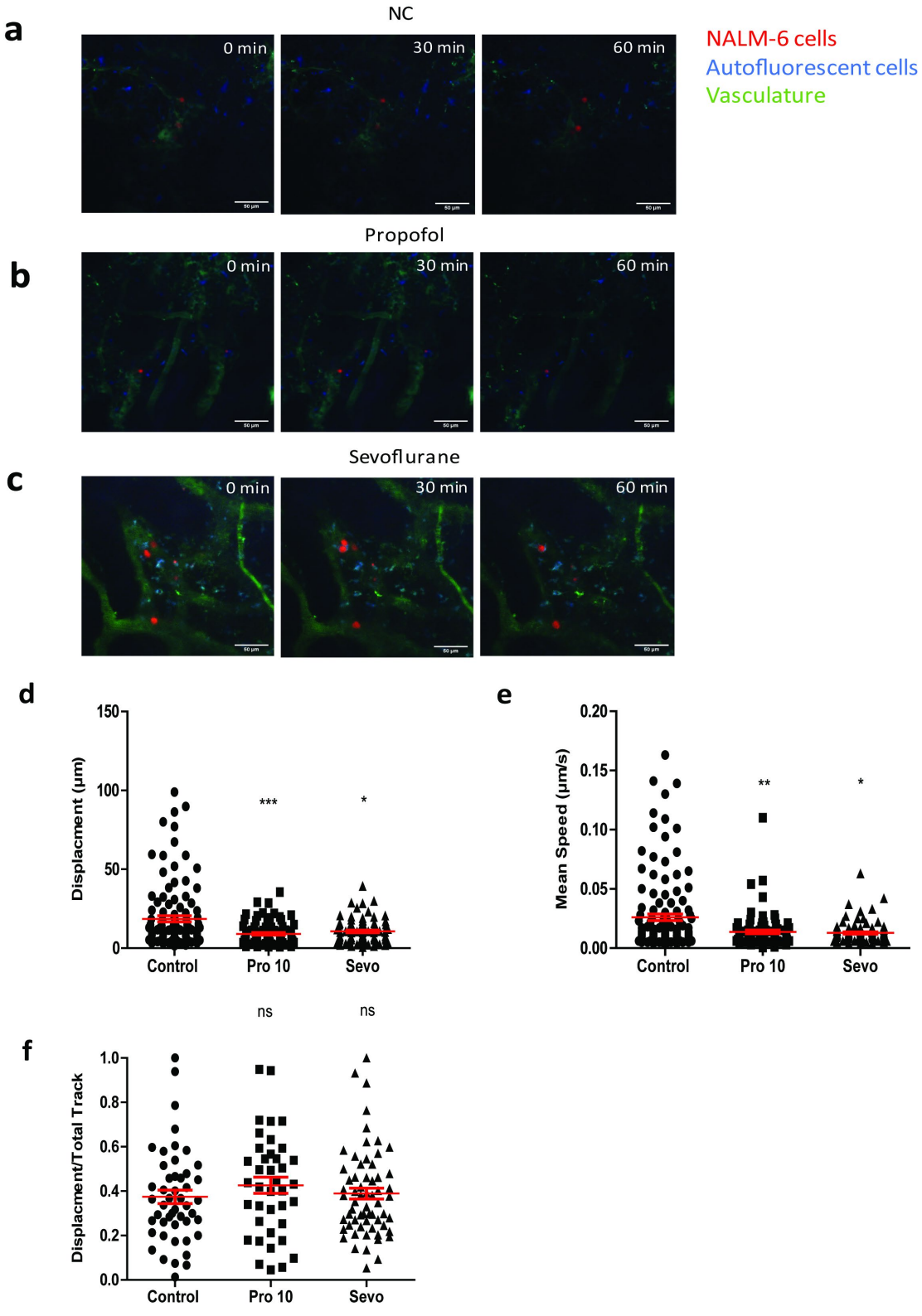
a
NC
0 min
30 min
60 min
NALM-6 cells
Autofluorescent cells
Vasculature
b
Propofol
0 min
30 min
60 min
c
Sevoflurane
0 min
30 min
60 min
d
Displacment (µm)
150
100
50
0
***
*
Control
Pro 10
Sevo
e
Mean Speed (µm/s)
0.20
0.15
0.10
0.05
0.00
**
*
Control
Pro 10
Sevo
f
Displacment/Total Track
1.0
0.8
0.6
0.4
0.2
0.0
ns
ns
Control
Pro 10
Sevo

Figure 5.8 General anaesthetics reduce migration of NALM-6 cells *in vivo*
a)-c) positions imaged at 3 min intervals for 66 minutes, bar: 50 μm. Red: NALM-6 cells, Blue: Autofluorescent cells, Green: Vasculature. We only investigated cells in the bone marrow. Cells in blood vessels were excluded. **a)** Naïve control cells were injected IV. NC: naïve control **b)** NALM-6 cells were pre-treated with 10μg/ml of propofol overnight before injection. **c)** NALM-6 cells were pre-treated with 3.6% (MAC 2.0) overnight before injection. **d)** The displacement of cells in bone marrow was measured. Data are pooled from 4 naïve control mice (N=4, 113 cells), 4 mice injected with propofol treated cells (n=4, 86 cells) and 4 mice injected with sevoflurane treated cells (n=4, 88 cells). Data are illustrated as mean±s.e.m. *P<0.05, ***P<0.001 vs Control. Data are analysed by one-way non-parametric ANOVA test (Kruskal-Wallis test). Pro 10: 10μg/ml of propofol, Sevo: 3.6% of sevoflurane. **e)** The mean speed of cells in bone marrow was measured. Data are pooled from 4 naïve control mice (N=4, 264 cells), 4 mice injected with propofol treated cells (n=4, 219 cells) and 4 mice injected with sevoflurane treated cells (n=4, 221 cells). Data are illustrated as mean±s.e.m. *P<0.05, **P<0.01 vs Control. Data are analysed by one-way non-parametric ANOVA test (Kruskal-Wallis test). Pro 10: 10μg/ml of propofol, Sevo: 3.6% of sevoflurane. **f)** The displacement /total track of cells in bone marrow was measured. Data are pooled from 4 naïve control mice (N=4, 113 cells), 4 mice injected with propofol treated cells (n=4, 86 cells) and 4 mice injected with sevoflurane treated cells (n=4, 88 cells). Data are illustrated as mean±s.e.m. ns: no significance. Data are analysed by one-way non-parametric ANOVA test (Kruskal-Wallis test). Pro 10: Cells were pre-treated with 10μg/ml of propofol overnight before injections, Sevo: Cells were pre-treated with 3.6% of sevoflurane overnight before injections.

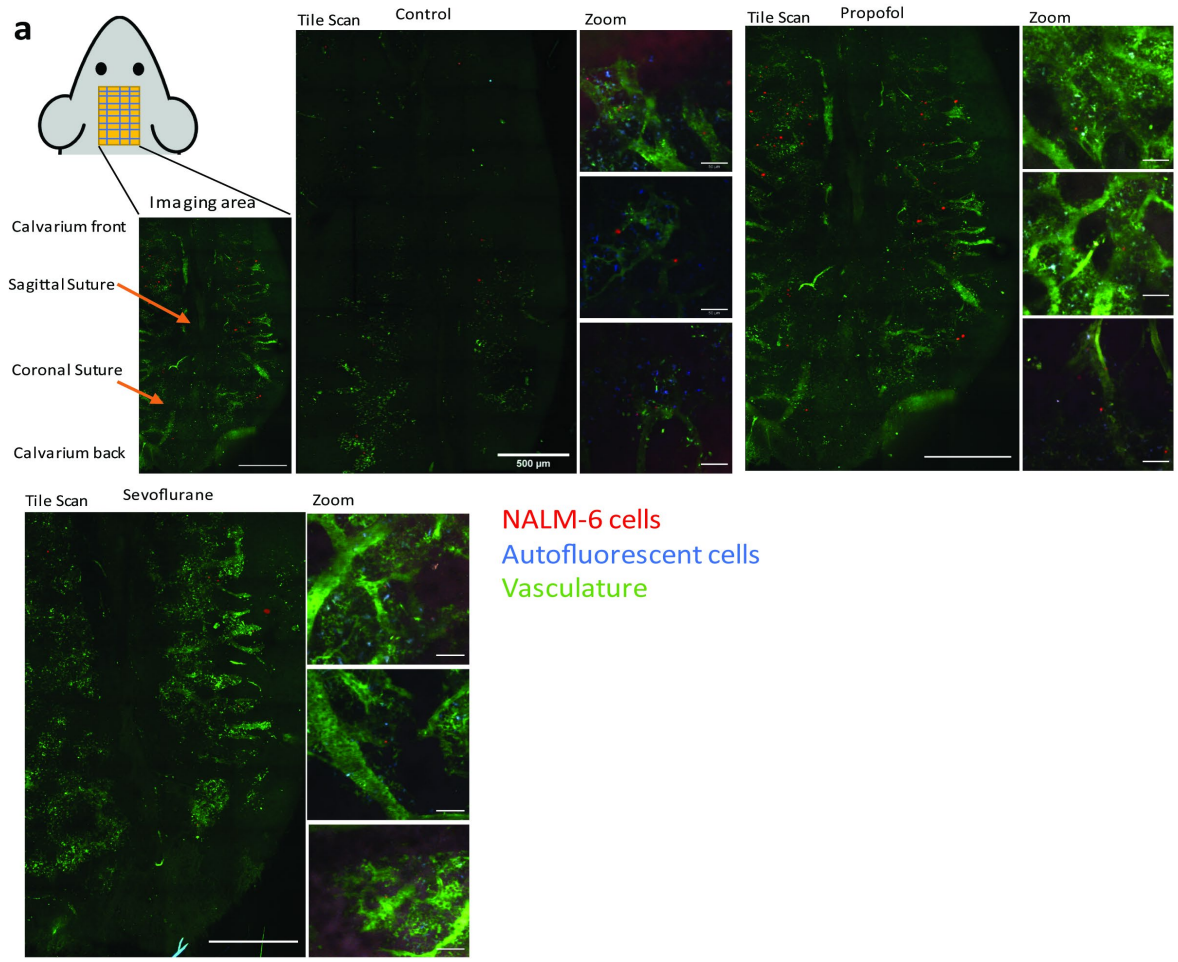
a
Tile Scan
Control
Zoom
Tile Scan
Propofol
Zoom
Imaging area
Calvarium front
Sagittal Suture
Coronal Suture
Calvarium back
500 µm
Tile Scan
Sevoflurane
Zoom
NALM-6 cells
Autofluorescent cells
Vasculature
b
Number of cells in BM
300
200
100
0
Control
Pro 10
Sevo
c
Distance to endosteal surface (µm)
400
300
200
100
0
Control
Pro 10
Sevo

Figure 5.9 General anaesthetics affect the number of cells entering BM and affect homing location of NALM-6 cells *in vivo*

a) upper left: diagram showing strategy for calvarium imaging. Lower left: Intravital confocal calvarium imaging of GFP transduced NLAM-6 cells (red) was performed after injection of GFP-NALM-6 cells into C57BL/6 mice IV. Representative maximum projection tile scans and corresponding high-magnification inserts were shown following IV injection of tritc-dextran to identify blood vessels (green); non leukaemia cells with high autofluorescent signals (blue) were recorded as well to improve the identification of target cells. Scale bar: 500µm for low magnification tile scan. 50 µm for high magnification images. **b)** summary graph showing the number of cells enter the BM. Data are illustrated as mean±s.e.m, (n=9). *P<0.05 vs Control. Non-parametric (Kruskal-Wallis) statistical test was used. Pro 10: cells were pre-treated with 10µg/ml of propofol overnight before injection, Sevo: cells were pre-treated with 3.6% sevoflurane overnight before injection. **c)** distance between nearest bone surface (not shown) to GFP-nalm-6 cells were measured. Data are pooled from 4 naïve control mice (N=4, 279 cells), 4 mice injected with propofol treated cells (n=4, 234 cells) and 4 mice injected with sevoflurane treated cells (n=4, 366 cells). Data are illustrated as mean±s.e.m (n=4). *P<0.05 non-parametric (Kruskal-Wallis) statistical test was used. Pro10: cells were pre-treated with 10µg/ml of propofol overnight. Sevo: cells were pre-treated with 3.6% of sevoflurane overnight.

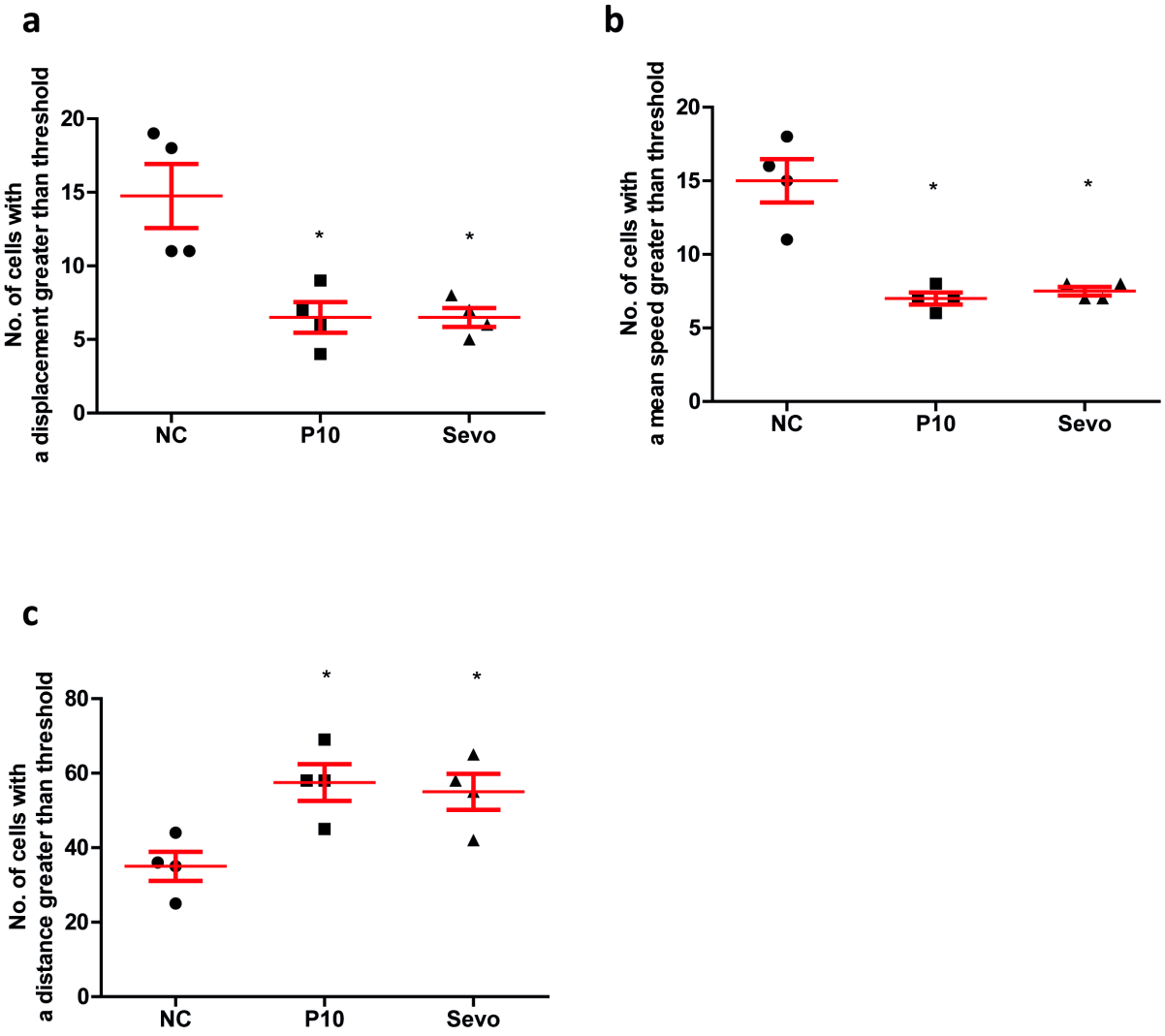
a
No. of cells with a displacement greater than threshold
20
15
10
5
0
NC
P10
Sevo
*
*
b
No. of cells with a mean speed greater than threshold
20
15
10
5
0
NC
P10
Sevo
*
*
c
No. of cells with a distance greater than threshold
80
60
40
20
0
NC
P10
Sevo
*
*

Figure 5.10 General anaesthetics affect the behaviour of NALM-6 cells *in vivo*
a) We analysed the data from Figure 5.8 d with a threshold approach. The median of the naïve control cells was set as the threshold value (Median=10.937µm). Then, we counted the number of cells with a displacement larger than the median in all treatment groups. We found that general anaesthetics reduced the number of cells with a displacement larger than 10.937µm. Data are illustrated as mean±s.e.m, (n=4). *P<0.05 vs Naïve control (NC). Non-parametric (Kruskal-Wallis) statistical test was used. NC: Naïve control, Pro 10: cells were pre-treated with 10µg/ml of propofol overnight before injections, Sevo: cells were pre-treated with 3.6% sevoflurane overnight before injections. **b)** We analysed the data from Figure 5.8 e with a threshold approach. The median of the naïve control cells was set as the threshold (Median=0.013µm/s). We found that general anaesthetics reduced the number of cells with a mean speed larger than 0.013µm/s. Data are illustrated as mean±s.e.m, (n=4). *P<0.05 vs Naïve control (NC). Non-parametric (Kruskal-Wallis) statistical test was used. NC: Naïve control, Pro 10: cells were pre-treated with 10µg/ml of propofol overnight before injections, Sevo: cells were pre-treated with 3.6% sevoflurane overnight before injections. **c)** We analysed the data from Figure 5.9 c with a threshold approach. The median of the naïve control cells was set as the threshold (Median=7.79µm). We found that general anaesthetics increased the number of cells with a distance to the nearest endosteal surface larger than 7.79µm. Data are illustrated as mean±s.e.m, (n=4). *P<0.05 vs Naïve control (NC). Non-parametric (Kruskal-Wallis) statistical test was used. NC: Naïve control, Pro 10: Cells were pre-treated with 10µg/ml of propofol overnight before injections, Sevo: Cells were pre-treated with 3.6% sevoflurane overnight before injections.

CHAPTER 6

Osteopontin (OPN) forms a positive feedback loop with HIF-1α in ALL cells, and it is disrupted by general anaesthetics

6.1 Introduction

OPN has functions in both physiological and pathophysiological conditions. In BM, OPN is secreted mainly by osteoblasts and stem cells[195]. Recently, it was discovered that leukaemia cells secrete OPN themselves[148]. The function of OPN in BM is complex. Also, the cleavage of OPN in BM by thrombin further contributes to the complex functions of OPN[148, 196]. The known functions include chemoresistance, cell quiescence and chemotaxis. A recent publication demonstrated stromal OPN anchored ALL cells in anatomic locations supporting cancer dormancy, avoiding chemotherapeutic agents. This process was mediated by α4ß1 integrin[148]. A group showed OPN maintained AML leukaemia stem cells survival by suppressing PUMA via using a mouse model of MLL-AF9 induced AML[197]. OPN was also shown to mediate bone marrow-derived macrophage chemotaxis through α4 and α9 integrins[198]. Recently, OPN was proposed as a prognostic factor in AML[195] by a recently published metanalysis consisting of 492 patients. It found that the serum concentration of OPN was inversely correlated with overall survival of AML patients. The difference was statistically significant (Hazard ratio= 1.83)[195].

OPN was observed to interact with HIF-1α in solid cancer models. OPN appeared to be an inducer of HIF-1α in ovarian cancer and breast cancer through activation of PI3K/AKT pathways[149, 150]. Increased HIF-1α led to enhanced cancer malignancy *in vitro*.

In this chapter, we explored the relationship between OPN and HIF-1α, and we also studied whether general anaesthetics might disrupt their reciprocal relationships *in vitro*. We studied the importance of OPN in ALL disease progression and prognostic value of OPN by using severe combined immunodeficient (SCID) mice.

6.2 Experiment design

6.2.1 In vitro

To study whether general anaesthetics modulate the expression of osteopontin, NALM-6 cells were treated with sevoflurane (3.6%) or propofol (5 to 10μg/ml) respectively. Then, cells were harvested for western blot analysis. Supernatant of cell culture was centrifuged and made ready for enzyme-linked immunosorbent assay (Figure 6.1).

Rising concentrations of OPN were given to NALM-6 cells, followed by western blot analysis (HIF-1α and AKT). OPN siRNA was also used in NALM-6 cells after which cells were harvested for western blot and flow cytometry analysis (Figure 6.2).

Both OPN treated and OPN siRNA treated cells were loaded onto the upper chamber of the migration chamber to study migration. After 6 hours of migration, cells in the lower chamber were collected and counted via flow cytometry (Figure 6.3).

6.2.2 *In vivo*

SCID mice were injected with 1 X 10^6 of NALM-6 cells IV. At 10 day intervals, mice were sacrificed with blood samples taken and bone marrow (femur) flushed. Blood serum was separated for ELISA analysis and the rest of the samples were prepared for flow cytometry analysis (Figure 6.4).

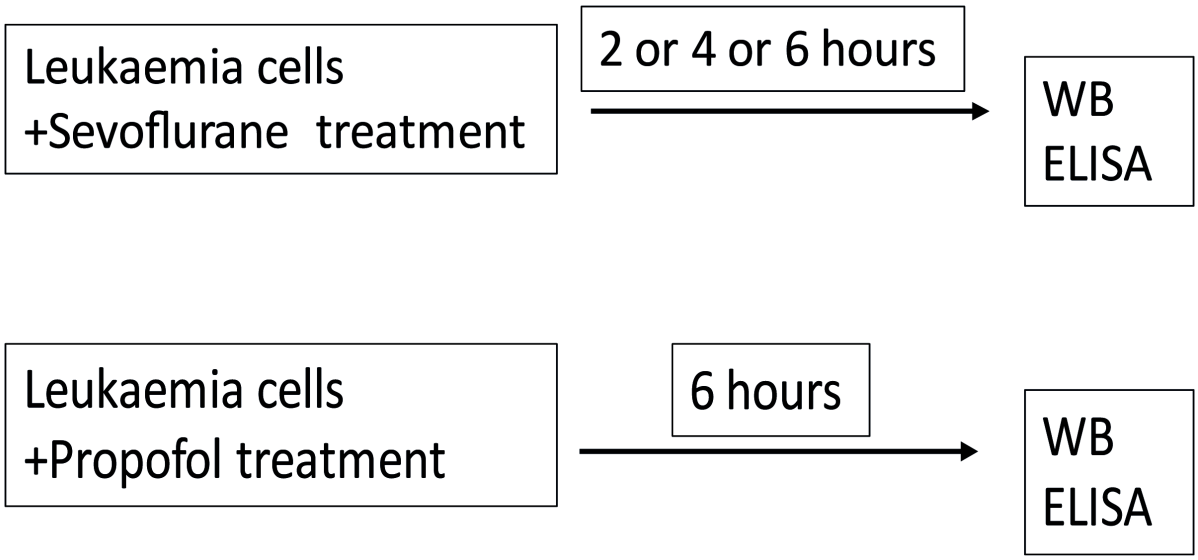

Figure 6.1 *In vitro* experiment design
WB: Western blot

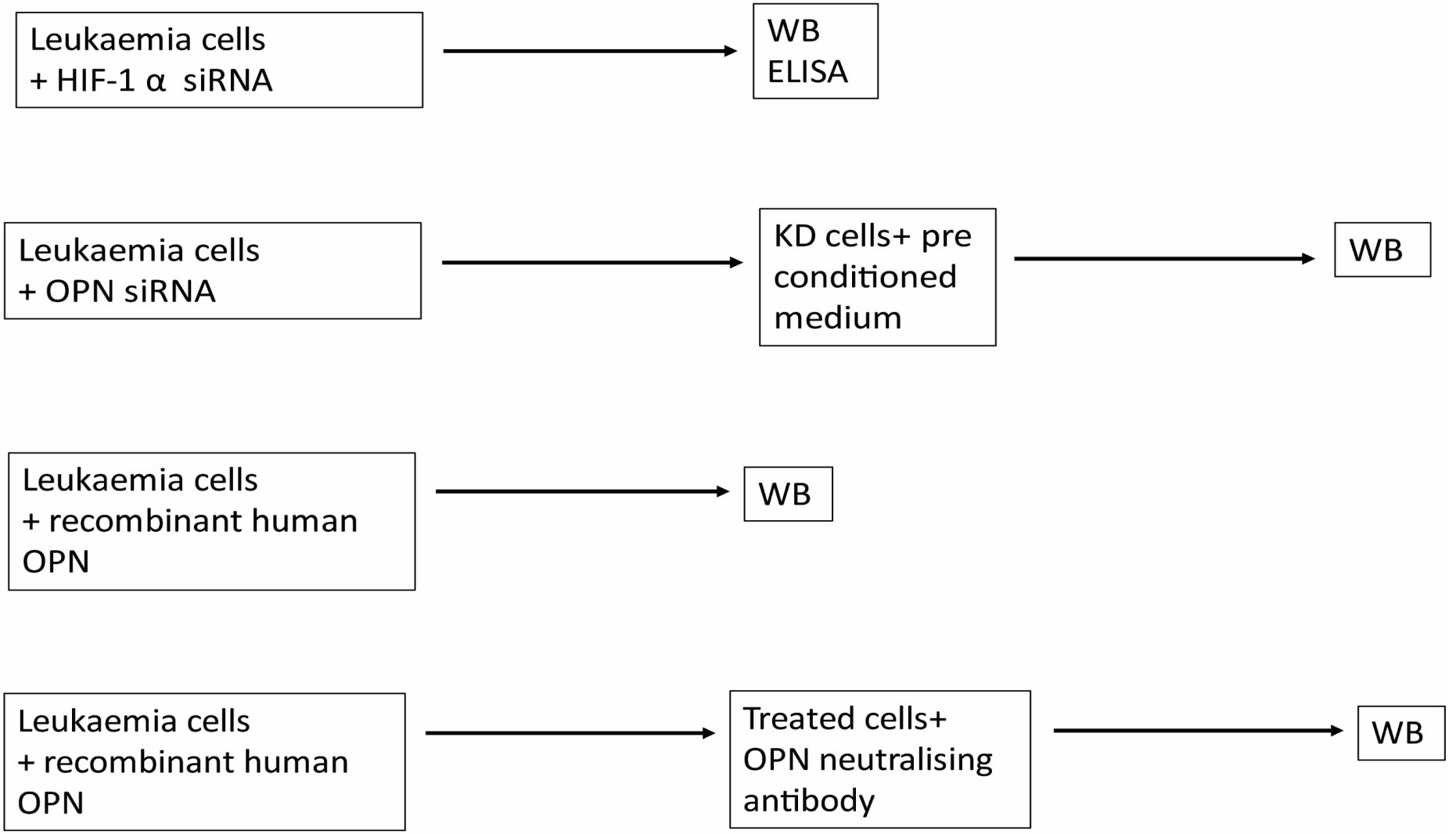

Figure 6.2 *In vitro* experiment design
KO cells: knocked cells
WB: Western blot

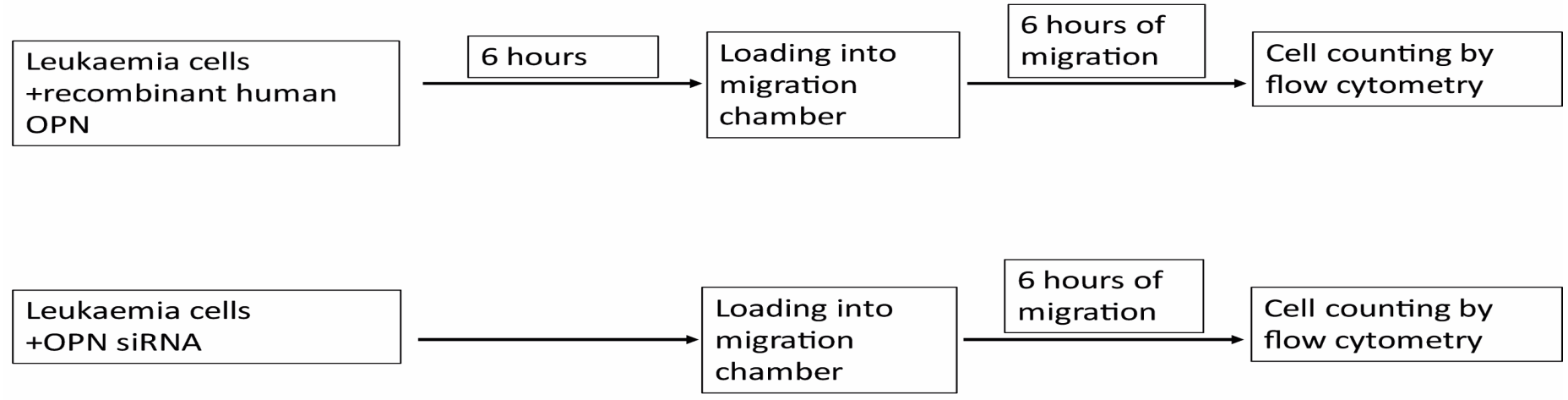

Figure 6.3 *In vitro* migration assay design

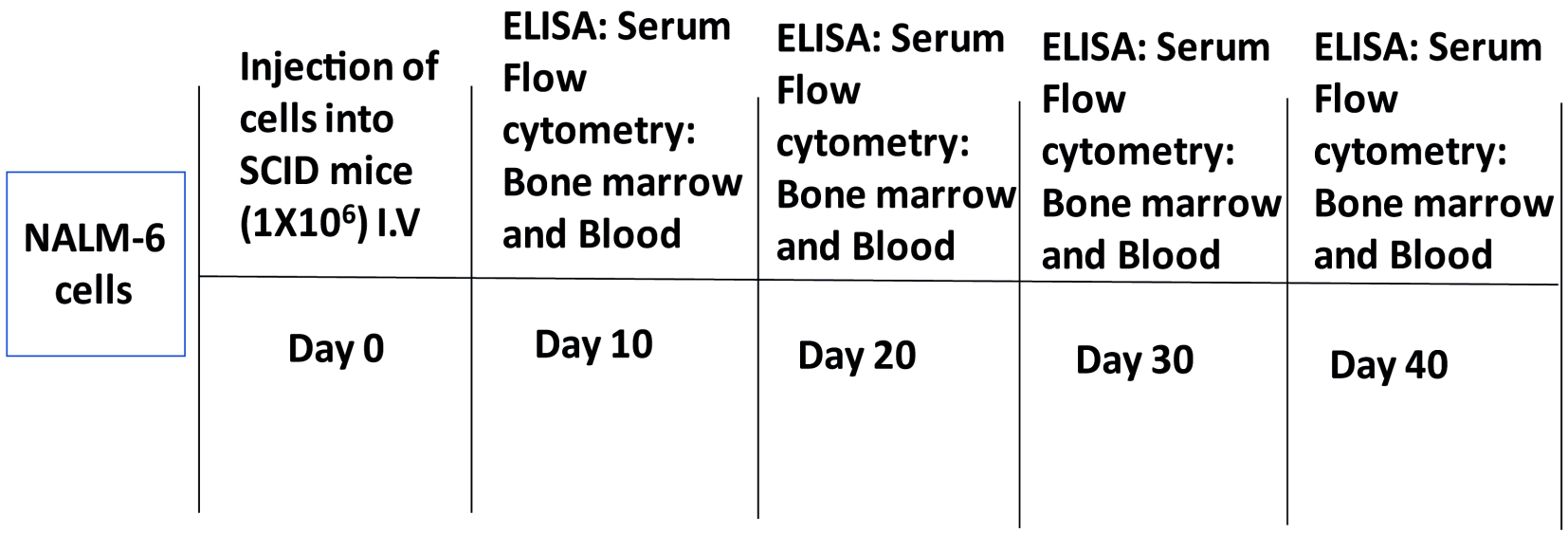

Figure 6.4 Disease induction and monitoring in the mouse model
At each 10 days interval, blood samples were taken via cardiac puncture. Bone marrow from femur was flushed by using PBS before being passed through cell retainer. Then, bone marrow samples were subject to flow cytometry analysis.

6.3 Results

6.3.1 General anaesthetics reduce protein synthesis and secretion of OPN

OPN protein expression was significantly reduced by propofol and sevoflurane in NALM-6 cells (Figure 6.5). 5 and 10μg/ml of propofol had similar inhibitory effects on OPN protein expression measured by western blot (Figure 6.5a). Only 6 hours of sevoflurane significantly reduced OPN protein synthesis measured by western blot (Figure 6.5b). ELISA analysis of OPN secretion showed a slightly different story in propofol. Only 10μg/ml of propofol was shown to decrease the secretion of OPN significantly (from 2.5 to around 1.5ng/ml) (Figure 6.5c). Six hours of sevoflurane dramatically declined the OPN secretion as shown by ELISA analysis (from 2.4 to 2ng/ml) (Figure 6.5d).

6.3.2 OPN is a downstream target of HIF-1α

After determining that general anaesthetics affecting the expression of OPN, we hypothesised OPN was a potential target of HIF-1α in NALM-6 cells. HIF-1α knocked down cells (knocked down via siRNA, the knock down of HIF-1α was validated via western blot, n=4) exhibited a reduction in OPN protein expression analysed by western blot (Figure 6.6a). ELISA analysis of samples with HIF-1α knocked down cells showed OPN secretion was reduced from 2.5ng/ml (control) to 1.5ng/ml (HIF siRNA) (Figure 6.6b). Twenty-four hours of hypoxia was given to cells after which OPN secretion was measured. After hypoxia, OPN secretion was increased to around 10ng/ml. Then, HIF siRNA treatment reduced the OPN secretion by almost half (5ng/ml) (Figure 6.6c).

6.3.3 OPN forms an auto feedback loop with HIF-1α

According to experimental data from breast and ovarian cancer models, OPN contributes to the increased level of HIF-1α. In addition, we found OPN was a downstream target of HIF-1α. Thus, we hypothesised leukaemia cells had an auto feedback loop between HIF-1α and OPN.

Firstly, rising concentration (50, 100 and 200ng/ml) of human recombinant OPN was used to treat NALM-6 cells for 6 hours. Then, HIF-1α expression was analysed via western blot. Expectedly, with the treatment of 100 and 200ng/ml of OPN, HIF-1α protein synthesis was significantly enhanced (Figure 6.7a). OPN neutralising antibody (2μg/ml) or control goat IgG were used for 6 hours (Figure 6.7b) to treat NALM-6 cells. Clearly, after OPN neutralising antibody treatment, HIF-1α expression was reduced. The control rabbit IgG did not affect the expression of HIF-1α (result not shown). To test this concept further, 200ng/ml of OPN and neutralising antibody were given to NALM-6 cells at the same time (Figure 6.7c). After treatment of 200ng/ml of OPN, HIF-1 α expression was increased but it was then reduced by the OPN neutralising antibody (Figure 6.7c). Finally, when NALM-6 cells were treated with OPN siRNA, the HIF-1α expression reduced dramatically (almost by half). However, after the treatment of pre-condition media (the media from the normal culture of NALM-6 cells), HIF-1α expression was restored (Figure 6.7d). Thus, these data are consistent with the findings that an OPN and HIF-1α have an autocrine feedback loop in NALM-6 cells.

After discovering the auto feedback loop between HIF and OPN, we studied the PI3K/AKT pathway as previous literature suggested. We observed that phosphorylation of AKT was largely enhanced with the treatment of human OPN at the concentration of 100 and 200ng/ml (Figure 6.7e). In addition, when NALM-6 cells were treated with neutralising OPN antibody, the phosphorylation of AKT was dramatically diminished by 50% (Figure 6.7f).

The current literature[148, 199-201] suggests that the potential receptor for OPN signalling is α4ß1 as NALM-6 cells do not process the CD44 receptor. Our results showed that the expression of α4ß1 integrin did not change after treatment of 200ng/ml of OPN and OPN siRNA in NALM-6 cells (results not shown, n=4), suggesting OPN did not induce subcellular signalling events through amplification of receptors.

6.3.4 OPN regulates CXCR4 expression and migration of NALM-6 cells

To further demonstrate the relationship between HIF-1α and OPN, we tested whether OPN regulated two downstream targets of HIF-1α. We observed that inhibition of OPN significantly reduced CXCR4 expression (20 to 25%) (Figure 6.8a). Furthermore, CXCR4 expression was increased after treatment of 200ng/ml of OPN in NALM-6 cells (Figure 6.8b). Similarly, when OPN was inhibited, fewer cells migrated from the upper chamber to the lower chamber presumably due to the reduction of CXCR4 (Figure 6.8c). When NALM-6 cells were pre-treated by 200ng/ml OPN, more cells migrated to the lower chamber (Figure 6.8d). These results suggest OPN can, to some degree, regulate downstream targets of HIF-1α.

6.3.5 Serum OPN level corresponds with leukaemia progression *in vivo*

Next, we determined the prognostic value of OPN in an established mouse model. Initially, SICD mice were injected with 1 X 10^6 of NALM-6 cells IV. Then, at each 10 day interval, blood and BM samples were taken for flow cytometry analysis and serum was separated for ELISA analysis (Figure 6.9a). Bone marrow and blood samples were stained with CD19-PE and CD10-APC. At day 10, the presence of leukaemia cells was not detectable in blood and BM. In addition, the serum OPN level was extremely low at around 5ng/ml (Figure 6.9a, b, and c). At day 20, the percentage of ALL cells in BM was increased. Serum OPN level increased to roughly 18ng/ml. At day 30, although 100% of mice did not have any symptoms of illness, bone marrow was filled with roughly 40% of ALL cells. In addition, the proportion of ALL cells in blood was around 5% and serum OPN concentration reached over 50ng/ml. 10 days later (day 40), surprisingly, all of the disease-bearing mice were either dead or terminated due to paralysis in lower limbs caused by CNS infiltration of ALL cells. At day 40, ALL cells made up 60% of cells in BM and they contributed to 8% of blood cells (Figure 6.9b, c). Serum OPN concentration reached an average of 150ng/ml. This is 30 times higher than that of day 10 (Figure 6.9d).

6.4 Discussion

Here, we have found a novel interaction between HIF-1α and OPN in leukaemia cells which has not been studied before. This autofeedback loop can be disrupted by general anaesthetics. In addition, we have also shown that the serum OPN level corresponds with disease progression.

HIF-1α potentially regulates over 100 genes[202]. It is not well known whether OPN is downstream to HIF-1α in leukaemia. Only one publication[203] mentioned hypoxia increasing the expression of OPN via HIF-1α mediated mechanisms in human AML cells. We confirmed this result by an siRNA-based strategy. The notion that OPN activates HIF-1α protein synthesis is illustrated before in breast and ovarian cancer cells via the PI3K/AKT pathway[149, 150]. In the breast cancer model, hypoxia increased the secretion of OPN in a HIF-1α independent manner[150]. The increased OPN secretion reciprocally elevated HIF-1α protein synthesis in breast cancer[150]. In addition to the PI3K/AKT pathway, the ILK pathway was also a signalling intermediate involved in OPN regulated HIF-1α expression. Unfortunately, neither ovarian nor breast cancer studies specified which receptor was responsible for OPN signalling. With our study, we only studied the α4ß1 integrin according to previous study[148] and found its expression was not affected by OPN treatment (data not shown, n=4).

In addition to HIF-1α, interaction of HIF-1ß and HIF-2α with OPN were studied. In the breast cancer model, they found HIF-1ß and HIF-2α had no potential interplay with OPN[150]. However, one publication showed OPN inhibited HIF-2α mRNA in osteoarthritic chondrocytes *in vitro*[204].

The major source of OPN in BM is secreted by host osteoblasts. In future experiments, we propose to study whether host-derived OPN could have similar signalling with HIF-1α in leukaemia cells. In other words, can host-derived OPN affect leukaemia malignancy? In order to achieve this, we plan to inject NALM-6 cells to OPN knocked out mice and study characterises associated with leukaemia malignancy.

Many publications reported the elevated plasma level of OPN in leukaemia patients and it has been proposed to have some prognostic value in leukaemia[205-209].

The median level of OPN in AML patients found in one particular publication appeared to be 7.4 ng/ml with a range of 0.3 to 30.5ng/ml. This was significantly higher than OPN levels found in blood serum of controls with a median of 2.1ng/ml and a range of 0.83 to 3.22ng/ml[205]. More importantly, they demonstrated bone marrow OPN level was significantly associated with overall survival (OS) and event-free survival (EFS). However, blood OPN concentration did not indicate any prognostic significance[205]. Considering the small patient size (n=41), future studies with a large sample size are still needed.

Interestingly, in our mouse model, we detected a much higher level of serum OPN. e.g. at day 40, the mean serum concentration of OPN was around 150ng/ml with around 8% of ALL cells in mouse blood. Unfortunately, the previous study[205] did not give the clinical data of the patients e.g. leukaemia

infiltration in blood and bone marrow. We could not draw any solid conclusion here why the human serum concentration of OPN was dramatically lower than that of mice.

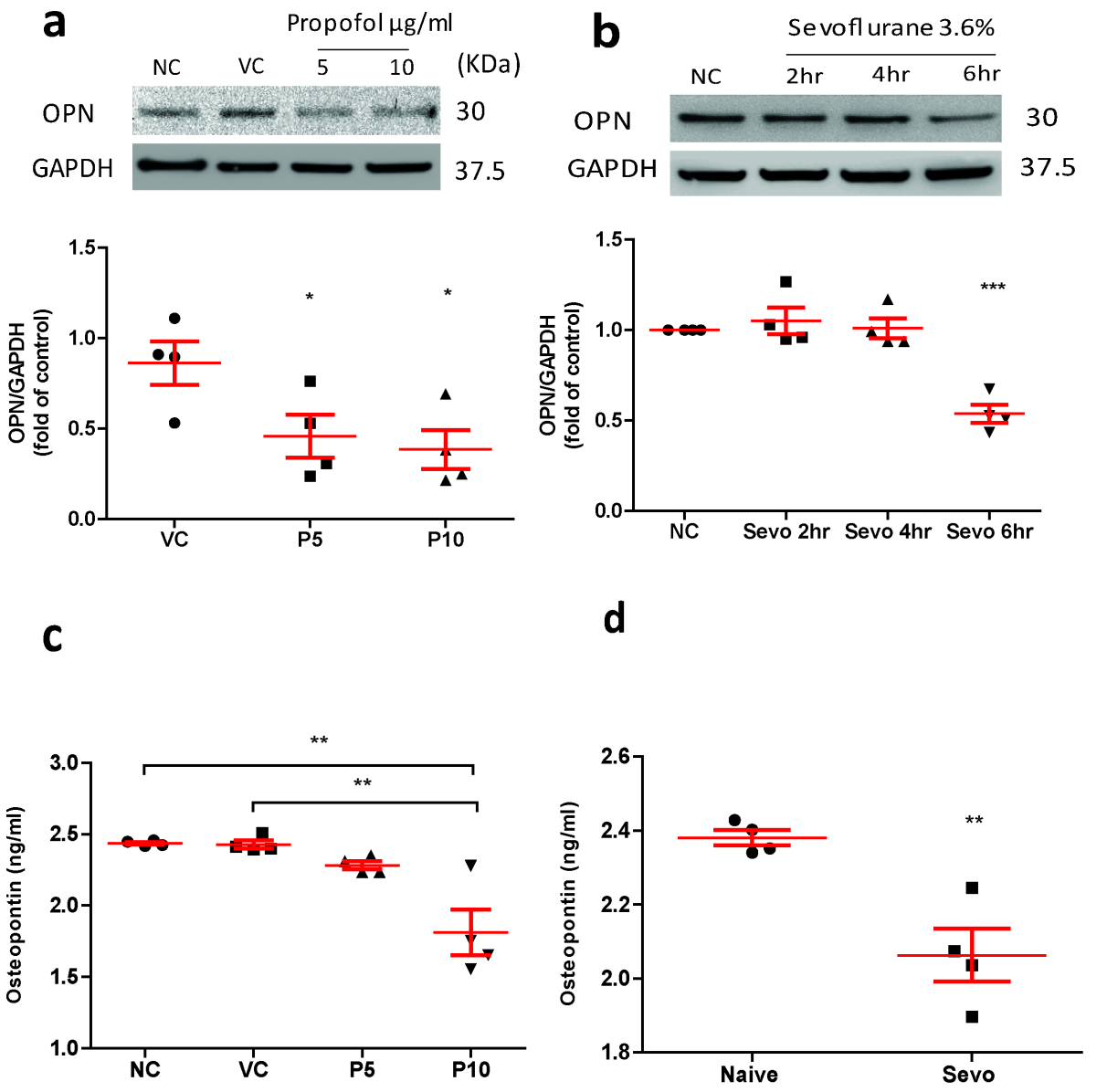

Figure 6.5 General anaesthetics reduce the expression and the secretion of OPN

a) Western blot and densitometry of OPN protein expression after the treatment of intralipid (VC) and propofol. Data are illustrated as mean±s.e.m (n=4) *P<0.05 vs Vehicle control (VC). Data are analysed by one-way ANOVA followed by Bonferroni's post-hoc test. NC: Naïve control, VC: Vehicle control, P5: 5μg/ml of propofol, P10: 10μg/ml of propofol. **b)** Western blot and densitometry of OPN protein expression after the treatment of 3.6% sevoflurane for 2, 4 and 6 hours. Data are shown as mean±s.e.m (n=4). ***P<0.001 vs Naïve control (NC). Data are analysed by one-way ANOVA followed by Bonferroni's post-hoc test. NC: Naïve control, Sevo 2hr: Sevoflurane 2 hours, Sevo 4hr: Sevoflurane 4 hours, Sevo 6hr: Sevoflurane 6 hours. **c)** ELSIA assay was used to measure OPN in supernatants after the treatment of propofol for 6 hours. Data are illustrated as mean±s.e.m (n=4). **P<0.01. Data are analysed by one-way ANOVA followed by Bonferroni's post-hoc test. NC: Naïve control, VC: intralipid P5: 5μg/ml of propofol, P10: 10μg/ml of propofol. **d)** ELSIA assay was used to measure OPN in supernatants after the treatment of 3.6% sevoflurane for 6 hours. Data are illustrated as mean±s.e.m (n=4). **P<0.01 vs Naïve control (Naïve). Data are analysed by unpaired T-test. Naïve: Naïve control, Sevo: Sevoflurane 6 hours.

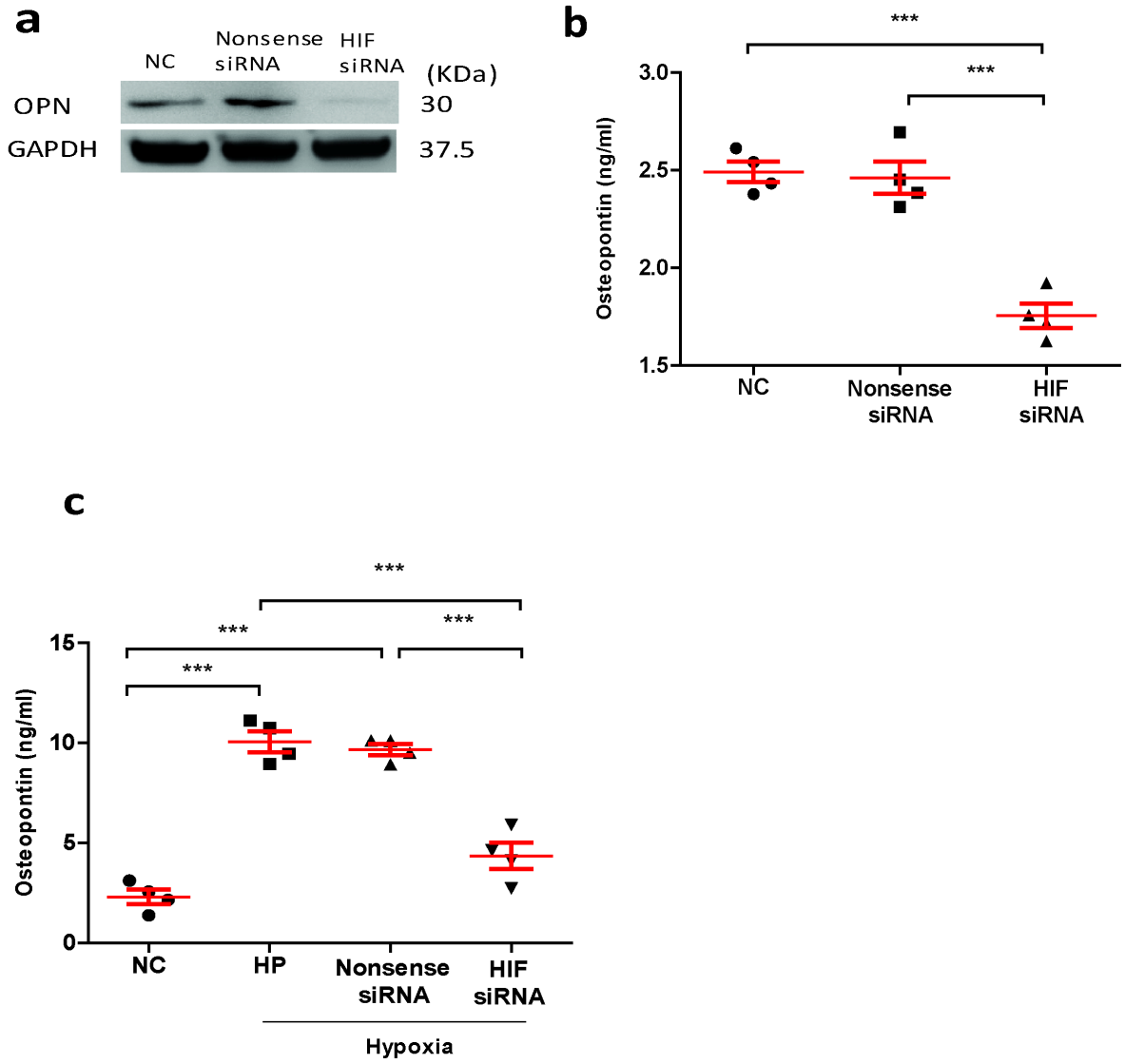

Figure 6.6 OPN is a downstream target of HIF-1α

a) OPN was shown to be a downstream target of HIF-1α. Western blot of OPN expression in cells treated with HIF-1α siRNA and nonsense siRNA. n=4. **b)** ELISA assay was used to measure OPN in culture after the treatment of HIF-1α siRNA and nonsense siRNA. Data are illustrated as mean±s.e.m (n=4). ***P<0.001. Data are analysed by one-way ANOVA followed by Bonferroni's post-hoc test. NC: Naïve control. **c)** ELISA assay was used to measure OPN in culture after the treatment of hypoxia, hypoxia + nonsense siRNA and hypoxia + HIF-1α siRNA. Data are shown as mean±s.e.m (n=4). ***P<0.001. Data are analysed by one-way ANOVA followed by Bonferroni's post-hoc test. NC: Naïve control, HP: Hypoxia.

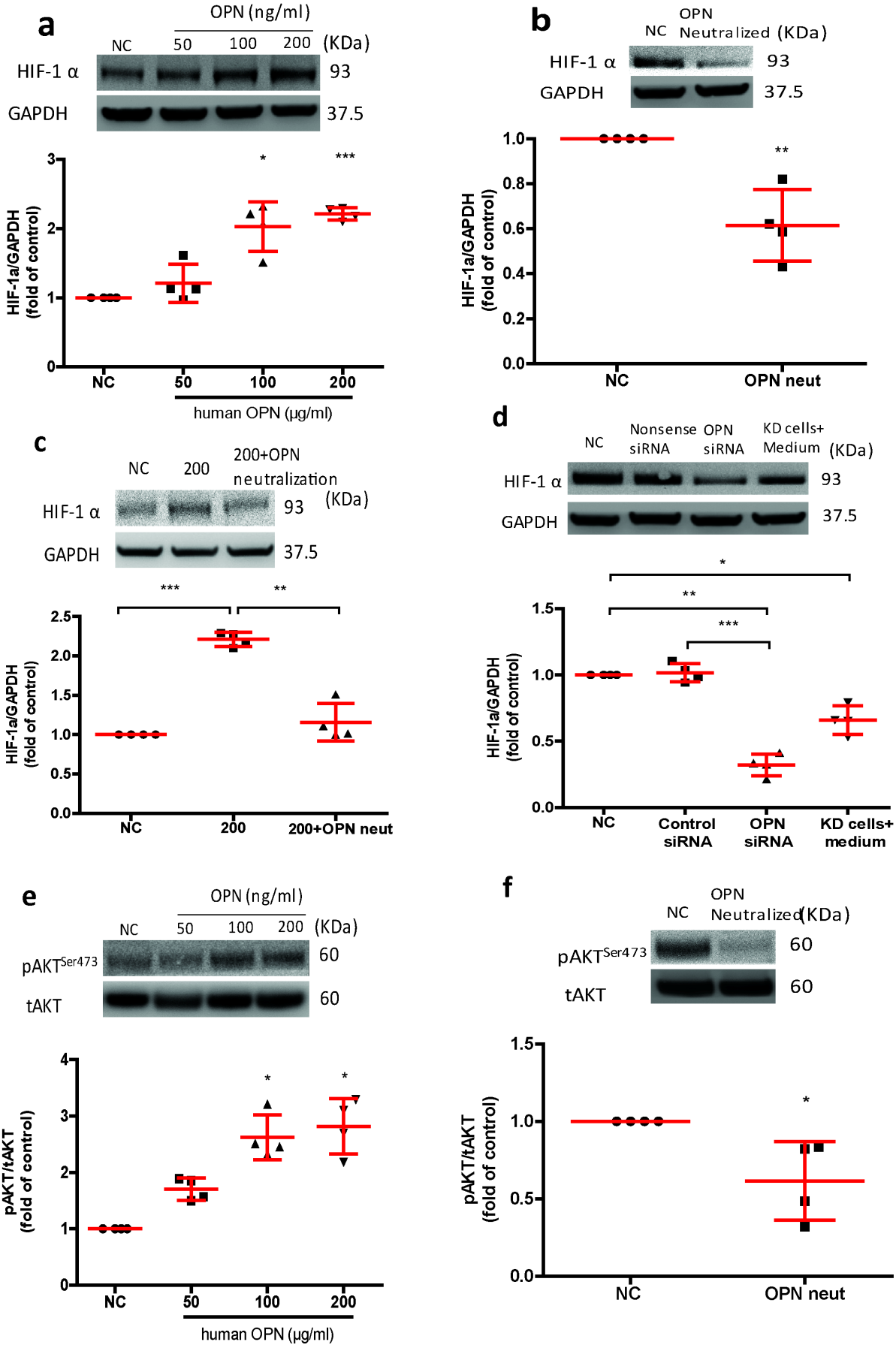
a
OPN (ng/ml)
NC 50 100 200 (KDa)
HIF-1 α
GAPDH
93
37.5
HIF-1a/GAPDH (fold of control)
NC 50 100 200
human OPN (μg/ml)
b
NC OPN Neutralized (KDa)
HIF-1 α
GAPDH
93
37.5
HIF-1a/GAPDH (fold of control)
NC OPN neut
c
NC 200 200+OPN neutralization (KDa)
HIF-1 α
GAPDH
93
37.5
HIF-1a/GAPDH (fold of control)
NC 200 200+OPN neut
d
NC Nonsense siRNA OPN siRNA KD cells+ Medium (KDa)
HIF-1 α
GAPDH
93
37.5
HIF-1a/GAPDH (fold of control)
NC Control siRNA OPN siRNA KD cells+ medium
e
OPN (ng/ml)
NC 50 100 200 (KDa)
pAKTSer473
tAKT
60
60
pAKT/tAKT (fold of control)
NC 50 100 200
human OPN (μg/ml)
f
NC OPN Neutralized (KDa)
pAKTSer473
tAKT
60
60
pAKT/tAKT (fold of control)
NC OPN neut

Figure 6.7 OPN forms an auto-feedback loop with HIF-1α

a) Western blot and densitometry of OPN protein expression after the treatment of concentrations of OPN (50 to 200ng/ml) for 6 hours. Data are illustrated as mean±s.e.m (n=4). *P<0.05, ***P<0.001 vs Naïve control (NC). Data are analysed by one-way ANOVA followed by Bonferroni's post-hoc test. NC: Naïve control. **b)** OPN neutralizing antibody (2μg/ml) was added to NALM-6 cells, then HIF-1α expression was analysed by western blot. Data are shown as mean±s.e.m (n=4). **P<0.01 vs Naïve control (NC). Data are analysed by unpaired T-test. NC: Naïve control, OPN neut: OPN neutralising antibody. **c)** NALM-6 cells were treated with 200ng/ml of OPN and OPN neutralisation antibody (2μg/ml) for 6 hours. Data are illustrated as mean±s.e.m (n=4). **P<0.01, ***P<0.001. Data are analysed by one-way ANOVA followed by Bonferroni's post-hoc test. NC: Naïve control, 200: 200ng/ml of human OPN. 200+OPN neut: 200ng/ml of human OPN+OPN neutralising antibody. **d)** OPN expression in NALM-6 cells was knocked down by OPN siRNA, then those cells were treated with preconditioned medium. Data are illustrated as mean±s.e.m (n=4). *P<0.05, **P<0.01, ***P<0.001. Data are analysed by one-way ANOVA followed by Bonferroni's post-hoc test. NC: Naïve control, KD cells+medium: HIF-1α knocked down cells+ preconditioned medium.

e) NALM-6 cells were treated with increasing concentrations of OPN (50 to 200ng/ml) for 6 hours, phosphorylation of AKT was elevated (analysed through western blot). Data are shown as mean±s.e.m (n=4). *P<0.05 vs Naïve control (NC). Data are analysed by one-way ANOVA followed by Bonferroni's post-hoc test. NC: Naïve control. **f)** OPN neutralizing antibody (2μg/ml) was added to NALM-6 cells, then phosphorylation of AKT was analysed by western blot. Data are shown as mean±s.e.m (n=4). *P<0.05 vs Naïve control (NC). Data are analysed by unpaired T-test. NC: Naïve control, OPN neut: OPN neutralising antibody.

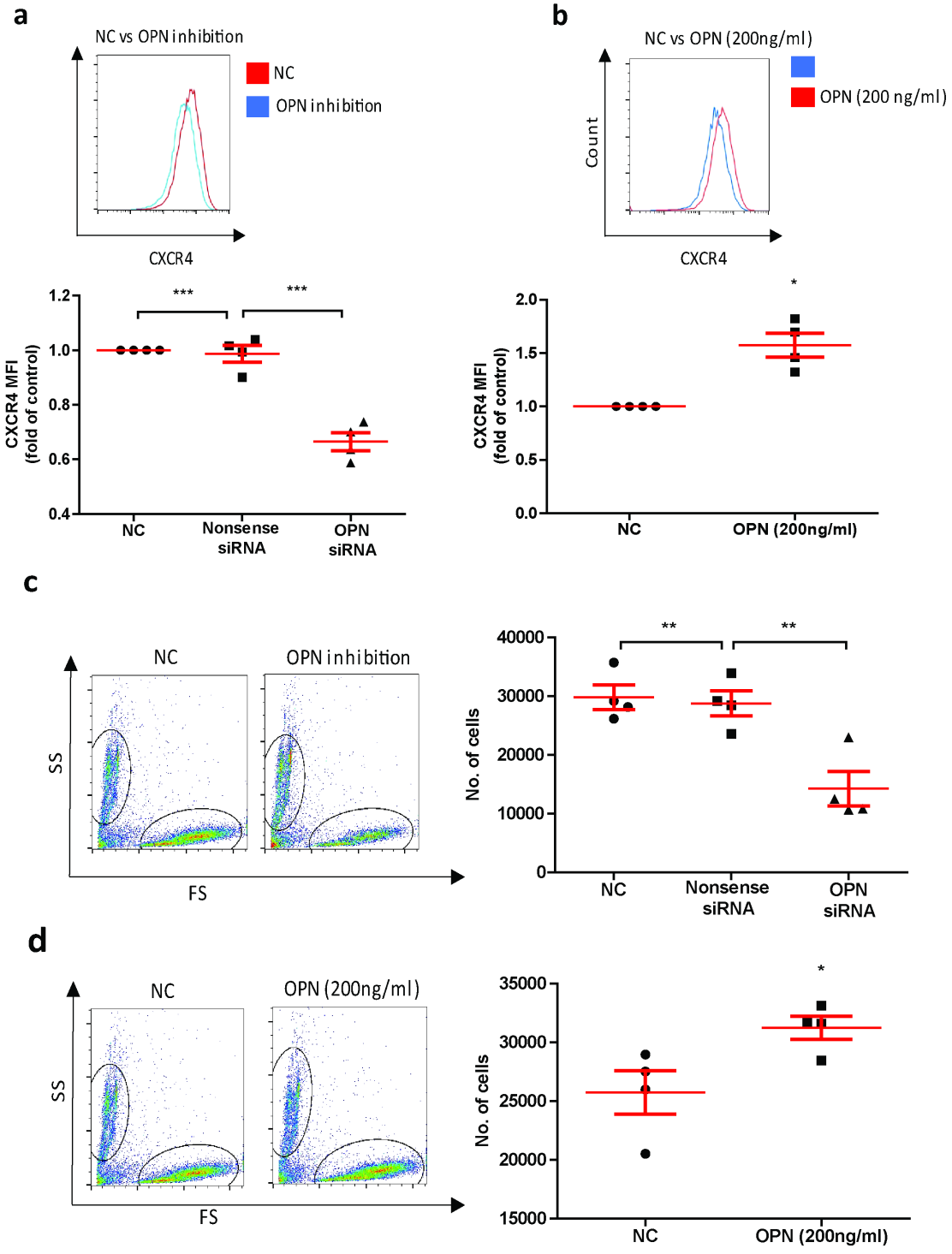
a
NC vs OPN inhibition
NC
OPN inhibition
CXCR4
CXCR4 MFI (fold of control)
***
***
NC
Nonsense siRNA
OPN siRNA
b
NC vs OPN (200ng/ml)
OPN (200 ng/ml)
Count
CXCR4
CXCR4 MFI (fold of control)
*
NC
OPN (200ng/ml)
c
NC
OPN inhibition
SS
FS
No. of cells
**
**
NC
Nonsense siRNA
OPN siRNA
d
NC
OPN (200ng/ml)
SS
FS
No. of cells
*
NC
OPN (200ng/ml)

Figure 6.8 OPN regulates CXCR4 and migration

a) OPN siRNA or nonsense siRNA were used to treat NALM-6 cells. After treatment, the CXCR4 expression was analysed by a flow cytometer. Data are shown as mean±s.e.m (n=4). ***P<0.001. Data are analysed by one-way ANOVA followed by Bonferroni's post-hoc test. NC: Naïve control. **b)** 200ng/ml of OPN was given to NALM-6 cells for 6 hours. After treatment, the CXCR4 expression was analysed by a flow cytometer. Data are shown as mean±s.e.m (n=4). *P<0.05 vs Naïve control (NC). Data are analysed by unpaired T-test. NC: Naïve control. **c)** OPN siRNA and nonsense siRNA were used to treat NALM-6 cells. Then, treated cells were loaded into migration chamber and they were allowed to migrate for 6 hours. After migration, cells in lower chamber were counted via flow cytometry. Data are shown as mean±s.e.m (n=4). **P<0.01. Data are analysed by one-way ANOVA followed by Bonferroni's post-hoc test. NC: Naïve control. **d)** 200ng/ml of OPN was used to treat NALM-6 cells for 6 hours. Then, treated cells were loaded into migration chamber and they were allowed to migrate for 6 hours. After migration, cells in lower chamber were counted via flow cytometry. Data are shown as mean±s.e.m (n=4). *P<0.05 vs Naïve control (NC). Data are analysed by unpaired T-test. NC: Naïve control.

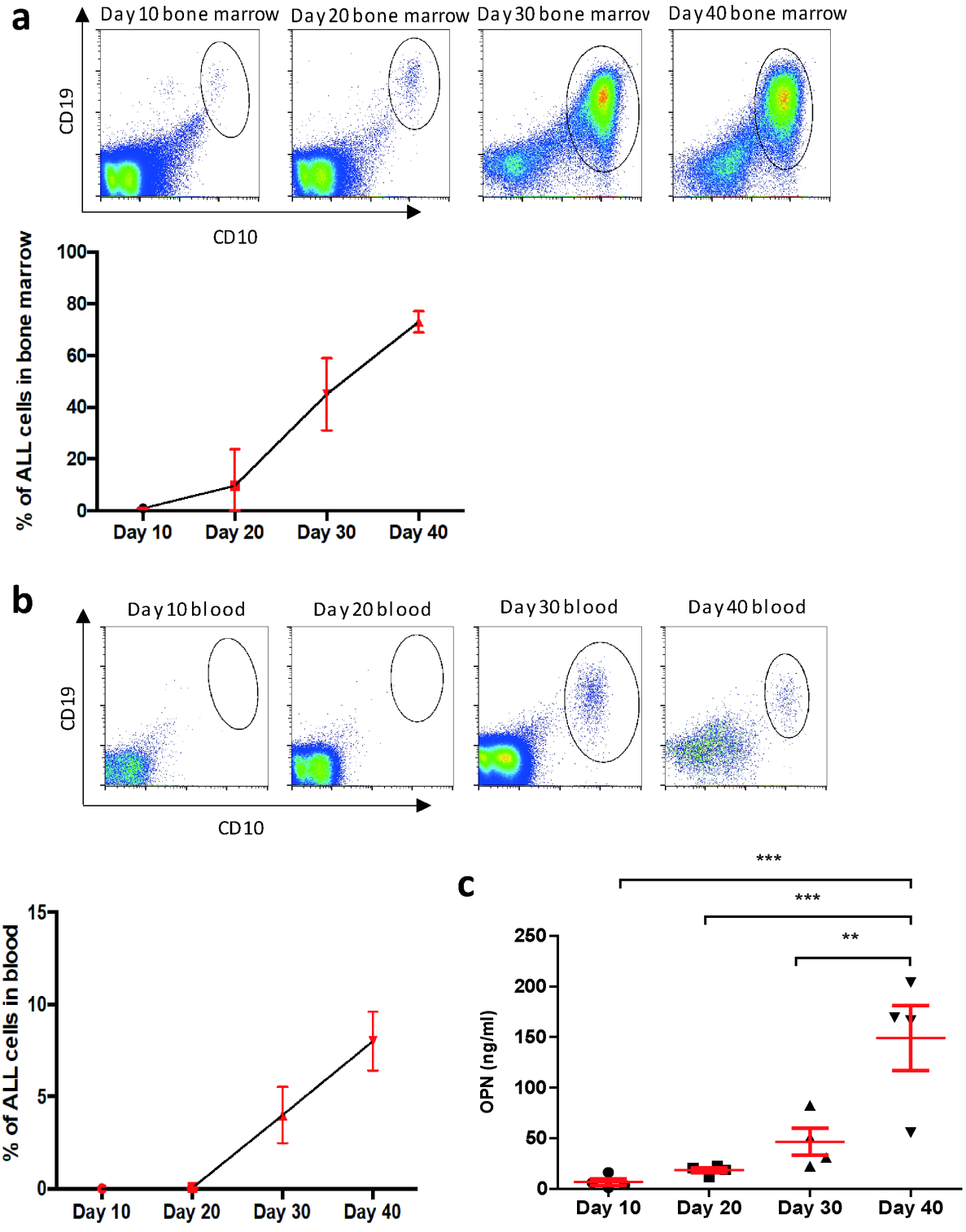
a
Day 10 bone marrow
Day 20 bone marrow
Day 30 bone marrov
Day 40 bone marrow
CD19
CD10
% of ALL cells in bone marrow
100
80
60
40
20
0
Day 10
Day 20
Day 30
Day 40
b
Day 10 blood
Day 20 blood
Day 30 blood
Day 40 blood
CD19
CD10
% of ALL cells in blood
15
10
5
0
Day 10
Day 20
Day 30
Day 40
c
***
***
**
OPN (ng/ml)
250
200
150
100
50
0
Day 10
Day 20
Day 30
Day 40

Figure 6.9 Serum OPN level corresponds with leukaemia disease progression
a) the proportion of CD19-PE+ CD10-APC+ NALM-6 cells increased in mouse BM (femur) as leukaemia manifests from day 10 to day 40. At day 40, all disease bearing mice died or terminated due to infiltration of leukaemia cells in CNS. Data are shown as mean±s.e.m (n=3). **b)** the proportion of CD19+ CD10+ NALM-6 cells increased in mouse blood as leukaemia manifests from day 10 to day 40. Bay day 40, all disease bearing mice died or terminated due to infiltration of leukaemia cells in CNS. Data are shown as mean±s.e.m (n=3). **c)** OPN concentration in mouse serum was increased dramatically from day 10 to day 40 post injection of leukaemia cells IV. And its pattern corresponds with proportion of leukaemia cells in blood and bone marrow. Data are illustrated as mean±s.e.m (n-=3). **P<0.01, ***P<0.001. Data are analysed by one-way ANOVA followed by Bonferroni's post-hoc test.

CHAPTER 7

General anaesthetics sensitise leukaemia cells to chemotherapy

7.1 Introduction

Chemotherapy is the backbone of modern-day leukaemia treatment and chemoresistance is the largest challenge. Although the treatment response for ALL patient is very good, those who have treatment failure are extremely difficult to recover. Almost all patients undergoing intrathecal chemotherapy require the frequent use of general anaesthetics[45]. This provides an opportunity for anaesthetics to have synergistic effects with chemotherapy on leukaemia cells. In this chapter, we studied whether general anaesthetics had any impact on the cytotoxic effects of chemotherapy. In particular, cytosine arabinoside (Ara-C) was chosen for our chemotherapy experiment. It is one of the four drugs approved for intrathecal use. Autophagy is regarded as one of the most frequent mechanisms induced by Ara-C (particularly at low does) in acute leukaemia chemoresistance[210-213]. Autophagy is a ubiquitous process in eukaryotic cells and it results in the breakdown of cytoplasm by the lysosome[214]. It was thought that autophagy allows cells to adapt to the environment and it is simply a degradative process with protective effects. However, current evidence demonstrates autophagy could either be cytotoxic or cytoprotective[215].

In the current literature, propofol and sevoflurane have been shown to affect chemoresistance. In particular, propofol is associated with sensitising cancer cells to chemotherapy in prostate cancer[4, 216] and endometrial cancer[189]. Sevoflurane has been shown to promote chemoresistance in non-small lung adenocarcinoma[121]. Our initial hypothesis was propofol and sevoflurane might sensitise ALL cells to Ara-C via autophagy-based mechanisms.

Our second hypothesis was OPN might regulate chemoresistance through autophagy via HIF-1α mediated mechanisms. We derived the second hypothesis from our previous results of OPN and HIF-1α. The role of HIF-1α was implicated in ALL chemoresistance[217]. We speculated OPN may play a part in chemoresistance of ALL cells.

However, our preliminary data showed no activation of the autophagy pathway in NALM-6 cells after the treatment of Ara-C and general anaesthetics (data not shown, n=4).

Then, we switched our focus to the apoptotic pathways, where we obtained significant results.

7.2 Experiment Design

We treated cells with rising concentrations of Ara-C (from 0.05 to 50μM) and general anaesthetics (10μg/ml of propofol and 3.6% of sevoflurane) for 6 hours. Then, cell viability was measured via propidium iodide-based flow cytometry analysis (Figure 7.2).

We then explored the underlying mechanisms. Cells were treated with Ara-C (from 0.05 to 50μM) and general anaesthetics (10μg/ml of propofol and 3.6% of sevoflurane) for 6 hours. Then, cells were harvested for western blot analysis. We particularly explored the extrinsic pathway of apoptosis

involving multiple caspases and poly ADP-ribose polymerase (PARP)[218]. In the extrinsic pathway, when a ligand binds to the death receptor, it activates death-inducing signalling complex (DISC) which includes caspase-8 and FADD. Then, activated caspase-8 cleaves pro-caspase-3 to form cleaved caspase 3. Cleaved caspase 3 facilitates the cleavage of PARP and stops its repair of DNA[219] (Figure 7.3). Finally, activated PARP leads to apoptosis.

For the OPN and chemoresistance experiment, NALM-6 cells were treated with Ara-C (0.05 to 100 μM) and 200 ng/ml of human recombinant OPN for 6 hours. Alternatively, NLAM-6 cells were treated with human OPN siRNA firstly to temporarily knock down OPN, then cells were treated with Ara-C (0.05 to 100μM) for 6 hours. After treatment, cell viability was analysed with flow cytometry (Figure 7.3).

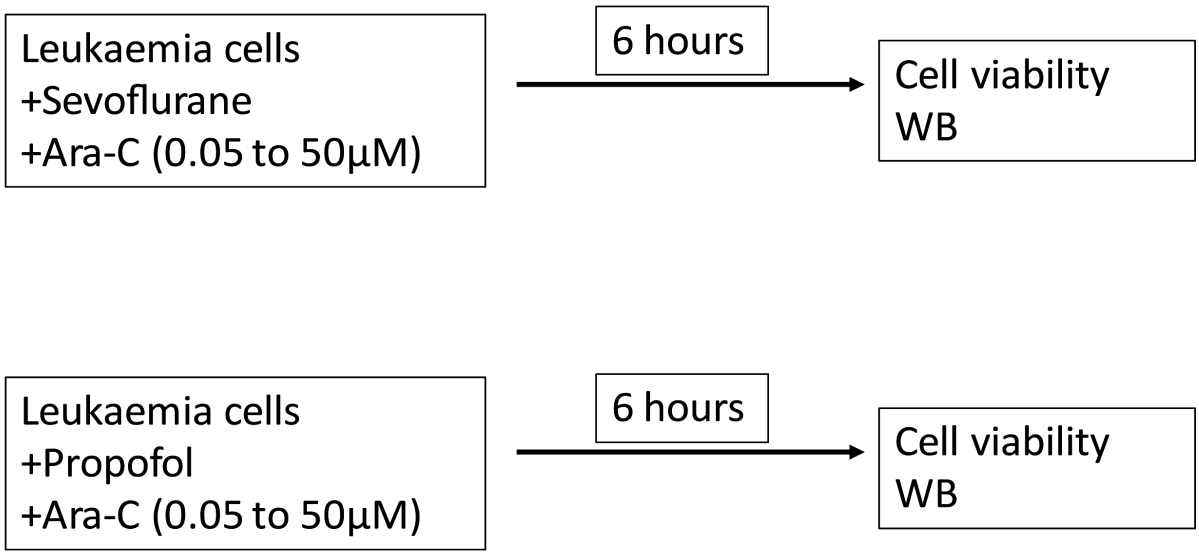

Figure 7.1 *In vitro* experiment design
WB: Western blot

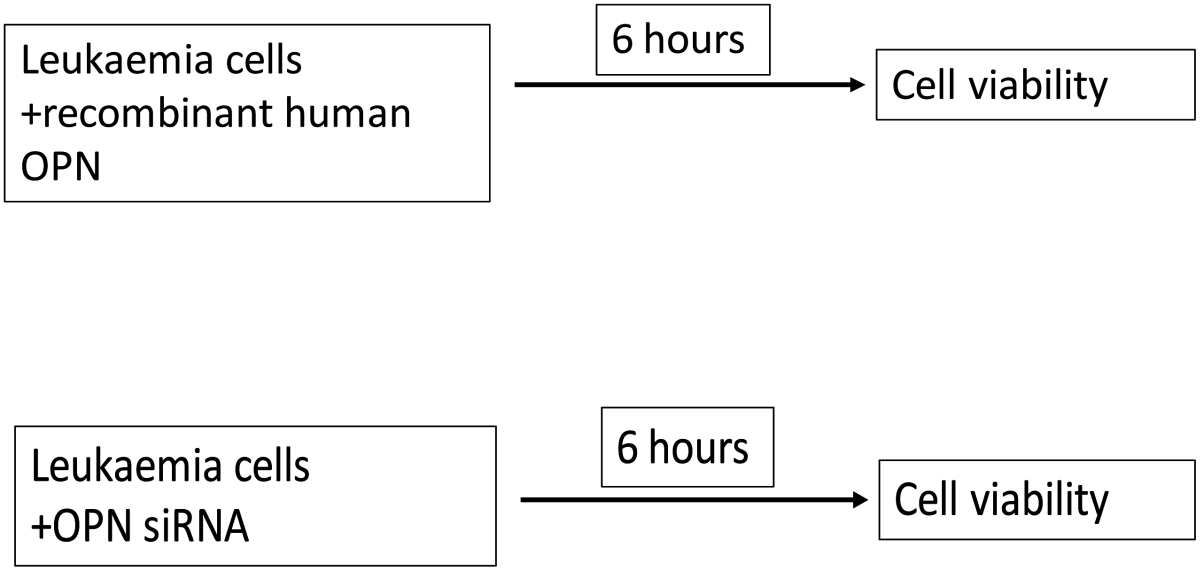

Figure 7.2 *In vitro* experiment design

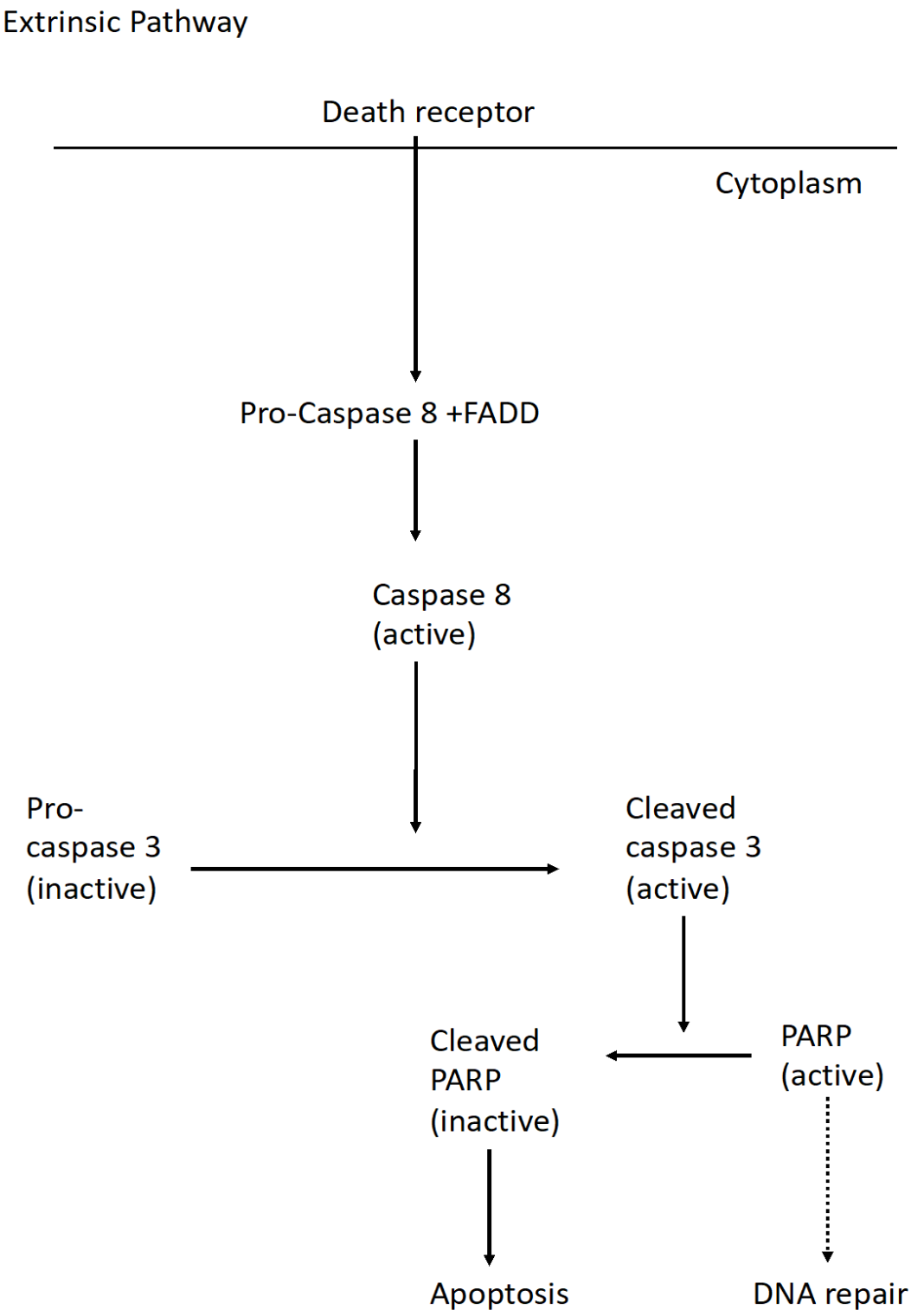

Figure 7.3 Extrinsic pathway of apoptosis
The death ligands bind to transmembrane death receptors present on the cell surface. The binding of ligand triggers receptor clustering on the cell surface. This results the adaptor proteins (FADD) cluster on the cytoplasmic site of the receptors, forming death inducing signalling complex (DISC). DISC then brings procaspase molecules close to one another, activating caspase cascade. Active caspase 8 cleaves pro-caspase 3 to active caspase 3 which then deactivates PARP to form cleaved PARP. Cleaved PARP triggers apoptotic machinery.

7.3 Results

7.3.1 General anaesthetics sensitise leukaemia cells to Ara-C

NALM-6 cells were treated with rising concentrations of Ara-C (0.05μM to 50μM) in combination with propofol (10μg/ml) or sevoflurane (3.6%) for 6 hours. Cell viability data was then obtained by propidium iodide-based flow cytometry analysis. We found a significant shift of the drug response curve to the left after treatment of Ara-C and propofol when compared to treatment of Ara-C alone, indicating enhanced cytotoxicity. Cell death induced by Ara-C increased dramatically from 0.05μM to 5μM then it plateaued between 5 to 50μM (Figure 7.4a). Even at 50μM, Ara-C only induced around 60% of cell death. With the help of propofol, cell death increased to around 70%. Similarly, sevoflurane shifted the drug response curve to the left (Figure 7.4b), indicating enhanced cytotoxicity. At maximum concentration of Ara-C, sevoflurane boosted the cytotoxicity of Ara-C from below 60% to around 70% (Figure 7.4b). Propofol and sevoflurane did not cause cell death in NALM-6 cells (Figure 7.4a and b).

7.3.2 General anaesthetics increase the expression of chemotherapy induced apoptotic markers in leukaemia cells

Following the discovery of the synergistic effect of general anaesthetics and Ara-C, we studied the apoptotic pathways.

As expected, after the treatment of low dose Ara-C (0.1μM) alone, we saw an increase in the expression of cleaved PARP. A reduction in the expression of pro-caspase 3 and an enhancement in the expression of cleaved caspase 8 were also seen (Figure 7.5a). When leukaemia cells were treated in the combination of 10μg/ml propofol and Ara-C, expression of above-mentioned apoptotic markers were altered. Propofol caused an elevation in cleaved PARP expression when compared to Ara-C treatment alone. In addition, elevated cleaved caspase 8 expression was also seen. In addition, pro-caspase 3 expression was further reduced when compared to Ara-C treatment alone (Figure 7.5a). The expression of cleaved PARP and cleaved caspase 8 increased 4-5 folds in Ara-C and propofol treated cells when compared to naïve control cells (Figure 7.5a). Pro-caspase 3 expression was reduced by 50% in propofol and Ara-C treated cells when compared to naïve control cells (Figure 7.5a). The combination treatment of Ara-C and sevoflurane affected the expression of apoptotic markers when compared to Ara-C treatment alone. Sevoflurane and Ara-C treated cells appeared to have a 7-fold increase in the expression of cleaved PARP when compared to naïve control cells (Figure 7.6a). In addition, cells treated with sevoflurane and Ara-C together also had a 3-fold elevation in cleaved caspase 8 and a 50% reduction in pro-caspase 3 expression when compared to naïve control cells (Figure 7.5a). When propofol or sevoflurane was given to NALM-6 cells alone, the expression of pro

caspase 3 was not affected, indicating the treatment of propofol or sevoflurane alone did not induce apoptosis (Figure 7.5 b and Figure 7.6 b).

7.3.3 OPN partially regulates chemoresistance of leukaemia cells

Out of curiosity, we investigated whether OPN may affect the sensitivity of chemotherapy in leukaemia cells.

Cells were treated with 200ng/ml of human OPN and Ara-C for 6 hours, then cell viability was recorded via flow cytometry. When NLAM-6 cells were given 200ng/ml of OPN, the chemo-sensitivity of NALM-6 was reduced dramatically (Figure 7.7a), suggesting a protective effect of OPN. At the maximum concentration of Ara-C (100μM), OPN treatment reduced cell death from roughly 70% to around 50% (Figure 7.7a). When OPN was inhibited by OPN siRNA in NLAM-6 cells, Ara-C induced cell death was increased (Figure 7.7b). This effect was particularly obvious in the mid-range concentrations of Ara-C (0.5 to 10μM) (Figure 7.7b). At the maximum concentration of Ara-C, OPN siRNA treated cells only achieved a very small increase in induced cell cytotoxicity when compared to Ara-C treated cells alone. Human OPN or OPN siRNA alone did not cause cell death in NALM-6 cells (Figure 7.7).

7.4 Discussion

In this chapter, we found propofol and sevoflurane might sensitise leukaemia cells to Ara-C. In addition, we confirmed OPN played a part in chemoresistance of leukaemia cells.

Inducing apoptosis is a primary means for cytotoxicity of Ara-C[220]. We found propofol and sevoflurane alone could not induce any form of cell death in clinically relevant concentrations. However, they seem to have a synergistic effect with chemotherapy. Others have confirmed our data on reduced chemoresistance by propofol[4, 216, 221]. Two mechanisms were studied in those publications including HIF-1 α[216] and NF- κB[221].

Existing research on the effect of sevoflurane on chemoresistance in others cancer cells contradicted our data. My colleagues Ciechanowicz et al found sevoflurane enhanced the chemoresistance of non-small cell lung cancer *in vitro* by using A549 cells[121].

Although we did not study the role of HIF in chemoresistance of leukaemia cells, OPN inhibition and OPN treatment experiments gave us some clues. As illustrated in chapter 6, HIF and OPN formed an autofeedback loop and it could be disrupted by general anaesthetics. It is highly likely that the results we have obtained on reduced chemoresistance by general anaesthetics are, partially, mediated by HIF-1α.

The role of OPN in cancer chemoresistance was briefly studied by us. Given the fact OPN has many splice variants, and they perform various functions in distinct anatomic location, its role in chemoresistance is still under investigation. OPN secreted by cancer cells induced chemoresistance in hepatocellular carcinoma cells via binding to integrin αvß3 and sustaining FoxO3a stability. This eventually led to an increase in autophagy in hepatocellular carcinoma cells *in vitro*[222].

In leukaemia, a recent publication confirmed that thrombin cleaved OPN in BM anchored leukaemia cells in the stem cell niche[148]. The stem cell niche is usually poorly perfused with blood and low in oxygen which is beneficial to stem cell quiescence. However, this provides a physical barrier in BM for leukaemia cells to avoid chemotherapy[148]. It is entirely possible that multiple variants of OPN from different origins e.g. cancer cell secreted OPN and host-derived OPN act together to promote chemoresistance of cancer.

We propose to validate our existing results via *in vivo* studies. Leukaemia bearing SCID mice will be treated with Ara-C or with combination of Ara-C and general anaesthetics for a few weeks to recreate clinical scenarios. Treatment response will be, then, monitored through tail bleed followed by flow cytometry detection of leukaemia cells. In addition, the survival curve for mice treated only with Ara-C and mice treated with both Ara-C plus general anaesthetics will be used to evaluate the effectiveness of general anaesthetics *in vivo*. In addition, the source of OPN (host-derived vs cancer cell-derived) exerting a protective effect against chemotherapy requires further investigation.

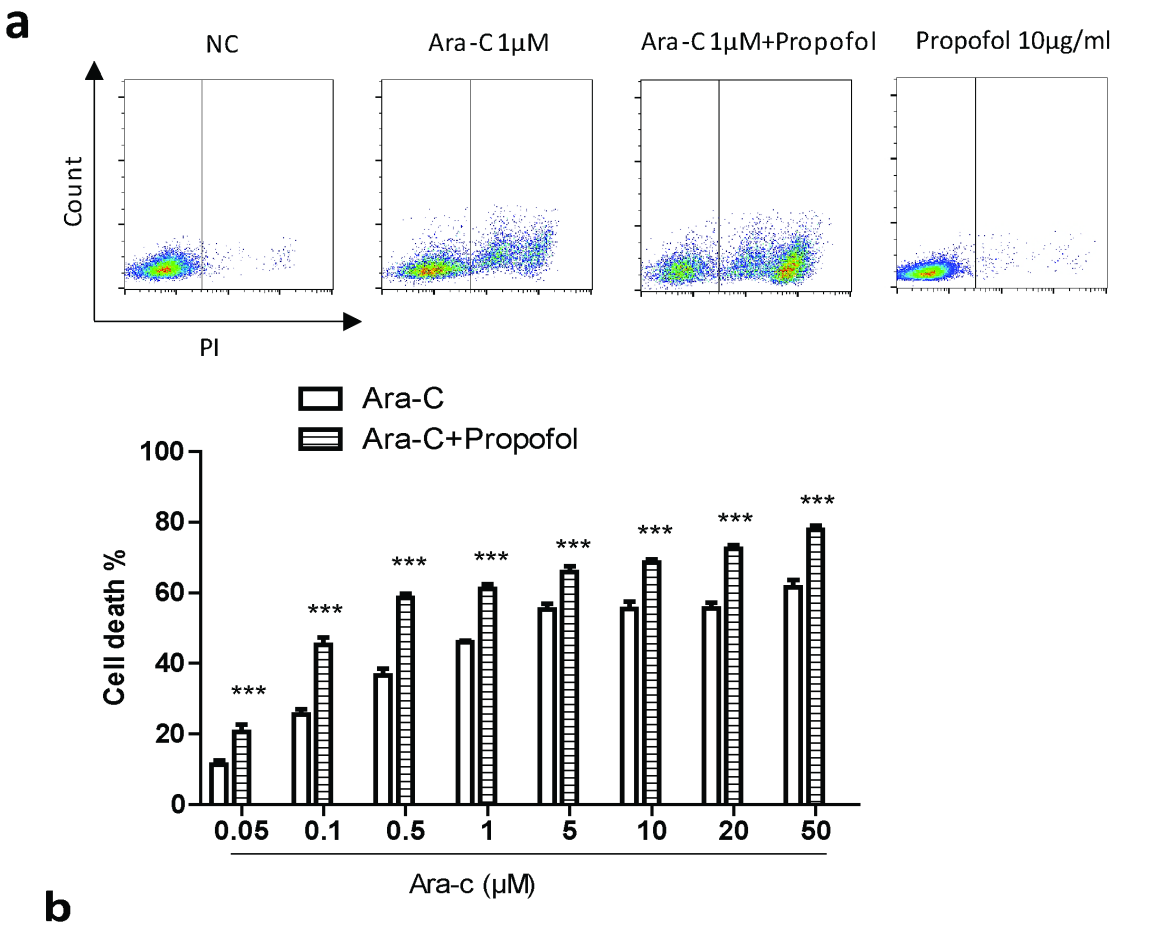
a
NC
Ara-C 1μM
Ara-C 1μM+Propofol
Propofol 10μg/ml
Count
PI
Ara-C
Ara-C+Propofol
Cell death %
100
80
60
40
20
0
***
0.05
0.1
0.5
1
5
10
20
50
Ara-c (μM)

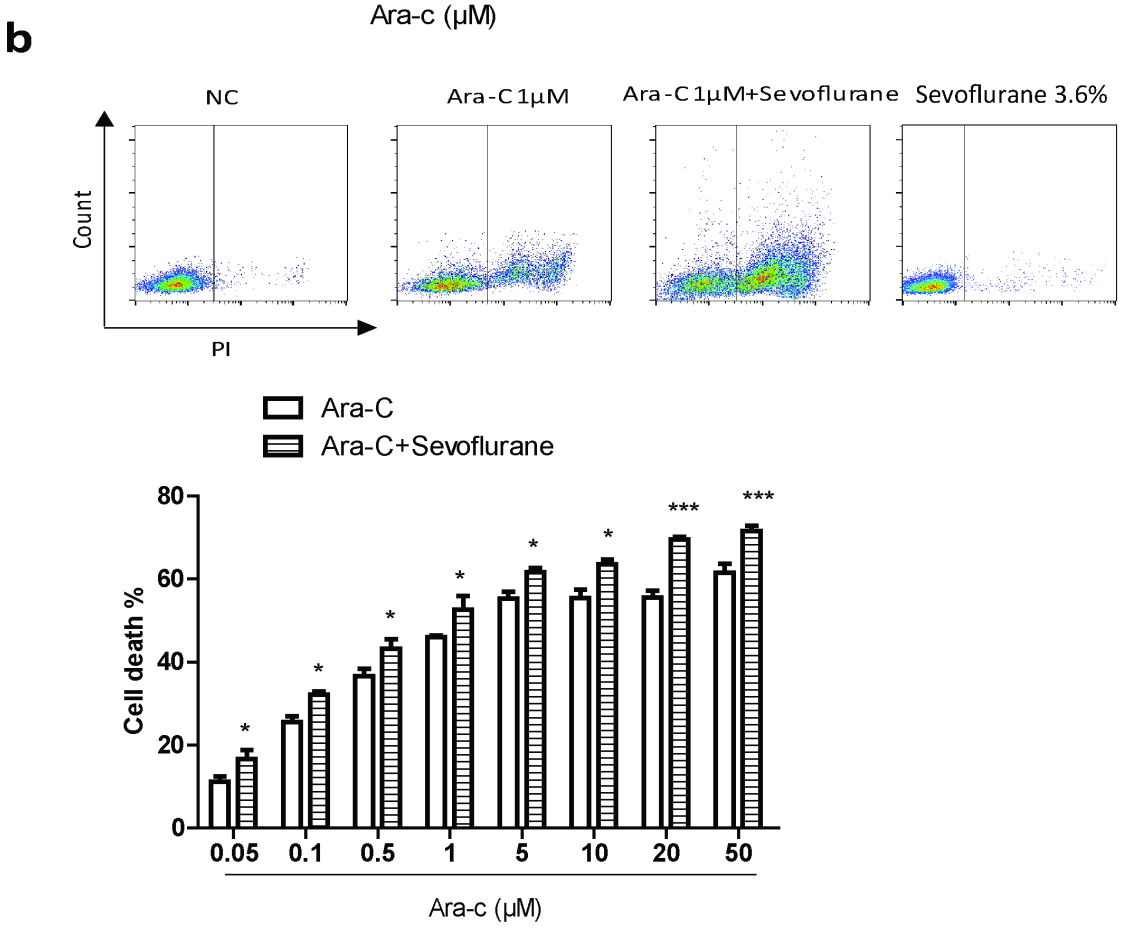
b
NC
Ara-C 1μM
Ara-C 1μM+Sevoflurane
Sevoflurane 3.6%
Count
PI
Ara-C
Ara-C+Sevoflurane
Cell death %
80
60
40
20
0
*
***
0.05
0.1
0.5
1
5
10
20
50
Ara-c (μM)

Figure 7.4 General anaesthetics reduce the chemoresistance of NALM-6 cells
a) Propofol has synergistic effects with Ara-c. NALM-6 cells were treated with 10 μg/ml of propofol and Ara-C (0.05 to 50μM) for 6 hours. Then, cell viability analysis was carried out by flow cytometry. Propofol alone did not induce cell death in NALM-6 cells. Data are shown as mean±s.e.m (n=4). ***P<0.001 vs Ara-C. Data are analysed by two-way ANOVA followed by Bonferroni's post-hoc test. **b)** Sevoflurane has synergistic effects with Ara-c. NALM-6 cells were treated with 3.6% of sevoflurane and Ara-C (0.05 to 50μM) for 6 hours. Then, cell viability analysis was carried out by flow cytometry. Sevoflurane alone did not induce cell death in NALM-6 cells. Data are shown as mean±s.e.m (n=4). *P<0.05, ***P<0.001 vs Ara-C. Data are analysed by two-way ANOVA followed by Bonferroni's post-hoc test.

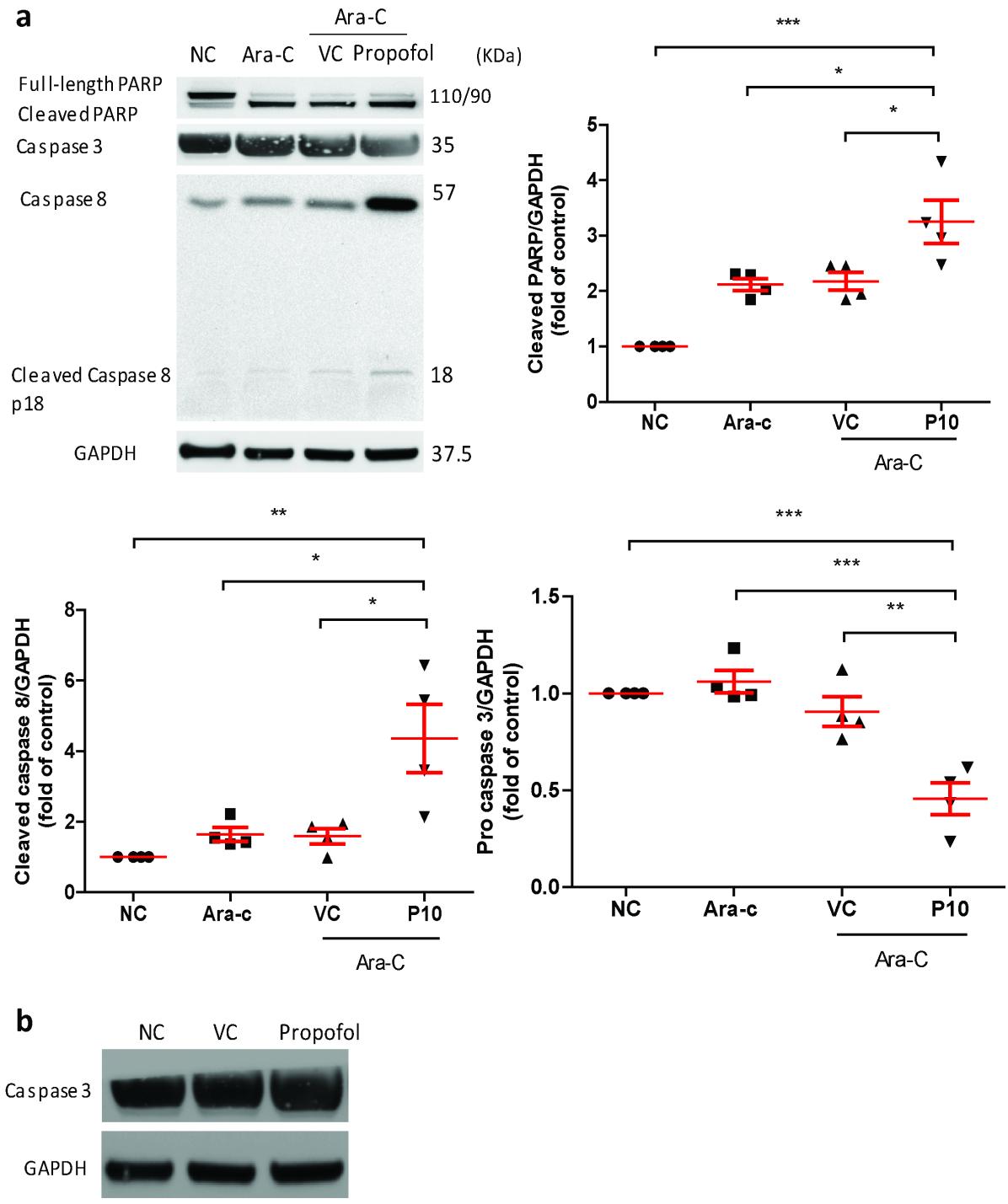

Figure 7.5 Propofol increases the expression of chemotherapy induced apoptotic markers
a) NALM-6 cells were treated with 0.1μM of Ara-C and 10μg/ml of propofol (or intralipid) for 6 hours. Then, cells were harvested for western blot analysis. The expression of cleaved PARP and cleaved caspase 8 were increased. The expression of pro-caspase 3 was reduced. Data are illustrated as mean±s.e.m (n=4). *P<0.05, **P<0.01, ***P<0.001. Data are analysed by one-way ANOVA followed by Bonferroni's post-hoc test. NC: Naïve control, VC: Vehicle control, P10: 10μg/ml of propofol. **b)** NALM-6 cells were treated with 10μg/ml of propofol or intralipid for 6 hours. Then, cells were harvested for western blot analysis. The expression of pro caspase 3 was not affected, indicating propofol alone did not induce apoptosis (n=4).

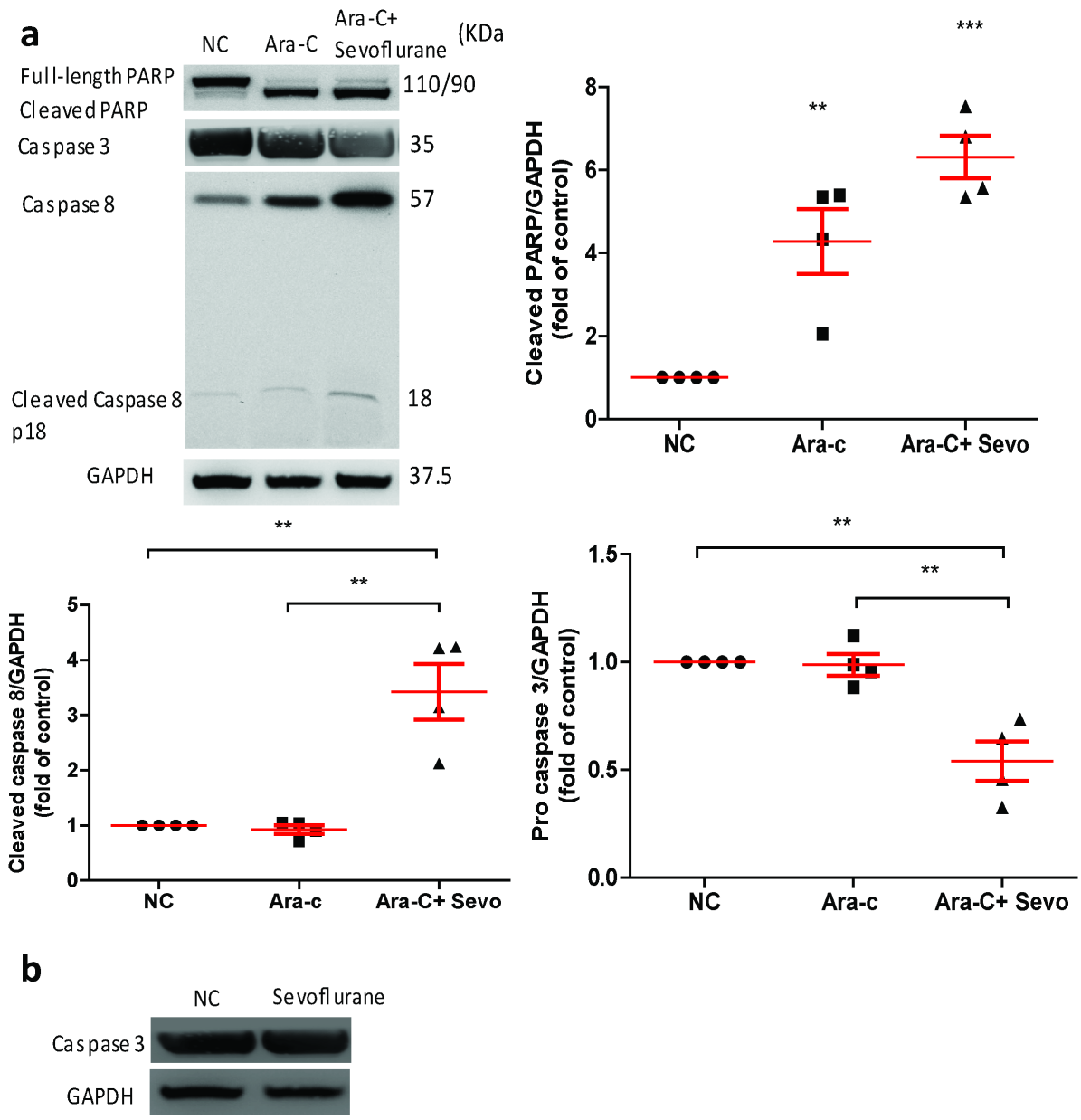

Figure 7.6 Sevoflurane increases the expression of chemotherapy induced apoptotic markers
a) NALM-6 cells were treated with 0.1µM of Ara-C and 3.6% of sevoflurane for 6 hours. Then, cells were harvested for western blot analysis. The Expression of cleaved PARP and cleaved caspase 8 were increased. The expression of procaspase 3 was reduced. Data are illustrated as mean±s.e.m (n=4). **P<0.01, ***P<0.001. Data are analysed by one-way ANOVA followed by Bonferroni's post-hoc test Sevo: 3.6% of sevoflurane. **b)** NALM-6 cells were treated with 3.6% sevoflurane for 6 hours. Then, cells were harvested for western blot analysis. The expression of pro caspase 3 was not affected, indicating sevoflurane alone did not induce apoptosis (n=4).

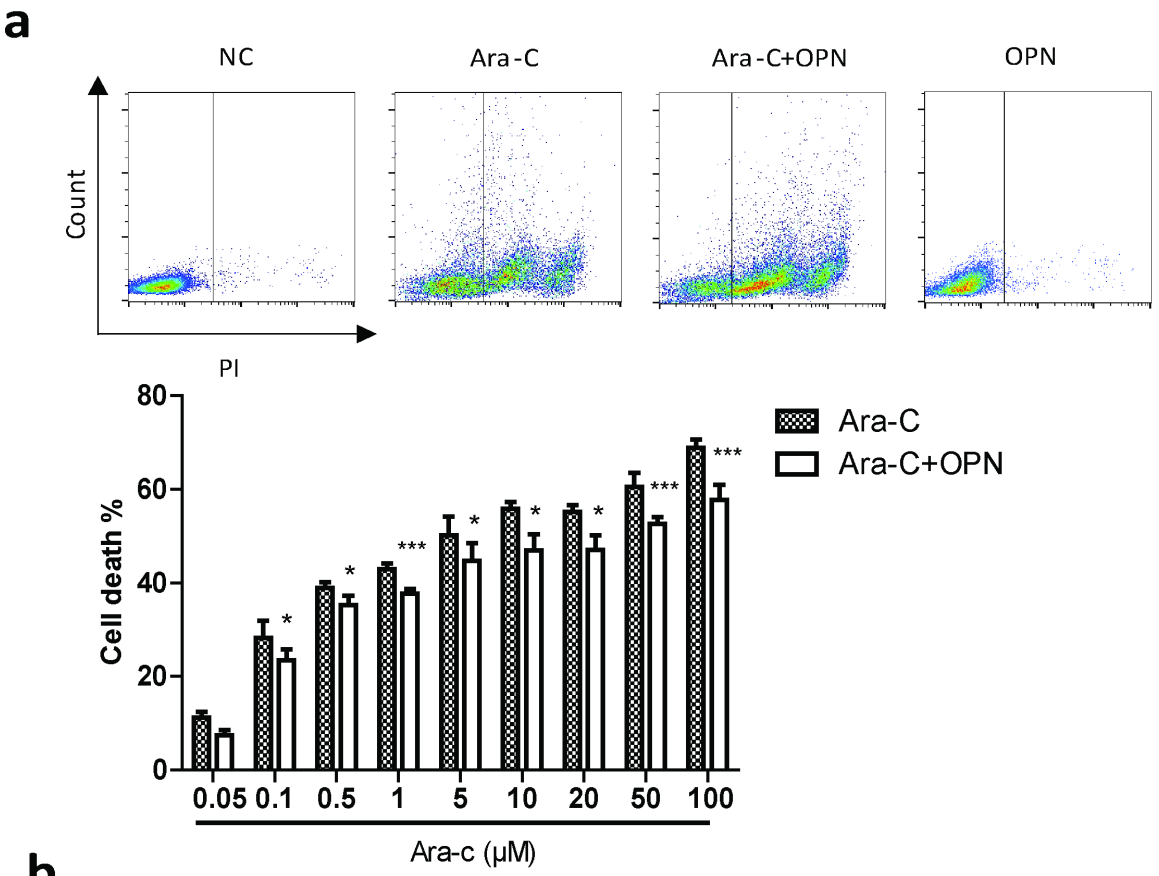
a
NC
Ara-C
Ara-C+OPN
OPN
Count
PI
Cell death %
Ara-C
Ara-C+OPN
0.05 0.1 0.5 1 5 10 20 50 100
Ara-c (μM)

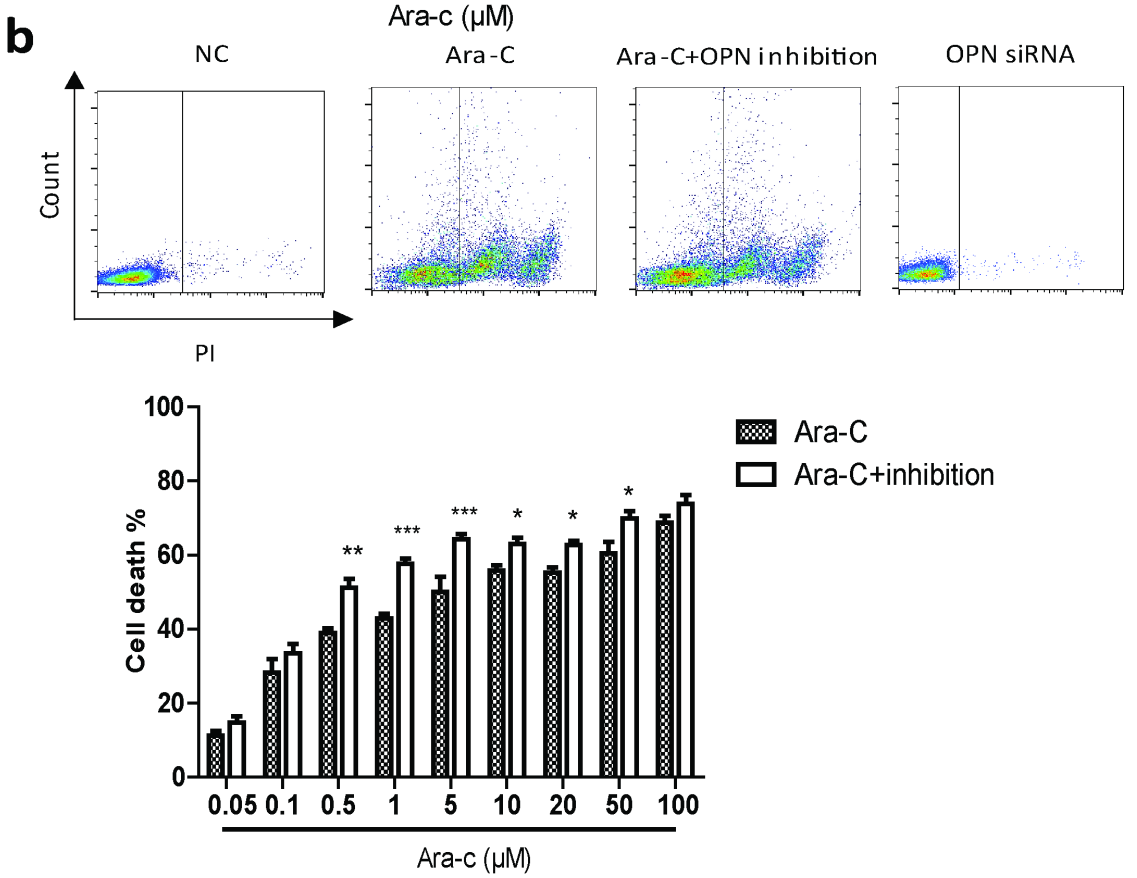
b
NC
Ara-C
Ara-C+OPN inhibition
OPN siRNA
Count
PI
Cell death %
Ara-C
Ara-C+inhibition
0.05 0.1 0.5 1 5 10 20 50 100
Ara-c (μM)

Figure 7.7 OPN regulates the chemoresistance of NALM-6 cells
a) NALM-6 cells were treated with 200ng/ml human recombinant OPN and Ara-C (0.05 to 100μM) for 6 hours. Then, cell viability analysis was carried out by flow cytometry. Human OPN alone did not affect the viability of NALM-6 cells. Data are illustrated as mean±s.e.m (n=4). *P<0.05, ***P<0.001 vs Ara-C. Data are analysed by two-way ANOVA followed by Bonferroni's post-hoc test. **b)** NALM-6 cells were treated with OPN siRNA initially. Then, siRNA treated cells were treated with Ara-c (0.05 to 100μM) for 6 hours. After treatment, cell viability analysis was carried out by flow cytometry. OPN siRNA did not affect the viability of NALM-6 cells. Data are shown as mean±s.e.m (n=4). *P<0.05, **P<0.01, ***P<0.001 vs Ara-C. Data are analysed by two-way ANOVA followed by Bonferroni's post-hoc test.

CHAPTER 8

Final Discussion

8.1 Summary of the findings

This study is the first of its kind to investigate the effects of general anaesthetics on human ALL *in vitro* and *in vivo*. Sevoflurane and propofol were shown to significantly reduce proliferation as determined ki-67 expression and flow cytometry, CXCR4 expression, migration and OPN secretion *in vitro.* In addition, both anaesthetics strongly affected the migration and homing of GFP-NALM-6 cells *in vivo*. Upon further investigation, we found that proliferation, CXCR4 expression, migration and the OPN expression were reduced in ALL cells *in vitro* after the treatment of HIF-1α siRNA. These results suggested that HIF-1α mediated pathways might be responsible for anaesthetics induced molecular changes in ALL cells *in vitro*.

Propofol was shown to reduce the phosphorylation of AKT and ERK. Sevoflurane reduced the phosphorylation of ERK only. General anaesthetics may reduce the expression of HIF-1α through inhibition of PI3K-AKT and ERK pathways. Results are summarised in Figure 8.1.

Chemoresistance study revealed that sevoflurane and propofol exhibited a synergistic effect with Ara-c *in vitro,* as general anaesthetics did not induce apoptosis themselves. The caspase-dependent apoptotic pathways were likely responsible for such effects.

The serum level of leukaemia cells derived OPN was shown to correlate with disease progression *in vivo.*

In addition to HIF-1α mediated mechanisms, we also identified that OPN might regulate some molecular pathways in leukaemia cells. We found that leukaemia cells secreted OPN formed an auto feedback loop with HIF-1α and regulated CXCR4 expression, migration and chemoresistance *in vitro* (Figure 8.2).

8.2 Molecular mechanisms responsible for general anaesthetics induced effects

8.2.1 HIF-1α

The role of HIF-1α in leukaemia is still under investigation. Limited evidence showed increased HIF-1α in human B cell ALL samples was associated with increased angiogenesis and poor outcome[223]. In addition, increased HIF-1α caused an increase in the potential of invasion and migration[135]. Enhanced chemoresistance was found with HIF-1α overexpression[159]. Our results indicated a reduction of HIF-1α resulted in the decrease of migration of ALL cells *in vitro* and *in vivo*. However, a reduction of HIF-1α was not correlated with decreased chemoresistance. Further investigation is still needed.

We found, unexpectedly, both IV and inhalational general anaesthetics reduced the protein expression of HIF-1α. However, most publications demonstrated IV anaesthetics reduced HIF expression whereas inhalational anaesthetics increased HIF expression[4, 108]. The exact reason for the contrasting phenomena is not known but is likely due to molecular actions and unique types of surface

receptor responding to anaesthetics on different cancer cells. Currently, both propofol and sevoflurane are thought to exert their effects on GABA receptors[224, 225]. Sevoflurane enhances the amplitude of responses to low concentrations of GABA and prolongs the duration of GABA mediated synaptic inhibition[224]. Propofol potentiates GABA responses and directly activates $GABA_AR$ function by binding to all α, ß and γ subunits of $GABA_AR$[226]. Propofol has also been shown to inhibit voltage-gated sodium channel NaChBac at multiple sites in bacteria[227] and in nerve terminals isolated from rat neurohypophysis[228]. The anaesthetic binding receptors on cancer cells are yet to be accurately identified for propofol and sevoflurane. The discovery of anaesthetic binding receptors may hold the key to predict the molecular changes induced by anaesthetics. Importantly, it seems a relatively common phenomenon for general anaesthetics to modulate HIF-1α expression across various cancer cell types originated from different tumours in distinct anatomical locations. It is reasonable to assume a generic family of receptor is responsible for such an effect induced by general anaesthetics.

The results we obtained from the anaesthetic recovery time are intriguing. The action of propofol was shown to be short-lived (<24 hours). We then further demonstrated propofol caused a temporary reduction in phosphorylation of ERK and AKT. Sevoflurane, on the other hand, was shown to have a long suppressive effect on the expression of HIF-1α protein even with a short initial exposure. According to our results, sevoflurane acted as a strong inhibitor of ERK phosphorylation with over 24 hours of inhibitory effect.

One publication[138] demonstrated that general anaesthetics did not affect the degradation pathway of HIF. Therefore, we did not investigate HIF-1α protein degradation pathways. There are mainly three pathways leading to HIF-1α protein expression. We found, of all three pathways, only STAT3-JAK was not affected by both sevoflurane and propofol. The phosphorylation of PI3K-AKT and MAPK-ERK were shown to be reduced by general anaesthetics. Several publications agreed with those findings[4, 229-231]. These results indicate that PI3K-AKT and MAPK-ERK pathways may play a role in the inhibitory effect of anaesthetics on HIF-1α expression. Additional experiments involving ERK and AKT inhibitors are needed to confirm that those two pathways are, indeed, responsible for the inhibitory effect of general anaesthetics on HIF-1 α expression.

In addition to HIF-1α, we also studied the expression HIF-1ß. It combines with HIF-1α to form a heterodimer which binds to the promoter region of the target gene. Like most publications, we did not find any significant difference in HIF-1ß expression after anaesthetic treatment. In addition to HIF-1α, some publications found HIF-2α was upregulated upon treatment of isoflurane and led to more malignant RCC phenotypes *in vitro*[108, 232]. Although the role of HIF-2α in leukaemia is not well defined, it would be interesting to investigate whether general anaesthetics may affect expression of HIF-2α in ALL cells in the future study.

8.2.2 Proliferation

In our study, we found both propofol and sevoflurane reduced the proliferation of NLAM-6 cells in HIF-1α mediated pathway. In addition, we established proliferation was positively correlated with HIF-1α in B-ALL cells. The role of HIF-1α in the proliferation of haematological cells is complex. On one hand, there is clear evidence that HIF-1α stabilisation in hemopoietic stem cells reduces cycling, proliferation and trafficking *in vivo*[233]. Essentially, with increased HIF-1α protein synthesis, hemopoietic stem cells commit cellular quiescence and it has been shown to be vital in maintaining the stem cell pool[233]. On the other hand, experiments on ALL cell lines showed increased HIF-1α activated Notch 1 signalling and eventually led to accelerated cell proliferation[234].

The techniques we deployed to investigate the proliferation were flow cytometry and ki-67 staining. Those two techniques are classical and accurate ways to detect cell proliferation. In addition to those two techniques, we may assess the expression of cyclin D and cyclin E in future experiments to confirm existing results.

8.2.3 CXCR4

The important role of CXCR4 in migration and homing of ALL cells has been investigated extensively[139, 235, 236]. Tavor et al showed CXCR4-SDF-1 axis was responsible for the migration of leukaemia cells *in vivo*[236]. In addition, ablation of CXCR4 resulted in poor engraftment of leukaemia cells *in vivo* but neutralisation of CXCR4 did not affect engraftment of human progenitors[236]. A few years later, spikins et al found that the homing of ALL cells in BM was entirely dependent on CXCR4[235].

Our *in vitro* data exhibited clearly that both propofol and sevoflurane reduced migration of leukaemia cells. Many current publications suggest that propofol reducs migration and invasion of cancer cells [169, 170, 186, 188, 237, 238]. However, existing data on sevoflurane and migration is more complex with contrasting evidence. Ecimovic P et al demonstrated that sevoflurane potentially increased migration of breast cancer cells *in vitro*[191]. Gao C et al recently illustrated that sevoflurane inhibited migration and invasion of glioma cells *in vitro* [239].

The mechanism by which general anaesthetics affect migration is under investigation in different cancer models. We found that general anaesthetics reduce migration of leukaemia cells via decreasing surface CXCR4 expressions. Published data on an ovarian cancer model stated otherwise. Iwasaki M et al found that volatile general anaesthetics (isoflurane, sevoflurane and desflurane) strongly increased CXC4 receptor expression and migration of ovarian cancer cells[122].

We found CXCR4 was a downstream target of HIF-1α. This pathway has been implicated in leukaemia and other cancer types. Valsecchi R et al showed HIF-1α was upstream of CXCR4 in chronic lymphoblastic leukaemia (CLL) and it regulated interactions between CLL cells and stromal

compartments through CXCR4[240]. Furthermore, a recent publication demonstrated that CXCR4 and HIF-1α formed a feed-forward loop in RCC cancer and the feed-forward loop promoted metastasis[184]. In their model, the nuclear translocation of CXCR4 enhanced transcriptional gene expression of HIF-1α[184]. Enhanced HIF-1α led to an increase in CXCR4 expression.

In addition to CXCR4, we also studied other receptors include VEGF receptor and glucose receptor (GLUT-1) (data not shown). However, only CXCR4 was responsive to the treatment of general anaesthetics.

Our *in vitro* data of migration were successfully validated *in vivo* by using intravital microscopy. The *in vivo* validation method (intravital microscopy) has not been seen in any previous publications regarding the effect of general anaesthetics on migration. We initially attempted to stain NALM-6 cells with PE-CD19, APC-CD10 and DiD dye. However, the resolution of direct staining was relatively poor. This rendered us to transduce NALM-6 cells with lentivirus packed GFP, which dramatically increased the resolution of images.

As expected, propofol and sevoflurane pre-treated GFP-NALM-6 cells had a huge reduction in migration displacement and migration speed. In addition, homing of leukaemia cells in BM was disrupted by general anaesthetics. Data of *in vivo* homing assay from other publications did not use the distance between an individual cell to nearest endosteal surface as a measure for homing location[139, 148, 235]. This resulted in no tangible comparison in terms of homing locations in BM between untreated cells and treated cells. The measurement of the distance between an individual cell and stromal compartment (vessel and bone) was initially pioneered by my co-supervisor (Professor Cristina Lo Celso)[241]. Distance measurement proved to be a more accurate means of assessing homing location as it can provide a clear and tangible comparison between naïve cells and treated cells.

8.2.4 Osteopontin

OPN (or secreted phosphoprotein 1) is a secreted protein with a variety of functions. Its functions include cell adhesion, migration, immune responses, tissue repair and bone minimisation. In BM, OPN is a non-collagenous protein present in bone matrix. Initially, OPN is thought to be only secreted by osteoblasts and stem cells[145]. However, both our results and a recent publication indicated that OPN can be secreted by B-ALL cells[148]. In addition to this finding, we observed the serum level of OPN was correlated with ALL disease progression (monitored by BM and blood samples). In AML patients, the serum OPN level was shown to correlate with AML disease advancement and OPN predicted prognosis and survival of AML patients[205].

Our *in vitro* data showed that both propofol and sevoflurane greatly reduced the secretion of OPN. A recent publication showed the opposite data. They demonstrated sevoflurane increased OPN expression in non-small cell lung cancer model[121]. The reason for this difference is likely due to different cancer type but warrants further investigation.

A positive autofeedback loop between HIF-1α and OPN was also identified. Leukaemia cells derived OPN was shown to increase HIF-1α protein synthesis via PI3K-AKT mediated mechanisms. A similar loop was suggested in a breast cancer model. However, in the breast cancer model, the elevated OPN expression was achieved through hypoxia only and it was in a HIF-1α independent manner[150]. According to our data, OPN is a direct downstream target of HIF which was implicated in previous clinical studies[242]. We also found that OPN knocked down cells had a dramatic reduction in migration and they were more sensitive to chemotherapy by Ara-C.

Taken together, all results suggested OPN, to some degree, positively regulated HIF-1α expression, migration and chemoresistance of leukaemia cells.

The importance of our findings lies in the fact that OPN is not only a structural anchorage protein in BM but also it acts as non-structural protein, activating protective mechanism for leukaemia cells.

Unfortunately, we did not study which integrin was responsible for OPN induced changes. NALM-6 cells do not have surface CD44 and they have a very low abundance of αV and α9ß1 integrin[148]. We suspect that α4ß1 is the most likely candidate. An *in vitro* interaction assay should be set up in the future experiment to find the exact integrin OPN binds to.

In vivo replication of our results is very important. We propose to study the homing and migration in OPN knocked out leukaemia cells by OPN shRNA *in vivo*. Furthermore, OPN knock out mice are used to investigate whether stromal-derived OPN plays any part in the protective effect of OPN. Finally, we propose to investigate whether an OPN specific inhibitor improves the outcome of ALL disease-bearing mice and whether it can be used as a novel targeted treatment for ALL.

8.2.5 Chemoresistance

Resistance to chemotherapy is the major cause of relapse in leukaemia treatment. In ALL, every time a patient has a relapse, the likelihood of subsequent remission is reduced by half.

In my PhD project, we studied the apoptosis pathways associated with Ara-C induced cell death in leukaemia cells and we discovered that general anaesthetics reduced leukaemia chemoresistance *in vitro* via potentiating caspase-based apoptosis. However, clinically relevant concentrations of propofol and sevoflurane do not induce any form of cell death in leukaemia cells.

Mounting evidence from neuroprotection studies showed that propofol and sevoflurane have long been associated with inducing apoptosis[243-245] on cells in CNS by activating both intrinsic and extrinsic

pathways of apoptosis. In cancer models, propofol was shown to induce apoptosis in ovarian cancer cells *in vitro*[246]. Sevoflurane was also demonstrated to induce apoptosis in lung cancer cells *in vitro*[247]. In terms of chemoresistance, one recent publication[4] also indicated that propofol reduced chemoresistance by increasing the cytochrome-c release in prostate cancer cells[4]. Another publication showed opposite data with sevoflurane enhancing chemoresistance in non-small cell lung cancer *in vitro*[121].

Future investigations are needed into this. It is interesting to investigate the role of HIF-1α in general anaesthetic mediated chemoresistance of leukaemia cells. We did briefly consider the HIF-1α when we studied the potential autophagy changes induced by general anaesthetics as autophagy is a known downstream target of HIF-1α[248]. Unfortunately, we were unable to observe autophagy induced by general anaesthetics (data not shown) in ALL cells. Given the fact, OPN regulates chemoresistance in ALL cells and OPN forms an auto feedback loop with HIF-1α, all indicating that the role of HIF-1α in ALL chemoresistance is important.

The interaction between leukaemia cells and the stromal compartment in patients undergoing chemotherapy is emerging as an important research topic. Recent research revealed novel chemoresistance mechanism. Structural proteins e.g. OPN and members of cell adhesion molecules family in BM matrix anchor cancer cells in distinct anatomic locations with poor perfusion, which creates a physical barrier for chemotherapeutic agents[148, 249]. In ALL, OPN was identified as one of those anchoring molecules[148]. However, in this publication, the source of OPN was ambiguous as they did not specify the origin of OPN (stromal-derived OPN or leukaemia derived OPN). According to our data, OPN secretion is reduced by general anaesthetics. Therefore, we hypothesise that general anaesthetics may alter the interaction between leukaemia cells and BM, thus making leukaemia cells more accessible to chemotherapy. In order to test this hypothesis, we will develop a treatment protocol consisting of chemotherapy and general anaesthetics for ALL disease-bearing mice. Then, we analyse the distance between leukaemia cells and BM stromal compartments (e.g. blood vessels and bone). The measurement data will be compared between general anaesthetics and chemotherapy-treated mice and chemotherapy-treated only mice.

In addition, the source of OPN responsible for anchorage is currently unknown. In future experiments, OPN knockout mice will be used to specify the source of OPN responsible for anchoring leukaemia cells.

8.3 Clinical implication

Most of the evidence regarding which general anaesthetic is beneficial to the outcome of cancer patients comes from pre-clinical and retrospective data. To this date, only one study is published with

the primary outcome set as cancer recurrence[90]. It found that paravertebral block and propofol did not reduce breast cancer recurrence after potentially curative surgery compared with sevoflurane and opioids[90].

In addition, there are a few ongoing trials investigating the question of which general anaesthetic is beneficial to the outcome of cancer patients. More importantly, they use cancer survival outcome or biomarkers associated with cancer prognosis as a primary or secondary outcome. Taking one trial as an example: this particular study with trial identifier: NCT03005860 is studying the serum biomarkers associated with breast cancer malignancy (include HIF-1α, VEGF, TGF, IL-17, IFN-g, TNF- α, IL-6 and MMP2) after (blood taken 24 hours post-surgery) breast cancer surgery. 40 patients are randomly put into propofol (total intravenous anaesthetics, TIVA) receiving group and sevoflurane receiving group. The trial is still ongoing with no results published. Longer-term follow-up is still needed to evaluate overall survival and occurrence of free survival in two groups receiving different general anaesthetics. Currently, there is no guidance to anaesthetists on which anaesthetic is beneficial to cancer patients in terms of cancer outcome. The use of anaesthetics is entirely down to each anaesthetist's belief, training and local capabilities. It is important we build upon our existing data and push for well-designed clinical trials. Ideally, anaesthetics should be stratified to different cancer patients according to their effects on cancer cells to improve patient outcome.

However, as far as general anaesthetics and cancer are concerned, there are mainly 2 challenges

1) There are over 100 cancer types in general. It is unrealistic to understand the effects of general anaesthetics on each one of them including subtypes in a relatively short time frame. According to WHO classification, there are 13 subtypes just in ALL with each one having its own genetic abnormalities[250]. Each subtype with different genetic abnormalities may have different responses to general anaesthetics.

2) Anaesthetics and other drugs are usually given in combination to achieve analgesia, amnesia, immobility, hypnosis and paralysis. No single anaesthetic can achieve all 5 properties. This combined use of anaesthetics may buffer each other's effects on cancer cells. For example, opioids are commonly used during surgery and procedures with general anaesthetics and they have been shown to influence cancer malignancy and metastasis[119]. One recent publication demonstrated that morphine increased cellular proliferation of Lewis lung carcinoma cells *in vitro* via the μ-opioid receptor[251]. One retrospective review[2] demonstrated the benefits of TIVA over inhalational general anaesthetics in breast cancer patients. However, it is not clear whether the source of the benefit arises directly from the avoidance of opioids in the TIVA group or an added benefit afforded by TIVA.

The clinical importance of our work is clear. Many ALL patients receive general anaesthetics 2-3 times per week during treatment. It provides sufficient opportunities for general anaesthetics to have

contact with leukaemia cells in the blood and BM. Importantly, our chemoresistance data showed synergistic effects between general anaesthetics and Ara-C. This result is particularly useful in a clinical setting. In leukaemia, intrathecal chemotherapy requires frequent use of general anaesthetics[252].

We hope the results from this PhD project can inspire further research into this important yet neglected research area. More importantly, we hope our data may encourage clinical trials in the near future and possibly modify clinical practice.

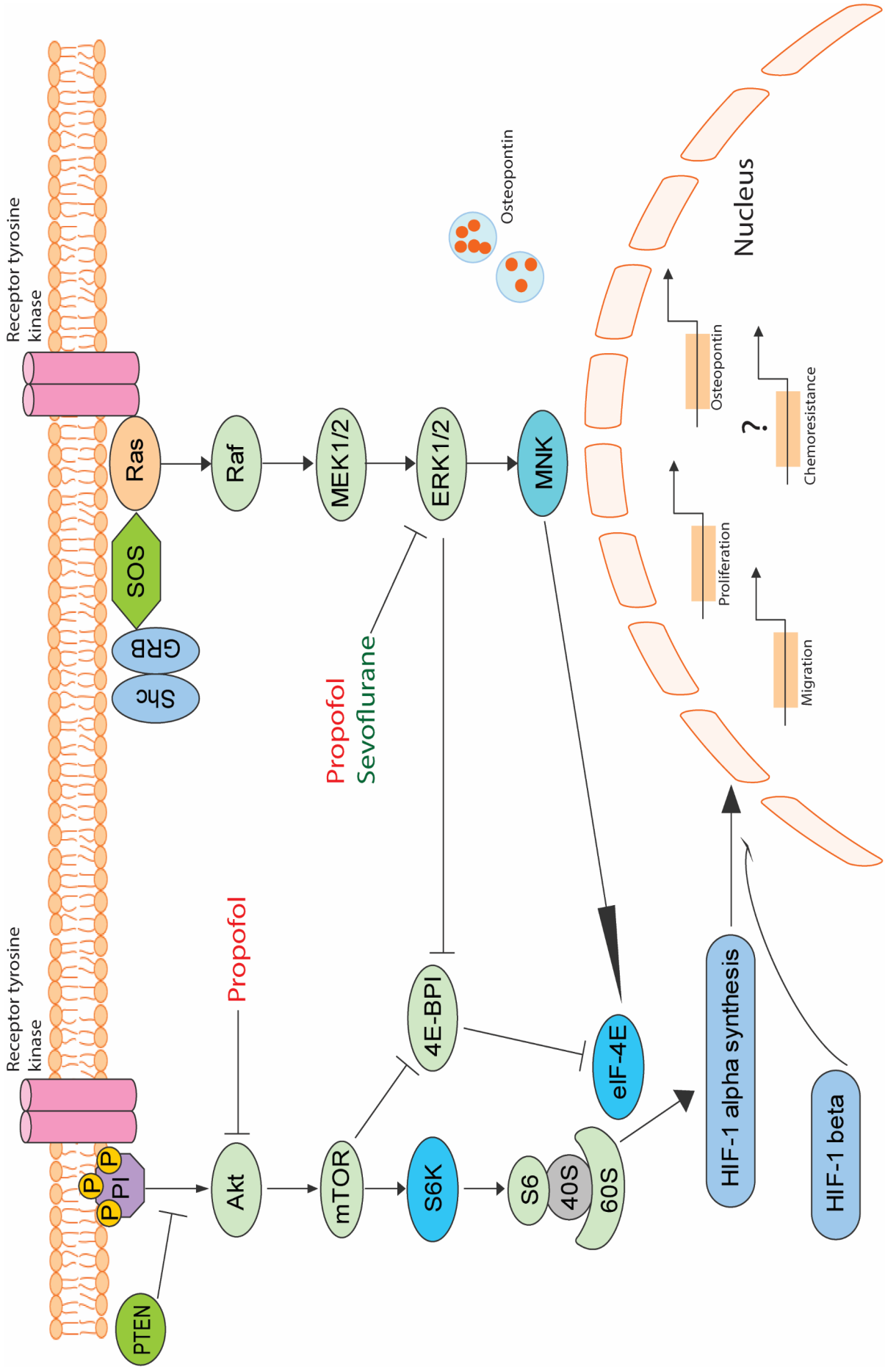
Receptor tyrosine kinase
Ras
SOS
GRB
Shc
Raf
MEK1/2
ERK1/2
MNK
Osteopontin
Nucleus
Osteopontin
?
Chemoresistance
Proliferation
Migration
Propofol
Sevoflurane
Receptor tyrosine kinase
PI
P
P
Akt
Propofol
mTOR
4E-BPI
eIF-4E
S6K
S6
40S
60S
HIF-1 alpha synthesis
HIF-1 beta
PTEN

Figure 8.1 General anaesthetics may reduce HIF-1α through MAPK-ERK and PI3K-AKT pathways
Two HIF-1α upstream pathways are usually mutated in B-ALL cells. Consistent activation of those two pathways contribute to elevated level of HIF-1α. Propofol inhibits the phosphorylation of both AKT and ERK 1/2. However, sevoflurane only inhibits the phosphorylation of ERK1/2. HIF-1ß expression and HIF-1α protein degradation are not affected by general anaesthetics. HIF siRNA experiemts reveal that proliferation, migration and osteopontin expression are downstream targets of HIF-1α in B-ALL cells. It is not clear whether molecular pathways associated with chemoresistance is a downstream target of HIF-1α. General anaesthetics reduce proliferation, migration, osteopontin expression and chemoresistance in B-ALL cells. The inhibitory effect of general anaesthetics on proliferation, migration and osteopontin expression may be due to HIF-1α mediated mechanisms.

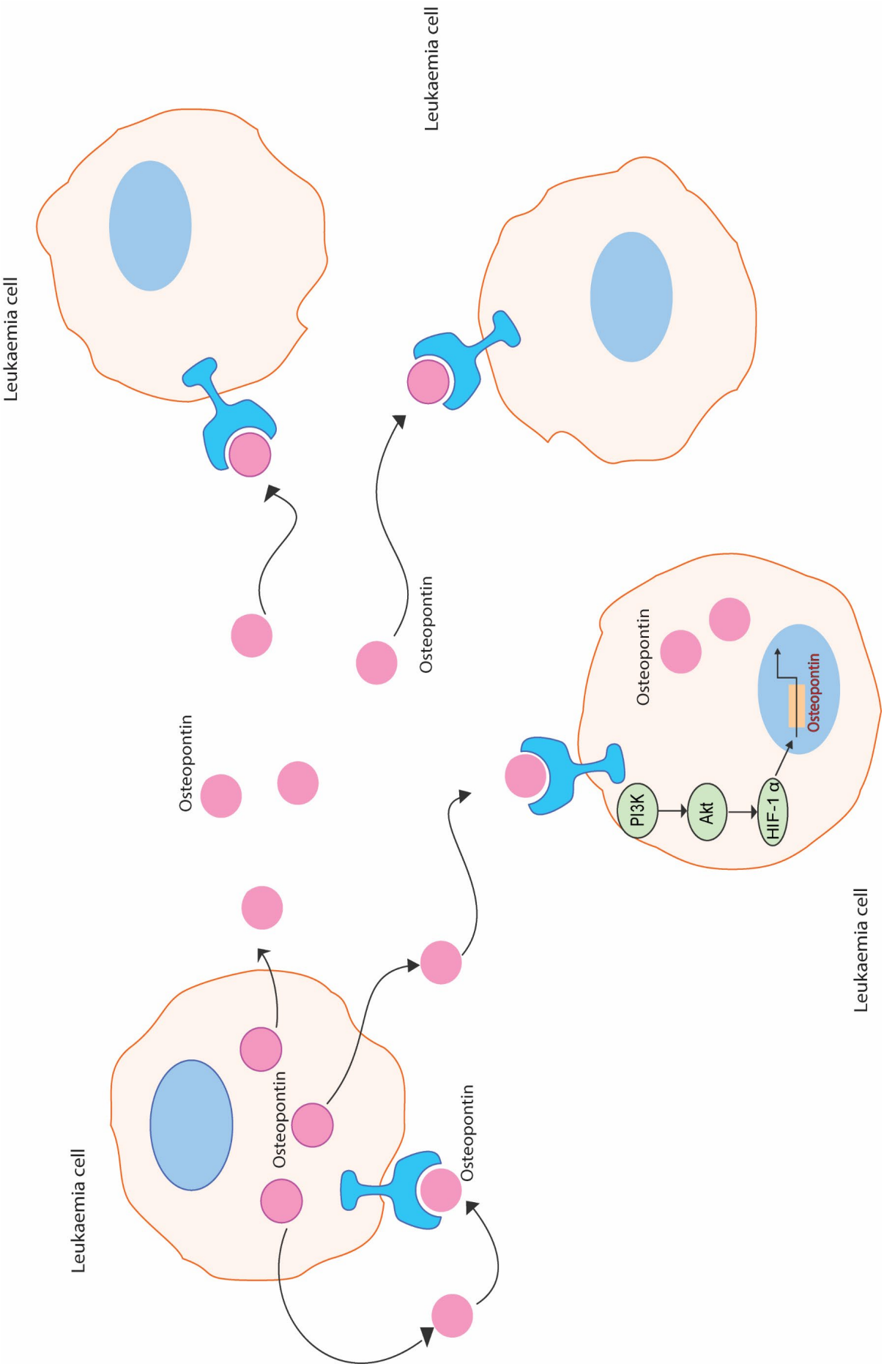
Leukaemia cell
Leukaemia cell
Osteopontin
Osteopontin
Osteopontin
Osteopontin
Leukaemia cell
Leukaemia cell
Osteopontin
PI3K
Akt
HIF-1 α
Osteopontin

Figure 8.2 Osteopontin forms an auto feedback loop with HIF-1α
OPN secreted by neighbouring leukaemia cells and self-secreted OPN activate PI3K by phosphorylating AKT. The phosphorylation of AKT leads to an increased gene transcription of HIF-1α which then, leads to an increased secretion of OPN. In addition to OPN, the increased expression of HIF-1α activates many other downstream targets. However, we cannot specific which surface receptor is responsible for OPN binding. In addition, we do not know whether stromal derived OPN contribute to this process.

Reference

1. Yap A, Lopez-Olivo MA, Dubowitz J, Hiller J, Riedel B, Global Onco-Anesthesia Research Collaboration G. Anesthetic technique and cancer outcomes: a meta-analysis of total intravenous versus volatile anesthesia. Can J Anaesth. 2019;66(5):546-61.
2. Yoo S, Lee HB, Han W, Noh DY, Park SK, Kim WH, et al. Total Intravenous Anesthesia versus Inhalation Anesthesia for Breast Cancer Surgery: A Retrospective Cohort Study. Anesthesiology. 2019;130(1):31-40.
3. Wigmore TJ, Mohammed K, Jhanji S. Long-term Survival for Patients Undergoing Volatile versus IV Anesthesia for Cancer Surgery: A Retrospective Analysis. Anesthesiology. 2016;124(1):69-79.
4. Huang H, Benzonana LL, Zhao H, Watts HR, Perry NJ, Bevan C, et al. Prostate cancer cell malignancy via modulation of HIF-1alpha pathway with isoflurane and propofol alone and in combination. Br J Cancer. 2014;111(7):1338-49.
5. Hunger SP, Mullighan CG. Acute Lymphoblastic Leukemia in Children. N Engl J Med. 2015;373(16):1541-52.
6. Inaba H, Greaves M, Mullighan CG. Acute lymphoblastic leukaemia. Lancet. 2013;381(9881):1943-55.
7. Lim JY, Bhatia S, Robison LL, Yang JJ. Genomics of racial and ethnic disparities in childhood acute lymphoblastic leukemia. Cancer. 2014;120(7):955-62.
8. Pui CH, Evans WE. A 50-year journey to cure childhood acute lymphoblastic leukemia. Semin Hematol. 2013;50(3):185-96.
9. Pui CH, Robison LL, Look AT. Acute lymphoblastic leukaemia. Lancet. 2008;371(9617):1030-43.
10. Mori H, Colman SM, Xiao Z, Ford AM, Healy LE, Donaldson C, et al. Chromosome translocations and covert leukemic clones are generated during normal fetal development. Proc Natl Acad Sci U S A. 2002;99(12):8242-7.
11. Ma X, Edmonson M, Yergeau D, Muzny DM, Hampton OA, Rusch M, et al. Rise and fall of subclones from diagnosis to relapse in pediatric B-acute lymphoblastic leukaemia. Nat Commun. 2015;6:6604.
12. Zhang J, Mullighan CG, Harvey RC, Wu G, Chen X, Edmonson M, et al. Key pathways are frequently mutated in high-risk childhood acute lymphoblastic leukemia: a report from the Children's Oncology Group. Blood. 2011;118(11):3080-7.
13. Buitenkamp TD, Izraeli S, Zimmermann M, Forestier E, Heerema NA, van den Heuvel-Eibrink MM, et al. Acute lymphoblastic leukemia in children with Down syndrome: a retrospective analysis from the Ponte di Legno study group. Blood. 2014;123(1):70-7.
14. Nachman JB, Heerema NA, Sather H, Camitta B, Forestier E, Harrison CJ, et al. Outcome of treatment in children with hypodiploid acute lymphoblastic leukemia. Blood. 2007;110(4):1112-5.
15. Russell LJ, Capasso M, Vater I, Akasaka T, Bernard OA, Calasanz MJ, et al. Deregulated expression of cytokine receptor gene, CRLF2, is involved in lymphoid transformation in B-cell precursor acute lymphoblastic leukemia. Blood. 2009;114(13):2688-98.
16. Russell LJ, De Castro DG, Griffiths M, Telford N, Bernard O, Panzer-Grumayer R, et al. A novel translocation, t(14;19)(q32;p13), involving IGH@ and the cytokine receptor for erythropoietin. Leukemia. 2009;23(3):614-7.
17. Clappier E, Auclerc MF, Rapion J, Bakkus M, Caye A, Khemiri A, et al. An intragenic ERG deletion is a marker of an oncogenic subtype of B-cell precursor acute lymphoblastic

leukemia with a favorable outcome despite frequent IKZF1 deletions. Leukemia. 2014;28(1):70-7.
18. Roberts KG, Li Y, Payne-Turner D, Harvey RC, Yang YL, Pei D, et al. Targetable kinase-activating lesions in Ph-like acute lymphoblastic leukemia. N Engl J Med. 2014;371(11):1005-15.
19. Coustan-Smith E, Sancho J, Hancock ML, Boyett JM, Behm FG, Raimondi SC, et al. Clinical importance of minimal residual disease in childhood acute lymphoblastic leukemia. Blood. 2000;96(8):2691-6.
20. Campana D. Minimal residual disease monitoring in childhood acute lymphoblastic leukemia. Curr Opin Hematol. 2012;19(4):313-8.
21. Borowitz MJ, Devidas M, Hunger SP, Bowman WP, Carroll AJ, Carroll WL, et al. Clinical significance of minimal residual disease in childhood acute lymphoblastic leukemia and its relationship to other prognostic factors: a Children's Oncology Group study. Blood. 2008;111(12):5477-85.
22. Piller G. Leukaemia - a brief historical review from ancient times to 1950. Br J Haematol. 2001;112(2):282-92.
23. Minot GR, Buckman TE, Isaacs R. CHRONIC MYELOGENOUS LEUKEMIA. Chicago: American Medical Association; 1924.
24. Farber S, Diamond LK. Temporary remissions in acute leukemia in children produced by folic acid antagonist, 4-aminopteroyl-glutamic acid. N Engl J Med. 1948;238(23):787-93.
25. Seibel NL. Acute lymphoblastic leukemia: an historical perspective. Hematology Am Soc Hematol Educ Program. 2008:365.
26. Pui CH, Evans WE. A 50-Year Journey to Cure Childhood Acute Lymphoblastic Leukemia. Seminars in Hematology. 2013;50(3):185-96.
27. Bhatia S, Landier W, Hageman L, Kim H, Chen Y, Crews KR, et al. 6MP adherence in a multiracial cohort of children with acute lymphoblastic leukemia: a Children's Oncology Group study. Blood. 2014;124(15):2345-53.
28. Krull KR, Brinkman TM, Li C, Armstrong GT, Ness KK, Srivastava DK, et al. Neurocognitive outcomes decades after treatment for childhood acute lymphoblastic leukemia: a report from the St Jude lifetime cohort study. J Clin Oncol. 2013;31(35):4407-15.
29. Nguyen K, Devidas M, Cheng SC, La M, Raetz EA, Carroll WL, et al. Factors influencing survival after relapse from acute lymphoblastic leukemia: a Children's Oncology Group study. Leukemia. 2008;22(12):2142-50.
30. Kim JY, Im SA, Lee JH, Lee JW, Chung NG, Cho B. Extramedullary Relapse of Acute Myeloid and Lymphoid Leukemia in Children: A Retrospective Analysis. Iran J Pediatr. 2016;26(3):e1711.
31. Mullighan CG, Zhang J, Kasper LH, Lerach S, Payne-Turner D, Phillips LA, et al. CREBBP mutations in relapsed acute lymphoblastic leukaemia. Nature. 2011;471(7337):235-9.
32. Tzoneva G, Perez-Garcia A, Carpenter Z, Khiabanian H, Tosello V, Allegretta M, et al. Activating mutations in the NT5C2 nucleotidase gene drive chemotherapy resistance in relapsed ALL. Nat Med. 2013;19(3):368-71.
33. Li B, Li H, Bai Y, Kirschner-Schwabe R, Yang JJ, Chen Y, et al. Negative feedback-defective PRPS1 mutants drive thiopurine resistance in relapsed childhood ALL. Nat Med. 2015;21(6):563-71.
34. Peters C, Schrappe M, von Stackelberg A, Schrauder A, Bader P, Ebell W, et al. Stem-cell transplantation in children with acute lymphoblastic leukemia: A prospective

international multicenter trial comparing sibling donors with matched unrelated donors-The ALL-SCT-BFM-2003 trial. J Clin Oncol. 2015;33(11):1265-74.
35. Bhamidipati PK, Kantarjian H, Cortes J, Cornelison AM, Jabbour E. Management of imatinib-resistant patients with chronic myeloid leukemia. Ther Adv Hematol. 2013;4(2):103-17.
36. Yamamoto M, Kurosu T, Kakihana K, Mizuchi D, Miura O. The two major imatinib resistance mutations E255K and T315I enhance the activity of BCR/ABL fusion kinase. Biochem Biophys Res Commun. 2004;319(4):1272-5.
37. Maude SL, Teachey DT, Porter DL, Grupp SA. CD19-targeted chimeric antigen receptor T-cell therapy for acute lymphoblastic leukemia. Blood. 2015;125(26):4017-23.
38. Maude SL, Frey N, Shaw PA, Aplenc R, Barrett DM, Bunin NJ, et al. Chimeric antigen receptor T cells for sustained remissions in leukemia. N Engl J Med. 2014;371(16):1507-17.
39. Topp MS, Gokbuget N, Stein AS, Zugmaier G, O'Brien S, Bargou RC, et al. Safety and activity of blinatumomab for adult patients with relapsed or refractory B-precursor acute lymphoblastic leukaemia: a multicentre, single-arm, phase 2 study. Lancet Oncol. 2015;16(1):57-66.
40. Hjortholm N, Jaddini E, Halaburda K, Snarski E. Strategies of pain reduction during the bone marrow biopsy. Ann Hematol. 2013;92(2):145-9.
41. Milligan DW, Howard MR, Judd A. Premedication with lorazepam before bone marrow biopsy. J Clin Pathol. 1987;40(6):696-8.
42. Zeltzer LK, Altman A, Cohen D, LeBaron S, Munuksela EL, Schechter NL. American Academy of Pediatrics Report of the Subcommittee on the Management of Pain Associated with Procedures in Children with Cancer. Pediatrics. 1990;86(5 Pt 2):826-31.
43. Gottschling S, Meyer S, Krenn T, Reinhard H, Lothschuetz D, Nunold H, et al. Propofol versus midazolam/ketamine for procedural sedation in pediatric oncology. J Pediatr Hematol Oncol. 2005;27(9):471-6.
44. Glaisyer HR, Sury MR. Recovery after anesthesia for short pediatric oncology procedures: propofol and remifentanil compared with propofol, nitrous oxide, and sevoflurane. Anesth Analg. 2005;100(4):959-63.
45. Meneses CF, de Freitas JC, Castro CG, Jr., Copetti F, Brunetto AL. Safety of general anesthesia for lumbar puncture and bone marrow aspirate/biopsy in pediatric oncology patients. J Pediatr Hematol Oncol. 2009;31(7):465-70.
46. Exadaktylos AK, Buggy DJ, Moriarty DC, Mascha E, Sessler DI. Can anesthetic technique for primary breast cancer surgery affect recurrence or metastasis? Anesthesiology. 2006;105(4):660-4.
47. Cata JP. Outcomes of regional anesthesia in cancer patients. Curr Opin Anaesthesiol. 2018;31(5):593-600.
48. Buggy DJ, Borgeat A, Cata J, Doherty DG, Doornebal CW, Forget P, et al. Consensus statement from the BJA Workshop on Cancer and Anaesthesia. Br J Anaesth. 2015;114(1):2-3.
49. Zimmitti G, Soliz J, Aloia TA, Gottumukkala V, Cata JP, Tzeng CW, et al. Positive Impact of Epidural Analgesia on Oncologic Outcomes in Patients Undergoing Resection of Colorectal Liver Metastases. Ann Surg Oncol. 2016;23(3):1003-11.
50. Lai R, Peng Z, Chen D, Wang X, Xing W, Zeng W, et al. The effects of anesthetic technique on cancer recurrence in percutaneous radiofrequency ablation of small hepatocellular carcinoma. Anesth Analg. 2012;114(2):290-6.

51. Kairaluoma P, Mattson J, Heikkila P, Pere P, Leidenius M. Perioperative Paravertebral Regional Anaesthesia and Breast Cancer Recurrence. Anticancer Res. 2016;36(1):415-8.
52. Cata JP, Chavez-MacGregor M, Valero V, Black W, Black DM, Goravanchi F, et al. The Impact of Paravertebral Block Analgesia on Breast Cancer Survival After Surgery. Reg Anesth Pain Med. 2016;41(6):696-703.
53. Starnes-Ott K, Goravanchi F, Meininger JC. Anesthetic choices and breast cancer recurrence: a retrospective pilot study of patient, disease, and treatment factors. Crit Care Nurs Q. 2015;38(2):200-10.
54. Finn DM, Ilfeld BM, Unkart JT, Madison SJ, Suresh PJ, Sandhu NPS, et al. Post-mastectomy cancer recurrence with and without a continuous paravertebral block in the immediate postoperative period: a prospective multi-year follow-up pilot study of a randomized, triple-masked, placebo-controlled investigation. J Anesth. 2017;31(3):374-9.
55. Cummings KC, 3rd, Patel M, Htoo PT, Bakaki PM, Cummings LC, Koroukian S. A comparison of the effects of epidural analgesia versus traditional pain management on outcomes after gastric cancer resection: a population-based study. Reg Anesth Pain Med. 2014;39(3):200-7.
56. Cummings KC, 3rd, Xu F, Cummings LC, Cooper GS. A comparison of epidural analgesia and traditional pain management effects on survival and cancer recurrence after colectomy: a population-based study. Anesthesiology. 2012;116(4):797-806.
57. Lee BM, Singh Ghotra V, Karam JA, Hernandez M, Pratt G, Cata JP. Regional anesthesia/analgesia and the risk of cancer recurrence and mortality after prostatectomy: a meta-analysis. Pain Manag. 2015;5(5):387-95.
58. Tsigonis AM, Al-Hamadani M, Linebarger JH, Vang CA, Krause FJ, Johnson JM, et al. Are Cure Rates for Breast Cancer Improved by Local and Regional Anesthesia? Reg Anesth Pain Med. 2016;41(3):339-47.
59. Hiller JG, Hacking MB, Link EK, Wessels KL, Riedel BJ. Perioperative epidural analgesia reduces cancer recurrence after gastro-oesophageal surgery. Acta Anaesthesiol Scand. 2014;58(3):281-90.
60. Heinrich S, Janitz K, Merkel S, Klein P, Schmidt J. Short- and long term effects of epidural analgesia on morbidity and mortality of esophageal cancer surgery. Langenbecks Arch Surg. 2015;400(1):19-26.
61. Shin S, Kim HI, Kim NY, Lee KY, Kim DW, Yoo YC. Effect of postoperative analgesia technique on the prognosis of gastric cancer: a retrospective analysis. Oncotarget. 2017;8(61):104594-604.
62. Wang Y, Wang L, Chen H, Xu Y, Zheng X, Wang G. The effects of intra- and post-operative anaesthesia and analgesia choice on outcome after gastric cancer resection: a retrospective study. Oncotarget. 2017;8(37):62658-65.
63. Wang J, Guo W, Wu Q, Zhang R, Fang J. Impact of Combination Epidural and General Anesthesia on the Long-Term Survival of Gastric Cancer Patients: A Retrospective Study. Med Sci Monit. 2016;22:2379-85.
64. Christopherson R, James KE, Tableman M, Marshall P, Johnson FE. Long-term survival after colon cancer surgery: a variation associated with choice of anesthesia. Anesth Analg. 2008;107(1):325-32.
65. Tsui BC, Rashiq S, Schopflocher D, Murtha A, Broemling S, Pillay J, et al. Epidural anesthesia and cancer recurrence rates after radical prostatectomy. Can J Anaesth. 2010;57(2):107-12.

66. Myles PS, Peyton P, Silbert B, Hunt J, Rigg JR, Sessler DI, et al. Perioperative epidural analgesia for major abdominal surgery for cancer and recurrence-free survival: randomised trial. BMJ. 2011;342:d1491.
67. Binczak M, Tournay E, Billard V, Rey A, Jayr C. Major abdominal surgery for cancer: does epidural analgesia have a long-term effect on recurrence-free and overall survival? Ann Fr Anesth Reanim. 2013;32(5):e81-8.
68. Holler JP, Ahlbrandt J, Burkhardt E, Gruss M, Rohrig R, Knapheide J, et al. Peridural analgesia may affect long-term survival in patients with colorectal cancer after surgery (PACO-RAS-Study): an analysis of a cancer registry. Ann Surg. 2013;258(6):989-93.
69. Lacassie HJ, Cartagena J, Branes J, Assel M, Echevarria GC. The relationship between neuraxial anesthesia and advanced ovarian cancer-related outcomes in the Chilean population. Anesth Analg. 2013;117(3):653-60.
70. Biki B, Mascha E, Moriarty DC, Fitzpatrick JM, Sessler DI, Buggy DJ. Anesthetic technique for radical prostatectomy surgery affects cancer recurrence: a retrospective analysis. Anesthesiology. 2008;109(2):180-7.
71. Ismail H, Ho KM, Narayan K, Kondalsamy-Chennakesavan S. Effect of neuraxial anaesthesia on tumour progression in cervical cancer patients treated with brachytherapy: a retrospective cohort study. Br J Anaesth. 2010;105(2):145-9.
72. Wuethrich PY, Hsu Schmitz SF, Kessler TM, Thalmann GN, Studer UE, Stueber F, et al. Potential influence of the anesthetic technique used during open radical prostatectomy on prostate cancer-related outcome: a retrospective study. Anesthesiology. 2010;113(3):570-6.
73. Wuethrich PY, Thalmann GN, Studer UE, Burkhard FC. Epidural analgesia during open radical prostatectomy does not improve long-term cancer-related outcome: a retrospective study in patients with advanced prostate cancer. PLoS One. 2013;8(8):e72873.
74. de Oliveira GS, Jr., Ahmad S, Schink JC, Singh DK, Fitzgerald PC, McCarthy RJ. Intraoperative neuraxial anesthesia but not postoperative neuraxial analgesia is associated with increased relapse-free survival in ovarian cancer patients after primary cytoreductive surgery. Reg Anesth Pain Med. 2011;36(3):271-7.
75. Gupta A, Bjornsson A, Fredriksson M, Hallbook O, Eintrei C. Reduction in mortality after epidural anaesthesia and analgesia in patients undergoing rectal but not colonic cancer surgery: a retrospective analysis of data from 655 patients in central Sweden. Br J Anaesth. 2011;107(2):164-70.
76. Forget P, Tombal B, Scholtes JL, Nzimbala J, Meulders C, Legrand C, et al. Do intraoperative analgesics influence oncological outcomes after radical prostatectomy for prostate cancer? Eur J Anaesthesiol. 2011;28(12):830-5.
77. Lin L, Liu C, Tan H, Ouyang H, Zhang Y, Zeng W. Anaesthetic technique may affect prognosis for ovarian serous adenocarcinoma: a retrospective analysis. Br J Anaesth. 2011;106(6):814-22.
78. Capmas P, Billard V, Gouy S, Lhomme C, Pautier P, Morice P, et al. Impact of epidural analgesia on survival in patients undergoing complete cytoreductive surgery for ovarian cancer. Anticancer Res. 2012;32(4):1537-42.
79. Day A, Smith R, Jourdan I, Fawcett W, Scott M, Rockall T. Retrospective analysis of the effect of postoperative analgesia on survival in patients after laparoscopic resection of colorectal cancer. Br J Anaesth. 2012;109(2):185-90.
80. Gottschalk A, Ford JG, Regelin CC, You J, Mascha EJ, Sessler DI, et al. Association between epidural analgesia and cancer recurrence after colorectal cancer surgery. Anesthesiology. 2010;113(1):27-34.

81. Roiss M, Schiffmann J, Tennstedt P, Kessler T, Blanc I, Goetz A, et al. Oncological long-term outcome of 4772 patients with prostate cancer undergoing radical prostatectomy: does the anaesthetic technique matter? Eur J Surg Oncol. 2014;40(12):1686-92.
82. Scavonetto F, Yeoh TY, Umbreit EC, Weingarten TN, Gettman MT, Frank I, et al. Association between neuraxial analgesia, cancer progression, and mortality after radical prostatectomy: a large, retrospective matched cohort study. Br J Anaesth. 2014;113 Suppl 1:i95-102.
83. Sprung J, Scavonetto F, Yeoh TY, Kramer JM, Karnes RJ, Eisenach JH, et al. Outcomes after radical prostatectomy for cancer: a comparison between general anesthesia and epidural anesthesia with fentanyl analgesia: a matched cohort study. Anesth Analg. 2014;119(4):859-66.
84. Merquiol F, Montelimard AS, Nourissat A, Molliex S, Zufferey PJ. Cervical epidural anesthesia is associated with increased cancer-free survival in laryngeal and hypopharyngeal cancer surgery: a retrospective propensity-matched analysis. Reg Anesth Pain Med. 2013;38(5):398-402.
85. Tseng KS, Kulkarni S, Humphreys EB, Carter HB, Mostwin JL, Partin AW, et al. Spinal anesthesia does not impact prostate cancer recurrence in a cohort of men undergoing radical prostatectomy: an observational study. Reg Anesth Pain Med. 2014;39(4):284-8.
86. Cata JP, Gottumukkala V, Thakar D, Keerty D, Gebhardt R, Liu DD. Effects of postoperative epidural analgesia on recurrence-free and overall survival in patients with nonsmall cell lung cancer. J Clin Anesth. 2014;26(1):3-17.
87. Cata JP, Bhavsar S, Hagan KB, Arunkumar R, Shi T, Grasu R, et al. Scalp blocks for brain tumor craniotomies: A retrospective survival analysis of a propensity match cohort of patients. J Clin Neurosci. 2018;51:46-51.
88. Zheng L, Hagan KB, Villarreal J, Keerty V, Chen J, Cata JP. Scalp block for glioblastoma surgery is associated with lower inflammatory scores and improved survival. Minerva Anestesiol. 2017;83(11):1137-45.
89. Gottschalk A, Brodner G, Van Aken HK, Ellger B, Althaus S, Schulze HJ. Can regional anaesthesia for lymph-node dissection improve the prognosis in malignant melanoma? Br J Anaesth. 2012;109(2):253-9.
90. Sessler DI, Pei L, Huang Y, Fleischmann E, Marhofer P, Kurz A, et al. Recurrence of breast cancer after regional or general anaesthesia: a randomised controlled trial. Lancet. 2019;394(10211):1807-15.
91. Jun IJ, Jo JY, Kim JI, Chin JH, Kim WJ, Kim HR, et al. Impact of anesthetic agents on overall and recurrence-free survival in patients undergoing esophageal cancer surgery: A retrospective observational study. Sci Rep. 2017;7(1):14020.
92. Piegeler T, Votta-Velis EG, Liu G, Place AT, Schwartz DE, Beck-Schimmer B, et al. Antimetastatic potential of amide-linked local anesthetics: inhibition of lung adenocarcinoma cell migration and inflammatory Src signaling independent of sodium channel blockade. Anesthesiology. 2012;117(3):548-59.
93. Onkal R, Djamgoz MB. Molecular pharmacology of voltage-gated sodium channel expression in metastatic disease: clinical potential of neonatal Nav1.5 in breast cancer. Eur J Pharmacol. 2009;625(1-3):206-19.
94. Li T, Chen L, Zhao H, Wu L, Masters J, Han C, et al. Both Bupivacaine and Levobupivacaine inhibit colon cancer cell growth but not melanoma cells in vitro. J Anesth. 2019;33(1):17-25.

95. House CD, Vaske CJ, Schwartz AM, Obias V, Frank B, Luu T, et al. Voltage-gated Na+ channel SCN5A is a key regulator of a gene transcriptional network that controls colon cancer invasion. Cancer Res. 2010;70(17):6957-67.
96. Tada M, Imazeki F, Fukai K, Sakamoto A, Arai M, Mikata R, et al. Procaine inhibits the proliferation and DNA methylation in human hepatoma cells. Hepatol Int. 2007;1(3):355-64.
97. Lirk P, Berger R, Hollmann MW, Fiegl H. Lidocaine time- and dose-dependently demethylates deoxyribonucleic acid in breast cancer cell lines in vitro. Br J Anaesth. 2012;109(2):200-7.
98. Fraser SP, Diss JK, Chioni AM, Mycielska ME, Pan H, Yamaci RF, et al. Voltage-gated sodium channel expression and potentiation of human breast cancer metastasis. Clin Cancer Res. 2005;11(15):5381-9.
99. Piegeler T, Schlapfer M, Dull RO, Schwartz DE, Borgeat A, Minshall RD, et al. Clinically relevant concentrations of lidocaine and ropivacaine inhibit TNFalpha-induced invasion of lung adenocarcinoma cells in vitro by blocking the activation of Akt and focal adhesion kinase. Br J Anaesth. 2015;115(5):784-91.
100. Dhennin-Duthille I, Gautier M, Faouzi M, Guilbert A, Brevet M, Vaudry D, et al. High expression of transient receptor potential channels in human breast cancer epithelial cells and tissues: correlation with pathological parameters. Cell Physiol Biochem. 2011;28(5):813-22.
101. Jiang Y, Gou H, Zhu J, Tian S, Yu L. Lidocaine inhibits the invasion and migration of TRPV6-expressing cancer cells by TRPV6 downregulation. Oncol Lett. 2016;12(2):1164-70.
102. Zhao J, Mo H. The Impact of Different Anesthesia Methods on Stress Reaction and Immune Function of the Patients with Gastric Cancer during Peri-Operative Period. J Med Assoc Thai. 2015;98(6):568-73.
103. Desmond F, McCormack J, Mulligan N, Stokes M, Buggy DJ. Effect of anaesthetic technique on immune cell infiltration in breast cancer: a follow-up pilot analysis of a prospective, randomised, investigator-masked study. Anticancer Res. 2015;35(3):1311-9.
104. Zhu J, Zhang XR, Yang H. Effects of combined epidural and general anesthesia on intraoperative hemodynamic responses, postoperative cellular immunity, and prognosis in patients with gallbladder cancer: A randomized controlled trial. Medicine (Baltimore). 2017;96(10):e6137.
105. Li JM, Shao JL, Zeng WJ, Liang RB. General/epidural anesthesia in combination preserves NK cell activity and affects cytokine response in cervical carcinoma patients undergoing radical resection: a cohort prospective study. Eur J Gynaecol Oncol. 2015;36(6):703-7.
106. Xu YJ, Chen WK, Zhu Y, Wang SL, Miao CH. Effect of thoracic epidural anaesthesia on serum vascular endothelial growth factor C and cytokines in patients undergoing anaesthesia and surgery for colon cancer. Br J Anaesth. 2014;113 Suppl 1:i49-55.
107. Aguirre JA, Lucchinetti E, Clanachan AS, Plane F, Zaugg M. Unraveling Interactions Between Anesthetics and the Endothelium: Update and Novel Insights. Anesth Analg. 2016;122(2):330-48.
108. Benzonana LL, Perry NJ, Watts HR, Yang B, Perry IA, Coombes C, et al. Isoflurane, a commonly used volatile anesthetic, enhances renal cancer growth and malignant potential via the hypoxia-inducible factor cellular signaling pathway in vitro. Anesthesiology. 2013;119(3):593-605.
109. Luo X, Zhao H, Hennah L, Ning J, Liu J, Tu H, et al. Impact of isoflurane on malignant capability of ovarian cancer in vitro. Br J Anaesth. 2015;114(5):831-9.

110. Wang P, Chen J, Mu LH, Du QH, Niu XH, Zhang MY. Propofol inhibits invasion and enhances paclitaxel- induced apoptosis in ovarian cancer cells through the suppression of the transcription factor slug. Eur Rev Med Pharmacol Sci. 2013;17(13):1722-9.
111. Chen X, Wu Q, Sun P, Zhao Y, Zhu M, Miao C. Propofol Disrupts Aerobic Glycolysis in Colorectal Cancer Cells via Inactivation of the NMDAR-CAMKII-ERK Pathway. Cell Physiol Biochem. 2018;46(2):492-504.
112. Connolly C, Buggy DJ. Opioids and tumour metastasis: does the choice of the anesthetic-analgesic technique influence outcome after cancer surgery? Curr Opin Anaesthesiol. 2016;29(4):468-74.
113. Lennon FE, Mirzapoiazova T, Mambetsariev B, Salgia R, Moss J, Singleton PA. Overexpression of the mu-opioid receptor in human non-small cell lung cancer promotes Akt and mTOR activation, tumor growth, and metastasis. Anesthesiology. 2012;116(4):857-67.
114. Singleton PA, Lingen MW, Fekete MJ, Garcia JG, Moss J. Methylnaltrexone inhibits opiate and VEGF-induced angiogenesis: role of receptor transactivation. Microvasc Res. 2006;72(1-2):3-11.
115. Gach K, Szemraj J, Fichna J, Piestrzeniewicz M, Delbro DS, Janecka A. The influence of opioids on urokinase plasminogen activator on protein and mRNA level in MCF-7 breast cancer cell line. Chem Biol Drug Des. 2009;74(4):390-6.
116. Harimaya Y, Koizumi K, Andoh T, Nojima H, Kuraishi Y, Saiki I. Potential ability of morphine to inhibit the adhesion, invasion and metastasis of metastatic colon 26-L5 carcinoma cells. Cancer Lett. 2002;187(1-2):121-7.
117. Hsiao PN, Chang MC, Cheng WF, Chen CA, Lin HW, Hsieh CY, et al. Morphine induces apoptosis of human endothelial cells through nitric oxide and reactive oxygen species pathways. Toxicology. 2009;256(1-2):83-91.
118. Hatsukari I, Hitosugi N, Ohno R, Hashimoto K, Nakamura S, Satoh K, et al. Induction of apoptosis by morphine in human tumor cell lines in vitro. Anticancer Res. 2007;27(2):857-64.
119. Juneja R. Opioids and cancer recurrence. Curr Opin Support Palliat Care. 2014;8(2):91-101.
120. Ma D, Lim T, Xu J, Tang H, Wan Y, Zhao H, et al. Xenon preconditioning protects against renal ischemic-reperfusion injury via HIF-1alpha activation. J Am Soc Nephrol. 2009;20(4):713-20.
121. Ciechanowicz S, Zhao H, Chen Q, Cui J, Mi E, Mi E, et al. Differential effects of sevoflurane on the metastatic potential and chemosensitivity of non-small-cell lung adenocarcinoma and renal cell carcinoma in vitro. Br J Anaesth. 2018;120(2):368-75.
122. Iwasaki M, Zhao H, Jaffer T, Unwith S, Benzonana L, Lian Q, et al. Volatile anaesthetics enhance the metastasis related cellular signalling including CXCR2 of ovarian cancer cells. Oncotarget. 2016;7(18):26042-56.
123. Wang GL, Jiang BH, Rue EA, Semenza GL. Hypoxia-inducible factor 1 is a basic-helix-loop-helix-PAS heterodimer regulated by cellular O2 tension. Proc Natl Acad Sci U S A. 1995;92(12):5510-4.
124. LaGory EL, Giaccia AJ. The ever-expanding role of HIF in tumour and stromal biology. Nat Cell Biol. 2016;18(4):356-65.
125. Hudson CC, Liu M, Chiang GG, Otterness DM, Loomis DC, Kaper F, et al. Regulation of hypoxia-inducible factor 1alpha expression and function by the mammalian target of rapamycin. Mol Cell Biol. 2002;22(20):7004-14.

126. Zhong H, Chiles K, Feldser D, Laughner E, Hanrahan C, Georgescu MM, et al. Modulation of hypoxia-inducible factor 1alpha expression by the epidermal growth factor/phosphatidylinositol 3-kinase/PTEN/AKT/FRAP pathway in human prostate cancer cells: implications for tumor angiogenesis and therapeutics. Cancer Res. 2000;60(6):1541-5.
127. Noman MZ, Buart S, Van Pelt J, Richon C, Hasmim M, Leleu N, et al. The cooperative induction of hypoxia-inducible factor-1 alpha and STAT3 during hypoxia induced an impairment of tumor susceptibility to CTL-mediated cell lysis. J Immunol. 2009;182(6):3510-21.
128. Irigoyen M, Garcia-Ruiz JC, Berra E. The hypoxia signalling pathway in haematological malignancies. Oncotarget. 2017;8(22):36832-44.
129. Spencer JA, Ferraro F, Roussakis E, Klein A, Wu J, Runnels JM, et al. Direct measurement of local oxygen concentration in the bone marrow of live animals. Nature. 2014;508(7495):269-73.
130. Deynoux M, Sunter N, Herault O, Mazurier F. Hypoxia and Hypoxia-Inducible Factors in Leukemias. Front Oncol. 2016;6:41.
131. Forristal CE, Brown AL, Helwani FM, Winkler IG, Nowlan B, Barbier V, et al. Hypoxia inducible factor (HIF)-2alpha accelerates disease progression in mouse models of leukemia and lymphoma but is not a poor prognosis factor in human AML. Leukemia. 2015;29(10):2075-85.
132. Wang Y, Liu Y, Malek SN, Zheng P, Liu Y. Targeting HIF1alpha eliminates cancer stem cells in hematological malignancies. Cell Stem Cell. 2011;8(4):399-411.
133. Coltella N, Percio S, Valsecchi R, Cuttano R, Guarnerio J, Ponzoni M, et al. HIF factors cooperate with PML-RARalpha to promote acute promyelocytic leukemia progression and relapse. EMBO Mol Med. 2014;6(5):640-50.
134. Zhang H, Li H, Xi HS, Li S. HIF1alpha is required for survival maintenance of chronic myeloid leukemia stem cells. Blood. 2012;119(11):2595-607.
135. Giambra V, Jenkins CE, Lam SH, Hoofd C, Belmonte M, Wang X, et al. Leukemia stem cells in T-ALL require active Hif1alpha and Wnt signaling. Blood. 2015;125(25):3917-27.
136. Velasco-Hernandez T, Hyrenius-Wittsten A, Rehn M, Bryder D, Cammenga J. HIF-1 alpha can act as a tumor suppressor gene in murine acute myeloid leukemia. Blood. 2014;124(24):3597-607.
137. Shi QY, Zhang SJ, Liu L, Chen QS, Yu LN, Zhang FJ, et al. Sevoflurane promotes the expansion of glioma stem cells through activation of hypoxia-inducible factors in vitro. British Journal of Anaesthesia. 2015;114(5):825-30.
138. Yang NL, Liang YF, Yang P, Ji FH. Propofol suppresses LPS-induced nuclear accumulation of HIF-1 alpha and tumor aggressiveness in non-small cell lung cancer. Oncology Reports. 2017;37(5):2611-9.
139. Sipkins DA, Wei XB, Wu JW, Runnels JM, Cote D, Means TK, et al. In vivo imaging of specialized bone marrow endothelial microdomains for tumour engraftment. Nature. 2005;435(7044):969-73.
140. Liou A, Delgado-Martin C, Teachey DT, Hermiston ML. The CXCR4/CXCL12 Axis Mediates Chemotaxis, Survival, and Chemoresistance in T-Cell Acute Lymphoblastic Leukemia. Blood. 2014;124(21).
141. D'Agostino G, Saporito A, Cecchinato V, Silvestri Y, Borgeat A, Anselmi L, et al. Lidocaine inhibits cytoskeletal remodelling and human breast cancer cell migration. British Journal of Anaesthesia. 2018;121(4):962-8.

142. Ceradini DJ, Kulkarni AR, Callaghan MJ, Tepper OM, Bastidas N, Kleinman ME, et al. Progenitor cell trafficking is regulated by hypoxic gradients through HIF-1 induction of SDF-1. Nature Medicine. 2004;10(8):858-64.
143. Staller P, Sulitkova J, Liszlwan J, Moch H, Oakeley EJ, Krek W. Chemokine receptor CXCR4 downregulated by von Hippel-Lindau tumour suppressor pVHL. Nature. 2003;425(6955):307-11.
144. Zhao HL, Chen Q, Alam A, Cui J, Suen KC, Soo AP, et al. The role of osteopontin in the progression of solid organ tumour. Cell Death & Disease. 2018;9.
145. Nilsson SK, Johnston HM, Whitty GA, Williams B, Webb RJ, Denhardt DT, et al. Osteopontin, a key component of the hematopoietic stem cell niche and regulator of primitive hematopoietic progenitor cells. Blood. 2005;106(4):1232-9.
146. Grassinger J, Haylock DN, Storan MJ, Haines GO, Williams B, Whitty GA, et al. Thrombin-cleaved osteopontin regulates hemopoietic stem and progenitor cell functions through interactions with alpha(9)beta(1) and alpha(4)beta(1) integrins. Blood. 2009;114(1):49-59.
147. Is there any correlation between levels of serum ostepontin, CEA, and FDG uptake in lung cancer patients with bone metastasis?
148. Boyerinas B, Zafrir M, Yesilkanal AE, Price TT, Hyjek EM, Sipkins DA. Adhesion to osteopontin in the bone marrow niche regulates lymphoblastic leukemia cell dormancy. Blood. 2013;121(24):4821-31.
149. Song G, Cai QF, Mao YB, Ming YL, Bao SD, Ouyang GL. Osteopontin promotes ovarian cancer progression and cell survival and increases HIF-1 alpha expression through the PI3-K/Akt pathway. Cancer Science. 2008;99(10):1901-7.
150. Raja R, Kale S, Thorat D, Soundararajan G, Lohite K, Mane A, et al. Hypoxia-driven osteopontin contributes to breast tumor growth through modulation of HIF1 alpha-mediated VEGF-dependent angiogenesis. Oncogene. 2014;33(16):2053-64.
151. Hawkins ED, Duarte D, Akinduro O, Khorshed RA, Passaro D, Nowicka M, et al. T-cell acute leukaemia exhibits dynamic interactions with bone marrow microenvironments. Nature. 2016;538(7626):518-+.
152. Wang XN, Dong YL, Zhang YY, Li TZ, Xie ZC. Sevoflurane induces cognitive impairment in young mice via autophagy. Plos One. 2019;14(5).
153. Zhang XM, Zhou YF, Xu MM, Chen G. Autophagy Is Involved in the Sevoflurane Anesthesia-Induced Cognitive Dysfunction of Aged Rats. Plos One. 2016;11(4).
154. Li ZQ, Li LX, Mo N, Cao YY, Kuerban B, Liang YX, et al. Duration-dependent regulation of autophagy by isoflurane exposure in aged rats. Neurosci Bull. 2015;31(4):505-13.
155. Hu DD, Lin EC, Kovach NL, Hoyer JR, Smith JW. A biochemical characterization of the binding of osteopontin to integrins alpha v beta 1 and alpha v beta 5. J Biol Chem. 1995;270(44):26232-8.
156. Lo Celso C, Fleming HE, Wu JW, Zhao CX, Miake-Lye S, Fujisaki J, et al. Live-animal tracking of individual haematopoietic stem/progenitor cells in their niche. Nature. 2009;457(7225):92-6.
157. Uphoff CC, MacLeod RA, Denkmann SA, Golub TR, Borkhardt A, Janssen JW, et al. Occurrence of TEL-AML1 fusion resulting from (12;21) translocation in human early B-lineage leukemia cell lines. Leukemia. 1997;11(3):441-7.
158. Mazoit JX, Samii K. Binding of propofol to blood components: implications for pharmacokinetics and for pharmacodynamics. Br J Clin Pharmacol. 1999;47(1):35-42.

159. Frolova O, Samudio I, Benito JM, Jacamo R, Kornblau SM, Markovic A, et al. Regulation of HIF-1alpha signaling and chemoresistance in acute lymphocytic leukemia under hypoxic conditions of the bone marrow microenvironment. Cancer Biol Ther. 2012;13(10):858-70.
160. Zhao J, Hao J, Fei X, Wang X, Hou Y, Deng C. Isoflurane inhibits occludin expression via up-regulation of hypoxia-inducible factor 1alpha. Brain Res. 2014;1562:1-10.
161. Li QF, Wang XR, Yang YW, Su DS. Up-regulation of hypoxia inducible factor 1alpha by isoflurane in Hep3B cells. Anesthesiology. 2006;105(6):1211-9.
162. Tasian SK, Teachey DT, Li Y, Shen F, Harvey RC, Chen IM, et al. Potent efficacy of combined PI3K/mTOR and JAK or ABL inhibition in murine xenograft models of Ph-like acute lymphoblastic leukemia. Blood. 2017;129(2):177-87.
163. Zhang Y, Gao Y, Zhang H, Zhang J, He F, Hnizda A, et al. PDGFRB mutation and tyrosine kinase inhibitor resistance in Ph-like acute lymphoblastic leukemia. Blood. 2018;131(20):2256-61.
164. Cook GJ, Pardee TS. Animal models of leukemia: any closer to the real thing? Cancer Metastasis Rev. 2013;32(1-2):63-76.
165. Hynds RE, Vladimirou E, Janes SM. The secret lives of cancer cell lines. Dis Model Mech. 2018;11(11).
166. Ben-David U, Siranosian B, Ha G, Tang H, Oren Y, Hinohara K, et al. Genetic and transcriptional evolution alters cancer cell line drug response. Nature. 2018;560(7718):325-30.
167. Scholzen T, Gerdes J. The Ki-67 protein: from the known and the unknown. J Cell Physiol. 2000;182(3):311-22.
168. Li R, Liu H, Dilger JP, Lin J. Effect of Propofol on breast Cancer cell, the immune system, and patient outcome. BMC Anesthesiol. 2018;18(1):77.
169. Liu SQ, Zhang JL, Li ZW, Hu ZH, Liu Z, Li Y. Propofol Inhibits Proliferation, Migration, Invasion and Promotes Apoptosis Through Down-Regulating miR-374a in Hepatocarcinoma Cell Lines. Cell Physiol Biochem. 2018;49(6):2099-110.
170. Sun H, Wang Y, Zhang W. Propofol inhibits proliferation and metastasis by up-regulation of miR-495 in JEG-3 choriocarcinoma cells. Artif Cells Nanomed Biotechnol. 2019;47(1):1738-45.
171. Hubbi ME, Semenza GL. Regulation of cell proliferation by hypoxia-inducible factors. Am J Physiol Cell Physiol. 2015;309(12):C775-82.
172. Chen S, Zhang M, Xing L, Wang Y, Xiao Y, Wu Y. HIF-1alpha contributes to proliferation and invasiveness of neuroblastoma cells via SHH signaling. PLoS One. 2015;10(3):e0121115.
173. Goda N, Ryan HE, Khadivi B, McNulty W, Rickert RC, Johnson RS. Hypoxia-inducible factor 1alpha is essential for cell cycle arrest during hypoxia. Mol Cell Biol. 2003;23(1):359-69.
174. Argano M, De Maria R, Vogl C, Rodlsberger K, Buracco P, Larenza Menzies MP. Canine mammary tumour cells exposure to sevoflurane: effects on cell proliferation and neuroepithelial transforming gene 1 expression. Vet Anaesth Analg. 2019;46(3):369-74.
175. Liu J, Yang L, Guo X, Jin G, Wang Q, Lv D, et al. Sevoflurane suppresses proliferation by upregulating microRNA-203 in breast cancer cells. Mol Med Rep. 2018;18(1):455-60.
176. Park JW, Lim MS, Ji SY, Cho MS, Park SJ, Han SH, et al. Effects of short-term exposure to sevoflurane on the survival, proliferation, apoptosis, and differentiation of neural precursor cells derived from human embryonic stem cells. J Anesth. 2017;31(6):821-8.

177. Koshiji M, Kageyama Y, Pete EA, Horikawa I, Barrett JC, Huang LE. HIF-1alpha induces cell cycle arrest by functionally counteracting Myc. EMBO J. 2004;23(9):1949-56.
178. Beyer S, Kristensen MM, Jensen KS, Johansen JV, Staller P. The histone demethylases JMJD1A and JMJD2B are transcriptional targets of hypoxia-inducible factor HIF. J Biol Chem. 2008;283(52):36542-52.
179. Leon KE, Aird KM. Jumonji C Demethylases in Cellular Senescence. Genes (Basel). 2019;10(1).
180. Hubbi ME, Luo W, Baek JH, Semenza GL. MCM proteins are negative regulators of hypoxia-inducible factor 1. Mol Cell. 2011;42(5):700-12.
181. Hubbi ME, Kshitiz, Gilkes DM, Rey S, Wong CC, Luo W, et al. A nontranscriptional role for HIF-1alpha as a direct inhibitor of DNA replication. Sci Signal. 2013;6(262):ra10.
182. Speth JM, Hoggatt J, Singh P, Pelus LM. Pharmacologic increase in HIF1alpha enhances hematopoietic stem and progenitor homing and engraftment. Blood. 2014;123(2):203-7.
183. Guo M, Cai C, Zhao G, Qiu X, Zhao H, Ma Q, et al. Hypoxia promotes migration and induces CXCR4 expression via HIF-1alpha activation in human osteosarcoma. PLoS One. 2014;9(3):e90518.
184. Bao Y, Wang Z, Liu B, Lu X, Xiong Y, Shi J, et al. A feed-forward loop between nuclear translocation of CXCR4 and HIF-1alpha promotes renal cell carcinoma metastasis. Oncogene. 2019;38(6):881-95.
185. Hofbauer R, Frass M, Salfinger H, Moser D, Hornykewycz S, Gmeiner B, et al. Propofol reduces the migration of human leukocytes through endothelial cell monolayers. Crit Care Med. 1999;27(9):1843-7.
186. Ye Z, Jingzhong L, Yangbo L, Lei C, Jiandong Y. Propofol inhibits proliferation and invasion of osteosarcoma cells by regulation of microRNA-143 expression. Oncol Res. 2013;21(4):201-7.
187. Zhang W, Wang Y, Zhu Z, Zheng Y, Song B. Propofol inhibits proliferation, migration and invasion of gastric cancer cells by up-regulating microRNA-195. Int J Biol Macromol. 2018;120(Pt A):975-84.
188. Yu X, Gao Y, Zhang F. Propofol inhibits pancreatic cancer proliferation and metastasis by up-regulating miR-328 and down-regulating ADAM8. Basic Clin Pharmacol Toxicol. 2019;125(3):271-8.
189. Du Q, Liu J, Zhang X, Zhang X, Zhu H, Wei M, et al. Propofol inhibits proliferation, migration, and invasion but promotes apoptosis by regulation of Sox4 in endometrial cancer cells. Braz J Med Biol Res. 2018;51(4):e6803.
190. Lai RC, Shan WR, Zhou D, Zeng XQ, Zuo K, Pan DF, et al. Sevoflurane promotes migration, invasion, and colony-forming ability of human glioblastoma cells possibly via increasing the expression of cell surface protein 44. Acta Pharmacol Sin. 2019.
191. Ecimovic P, McHugh B, Murray D, Doran P, Buggy DJ. Effects of sevoflurane on breast cancer cell function in vitro. Anticancer Res. 2013;33(10):4255-60.
192. Miyazaki K, Oyanagi J, Hoshino D, Togo S, Kumagai H, Miyagi Y. Cancer cell migration on elongate protrusions of fibroblasts in collagen matrix. Sci Rep. 2019;9(1):292.
193. Moratz C, Kehrl JH. In vitro and in vivo assays of B-lymphocyte migration. Methods Mol Biol. 2004;271:161-71.
194. De Bie J, Demeyer S, Alberti-Servera L, Geerdens E, Segers H, Broux M, et al. Single-cell sequencing reveals the origin and the order of mutation acquisition in T-cell acute lymphoblastic leukemia. Leukemia. 2018;32(6):1358-69.

195. Chen YB, Ren SM, Li SD, Du Z. Prognostic significance of osteopontin in acute myeloid leukemia: A meta-analysis. Mol Clin Oncol. 2017;7(2):275-80.
196. Grassinger J, Haylock DN, Storan MJ, Haines GO, Williams B, Whitty GA, et al. Thrombin-cleaved osteopontin regulates hemopoietic stem and progenitor cell functions through interactions with alpha9beta1 and alpha4beta1 integrins. Blood. 2009;114(1):49-59.
197. Yu H, Shen H, Yuan Y, XuFeng R, Hu X, Garrison SP, et al. Deletion of Puma protects hematopoietic stem cells and confers long-term survival in response to high-dose gamma-irradiation. Blood. 2010;115(17):3472-80.
198. Lund SA, Wilson CL, Raines EW, Tang J, Giachelli CM, Scatena M. Osteopontin mediates macrophage chemotaxis via alpha4 and alpha9 integrins and survival via the alpha4 integrin. J Cell Biochem. 2013;114(5):1194-202.
199. Blase L, Merling A, Engelmann S, Moller P, Schwartz-Albiez R. Characterization of cell surface-expressed proteochondroitin sulfate of pre-B Nalm-6 cells and its possible role in laminin adhesion. Leukemia. 1996;10(6):1000-11.
200. Shen W, Bendall LJ, Gottlieb DJ, Bradstock KF. The chemokine receptor CXCR4 enhances integrin-mediated in vitro adhesion and facilitates engraftment of leukemic precursor-B cells in the bone marrow. Exp Hematol. 2001;29(12):1439-47.
201. Patrick CW, Jr., Juneja HS, Lee S, Schmalstieg FC, McIntire LV. Heterotypic adherence between human B-lymphoblastic and pre-B-lymphoblastic cells and marrow stromal cells is a biphasic event: integrin very late antigen-4 alpha mediates only the early phase of the heterotypic adhesion. Blood. 1995;85(1):168-78.
202. Meng X, Grotsch B, Luo Y, Knaup KX, Wiesener MS, Chen XX, et al. Hypoxia-inducible factor-1alpha is a critical transcription factor for IL-10-producing B cells in autoimmune disease. Nat Commun. 2018;9(1):251.
203. Hatfield KJ, Bedringsaas SL, Ryningen A, Gjertsen BT, Bruserud O. Hypoxia increases HIF-1alpha expression and constitutive cytokine release by primary human acute myeloid leukaemia cells. Eur Cytokine Netw. 2010;21(3):154-64.
204. Cheng C, Zhang FJ, Tian J, Tu M, Xiong YL, Luo W, et al. Osteopontin inhibits HIF-2alpha mRNA expression in osteoarthritic chondrocytes. Exp Ther Med. 2015;9(6):2415-9.
205. Liersch R, Gerss J, Schliemann C, Bayer M, Schwoppe C, Biermann C, et al. Osteopontin is a prognostic factor for survival of acute myeloid leukemia patients. Blood. 2012;119(22):5215-20.
206. Lee CY, Tien HF, Hou HA, Chou WC, Lin LI. Marrow osteopontin level as a prognostic factor in acute myeloid leukaemia. Br J Haematol. 2008;141(5):736-9.
207. Powell JA, Thomas D, Barry EF, Kok CH, McClure BJ, Tsykin A, et al. Expression profiling of a hemopoietic cell survival transcriptome implicates osteopontin as a functional prognostic factor in AML. Blood. 2009;114(23):4859-70.
208. Saeki Y, Mima T, Ishii T, Ogata A, Kobayashi H, Ohshima S, et al. Enhanced production of osteopontin in multiple myeloma: clinical and pathogenic implications. Br J Haematol. 2003;123(2):263-70.
209. Sfiridaki A, Miyakis S, Pappa C, Tsirakis G, Alegakis A, Kotsis V, et al. Circulating osteopontin: a dual marker of bone destruction and angiogenesis in patients with multiple myeloma. J Hematol Oncol. 2011;4:22.
210. Chen L, Guo P, Zhang Y, Li X, Jia P, Tong J, et al. Autophagy is an important event for low-dose cytarabine treatment in acute myeloid leukemia cells. Leuk Res. 2017;60:44-52.

211. Cheong JW, Kim Y, Eom JI, Jeung HK, Min YH. Enhanced autophagy in cytarabine arabinoside-resistant U937 leukemia cells and its potential as a target for overcoming resistance. Mol Med Rep. 2016;13(4):3433-40.
212. Evangelisti C, Evangelisti C, Chiarini F, Lonetti A, Buontempo F, Neri LM, et al. Autophagy in acute leukemias: a double-edged sword with important therapeutic implications. Biochim Biophys Acta. 2015;1853(1):14-26.
213. Kim Y, Eom JI, Jeung HK, Jang JE, Kim JS, Cheong JW, et al. Induction of cytosine arabinoside-resistant human myeloid leukemia cell death through autophagy regulation by hydroxychloroquine. Biomed Pharmacother. 2015;73:87-96.
214. Klionsky DJ. Autophagy: from phenomenology to molecular understanding in less than a decade. Nat Rev Mol Cell Biol. 2007;8(11):931-7.
215. Sharma K, Le N, Alotaibi M, Gewirtz DA. Cytotoxic autophagy in cancer therapy. Int J Mol Sci. 2014;15(6):10034-51.
216. Qian J, Shen S, Chen W, Chen N. Propofol Reversed Hypoxia-Induced Docetaxel Resistance in Prostate Cancer Cells by Preventing Epithelial-Mesenchymal Transition by Inhibiting Hypoxia-Inducible Factor 1alpha. Biomed Res Int. 2018;2018:4174232.
217. Frolova O SI, Benito JM, Jacamo R, Knornblau SM, Markovic A, Schober W, Lu HB, Qiu YH, Bugli D and Konopleva M. Regulation of HIF-1α signaling and chemoresistance in acute lymphocytic leukemia under hypoxic conditions of the bone marrow microenvironment. Cancer Biology & therapy 2012;13(10):858-70.
218. Boulares AH, Yakovlev AG, Ivanova V, Stoica BA, Wang G, Iyer S, et al. Role of poly(ADP-ribose) polymerase (PARP) cleavage in apoptosis. Caspase 3-resistant PARP mutant increases rates of apoptosis in transfected cells. J Biol Chem. 1999;274(33):22932-40.
219. Malhotra U, Zaidi AH, Kosovec JE, Kasi PM, Komatsu Y, Rotoloni CL, et al. Prognostic value and targeted inhibition of survivin expression in esophageal adenocarcinoma and cancer-adjacent squamous epithelium. PLoS One. 2013;8(11):e78343.
220. Zhao H, Shi P, Deng M, Jiang Z, Li Y, Kannappan V, et al. Low dose triptolide reverses chemoresistance in adult acute lymphoblastic leukemia cells via reactive oxygen species generation and DNA damage response disruption. Oncotarget. 2016;7(51):85515-28.
221. Qi-Hang D Y-BX, Meng-Yuan Z, Peng Y, Chang-Yao H. Propofol induces apoptosis and increases gemcitabine sensitivity in pancreatic cancer cells in vitro by inhibition of nuclear factor-κB activity. World Journal of Gastroenterology 2013;19(33):5485-92
222. Liu G, Fan X, Tang M, Chen R, Wang H, Jia R, et al. Osteopontin induces autophagy to promote chemo-resistance in human hepatocellular carcinoma cells. Cancer Lett. 2016;383(2):171-82.
223. Wellmann S, Guschmann M, Griethe W, Eckert C, von Stackelberg A, Lottaz C, et al. Activation of the HIF pathway in childhood ALL, prognostic implications of VEGF. Leukemia. 2004;18(5):926-33.
224. Hayashiuchi M, Kitayama T, Morita K, Yamawaki Y, Oue K, Yoshinaka T, et al. General anesthetic actions on GABAA receptors in vivo are reduced in phospholipase C-related catalytically inactive protein knockout mice. J Anesth. 2017;31(4):531-8.
225. Hales TG, Lambert JJ. The actions of propofol on inhibitory amino acid receptors of bovine adrenomedullary chromaffin cells and rodent central neurones. Br J Pharmacol. 1991;104(3):619-28.

226. Lam DW, Reynolds JN. Modulatory and direct effects of propofol on recombinant GABAA receptors expressed in xenopus oocytes: influence of alpha- and gamma2-subunits. Brain Res. 1998;784(1-2):179-87.
227. Wang Y, Yang E, Wells MM, Bondarenko V, Woll K, Carnevale V, et al. Propofol inhibits the voltage-gated sodium channel NaChBac at multiple sites. J Gen Physiol. 2018;150(9):1317-31.
228. Ouyang W, Wang G, Hemmings HC, Jr. Isoflurane and propofol inhibit voltage-gated sodium channels in isolated rat neurohypophysial nerve terminals. Mol Pharmacol. 2003;64(2):373-81.
229. Feng J, Lucchinetti E, Fischer G, Zhu M, Zaugg K, Schaub MC, et al. Cardiac remodelling hinders activation of cyclooxygenase-2, diminishing protection by delayed pharmacological preconditioning: role of HIF1 alpha and CREB. Cardiovasc Res. 2008;78(1):98-107.
230. Zhang L, Huang H, Cheng J, Liu J, Zhao H, Vizcaychipi MP, et al. Pre-treatment with isoflurane ameliorates renal ischemic-reperfusion injury in mice. Life Sci. 2011;88(25-26):1102-7.
231. Ye Z, Guo Q, Xia P, Wang N, Wang E, Yuan Y. Sevoflurane postconditioning involves an up-regulation of HIF-1alpha and HO-1 expression via PI3K/Akt pathway in a rat model of focal cerebral ischemia. Brain Res. 2012;1463:63-74.
232. Sumi C, Matsuo Y, Kusunoki M, Shoji T, Uba T, Iwai T, et al. Cancerous phenotypes associated with hypoxia-inducible factors are not influenced by the volatile anesthetic isoflurane in renal cell carcinoma. PLoS One. 2019;14(4):e0215072.
233. Morikawa T, Takubo K. Hypoxia regulates the hematopoietic stem cell niche. Pflugers Arch. 2016;468(1):13-22.
234. Zou J, Li P, Lu F, Liu N, Dai J, Ye J, et al. Notch1 is required for hypoxia-induced proliferation, invasion and chemoresistance of T-cell acute lymphoblastic leukemia cells. J Hematol Oncol. 2013;6:3.
235. Colmone A, Amorim M, Pontier AL, Wang S, Jablonski E, Sipkins DA. Leukemic cells create bone marrow niches that disrupt the behavior of normal hematopoietic progenitor cells. Science. 2008;322(5909):1861-5.
236. Tavor S, Petit I, Porozov S, Avigdor A, Dar A, Leider-Trejo L, et al. CXCR4 regulates migration and development of human acute myelogenous leukemia stem cells in transplanted NOD/SCID mice. Cancer Res. 2004;64(8):2817-24.
237. Du Q, Zhang X, Zhang X, Wei M, Xu H, Wang S. Propofol inhibits proliferation and epithelial-mesenchymal transition of MCF-7 cells by suppressing miR-21 expression. Artif Cells Nanomed Biotechnol. 2019;47(1):1265-71.
238. Zheng H, Fu Y, Yang T. Propofol inhibits proliferation, migration, and invasion of hepatocellular carcinoma cells by downregulating Twist. J Cell Biochem. 2019;120(8):12803-9.
239. Gao C, Shen J, Meng ZX, He XF. Sevoflurane Inhibits Glioma Cells Proliferation and Metastasis through miRNA-124-3p/ROCK1 Axis. Pathol Oncol Res. 2019.
240. Valsecchi R, Coltella N, Belloni D, Ponente M, Ten Hacken E, Scielzo C, et al. HIF-1alpha regulates the interaction of chronic lymphocytic leukemia cells with the tumor microenvironment. Blood. 2016;127(16):1987-97.
241. Duarte D, Hawkins ED, Akinduro O, Ang H, De Filippo K, Kong IY, et al. Inhibition of Endosteal Vascular Niche Remodeling Rescues Hematopoietic Stem Cell Loss in AML. Cell Stem Cell. 2018;22(1):64-77 e6.

242. Song X, Yang C, Zhang H, Wang J, Sun X, Hu L, et al. Hypoxia-Inducible Factor-1alpha (HIF-1alpha) Expression on Endothelial Cells in Juvenile Nasopharyngeal Angiofibroma: A Review of 70 cases and Tissue Microarray Analysis. Ann Otol Rhinol Laryngol. 2018;127(6):357-66.
243. Yan Y, Qiao S, Kikuchi C, Zaja I, Logan S, Jiang C, et al. Propofol Induces Apoptosis of Neurons but Not Astrocytes, Oligodendrocytes, or Neural Stem Cells in the Neonatal Mouse Hippocampus. Brain Sci. 2017;7(10).
244. Dong Y, Zhang G, Zhang B, Moir RD, Xia W, Marcantonio ER, et al. The common inhalational anesthetic sevoflurane induces apoptosis and increases beta-amyloid protein levels. Arch Neurol. 2009;66(5):620-31.
245. Zhou X, Li W, Chen X, Yang X, Zhou Z, Lu D, et al. Dose-dependent effects of sevoflurane exposure during early lifetime on apoptosis in hippocampus and neurocognitive outcomes in Sprague-Dawley rats. Int J Physiol Pathophysiol Pharmacol. 2016;8(3):111-9.
246. Su Z, Hou XK, Wen QP. Propofol induces apoptosis of epithelial ovarian cancer cells by upregulation of microRNA let-7i expression. Eur J Gynaecol Oncol. 2014;35(6):688-91.
247. Wang L, Wang T, Gu JQ, Su HB. Volatile anesthetic sevoflurane suppresses lung cancer cells and miRNA interference in lung cancer cells. Onco Targets Ther. 2018;11:5689-93.
248. Papandreou I, Lim AL, Laderoute K, Denko NC. Hypoxia signals autophagy in tumor cells via AMPK activity, independent of HIF-1, BNIP3, and BNIP3L. Cell Death Differ. 2008;15(10):1572-81.
249. Windisch R, Pirschtat N, Kellner C, Chen-Wichmann L, Lausen J, Humpe A, et al. Oncogenic Deregulation of Cell Adhesion Molecules in Leukemia. Cancers (Basel). 2019;11(3).
250. Arber DA, Orazi A, Hasserjian R, Thiele J, Borowitz MJ, Le Beau MM, et al. The 2016 revision to the World Health Organization classification of myeloid neoplasms and acute leukemia. Blood. 2016;127(20):2391-405.
251. Mathew B, Lennon FE, Siegler J, Mirzapoiazova T, Mambetsariev N, Sammani S, et al. The novel role of the mu opioid receptor in lung cancer progression: a laboratory investigation. Anesth Analg. 2011;112(3):558-67.
252. Rhondali O, Pouyau A, Bonnard C, Chassard D. [Anaesthetic management of a child with hemoglobinopathy]. Ann Fr Anesth Reanim. 2013;32(12):e193-7.

Appendix

Results from this thesis is being submitted for publication.

Two memory sticks are submitted to two examiners. Information in these two memory sticks include

1) 3 examples of time lapses captured by intravital microscopy.

2) 3 examples of tile scans captured by intravital microscopy.